IV.D Fuel Cell Stack Subsystem and Components

IV.D.1 R&D of a 50 kW, High Efficiency, High Power Density, CO-Tolerant PEM Fuel Cell Stack System

Tim Rehg (Primary Contact), Nguyen Minh (Program Manager)
Honeywell International
2525 W. 190th Street, MS-36-1-93193
Torrance, CA 90504-6099
(310) 538-7220, fax: (310) 512-3432, e-mail: Timothy.Rehg@ ps.ge.com

DOE Technology Development Manager: Patrick Davis
(202) 586-8061, fax: (202) 586-9811, e-mail: Patrick.Davis@ee.doe.gov

ANL Technical Advisor: William Swift
(630) 252-5964, fax: (630) 972-4473, e-mail: swift@cmt.anl.gov

Objectives

- Research, develop, assemble, and test a 50 kW net polymer electrolyte membrane (PEM) fuel cell stack system comprised of a PEM fuel cell stack and the supporting gas, thermal, and water management subsystems. The PEM fuel cell stack system will be capable of integration with at least one of the fuel processors currently under development by Hydrogen Burner Technology (HBT) and Arthur D. Little, Inc.

Approach

This phased program includes the fabrication and testing of three 10-kW subscale PEM fuel cell stacks leading up to the final 50 kW system. Stack technology development and system analysis were conducted iteratively to identify pertinent technology advances to be incorporated into successive subscale stack builds. The final system analysis will define the 50 kW stack and system configuration.

Phase I:

- PEM stack R&D to demonstrate multi-fuel capability and CO tolerance
- PEM stack R&D to advance technologies toward DOE targets

Phase II:

- Subscale integration, electronic control system development, transient characteristics, and durability testing

Phase III:

- Testing of the 50 kW PEM fuel cell stack system
- Hardware delivery of 50 kW PEM fuel cell stack system to Argonne National Laboratory

Accomplishments

- Testing of the balance-of-plant with the integrated turbocompressor has been completed.
- A 3rd generation 10-kW class PEM stack with compression molded bipolar plates has been completed and tested, and anode stoichiometry of 1.15 has been demonstrated.
- The 50-kW class PEM fuel cell stack has been built and integrated into the brassboard system.

Future Directions

- Conduct performance testing of the 50 kW net PEM fuel cell stack system brassboard at nominal load, peak load, and different intermediate partial loads and determine system efficiency.
- Deliver 50 kW net PEM fuel cell stack system brassboard to Argonne National Laboratory at the conclusion of the project (07/02).

Introduction

Fuel cell power plants will become viable substitutes for the internal combustion engine (ICE) in automotive applications only when their benefits of increased fuel efficiency and reduced emissions are accompanied by performance and cost comparable to the ICE. Meeting these requirements is a significant technical challenge that requires an integrated systems approach. This effort encompasses the technical and developmental activities required to incorporate innovations necessary to develop a 50 kW fuel cell stack system to meet the requirements set forth by the DOE.

Approach and Results

Fuel Cell Stack System

The PEM fuel cell stack system consists of the fuel cell stack and supporting gas, thermal and water management systems as shown in Figure 1. Overall system performance depends on the careful integration of these subsystems. The system developed under this contract was designed to accept reformed gasoline from a fuel processor. Development of the fuel processor was not part of this program.

The 50 kW fuel cell stack brassboard system design has been completed. The three-dimensional layout including six hexagonally shaped stacks can be seen in Figure 2. During this reporting period, all major components have been procured, and the balance of plant has been assembled. A photograph of the system is shown in Figure 3. The brassboard has been designed for 50 kW electric power output, operating at high-efficiency on simulated gasoline reformate. It incorporates full integration and management of on-board thermal, water and air subsystems, and makes use of off-the-shelf components to minimize cost and assembly time.

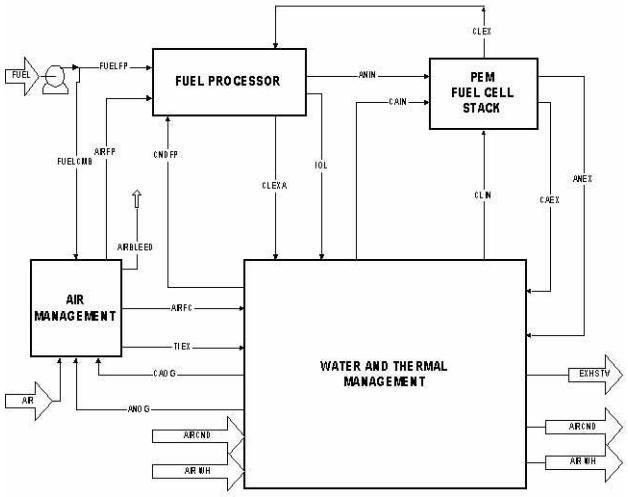

Figure 1. PEM Fuel Cell Stack System Diagram

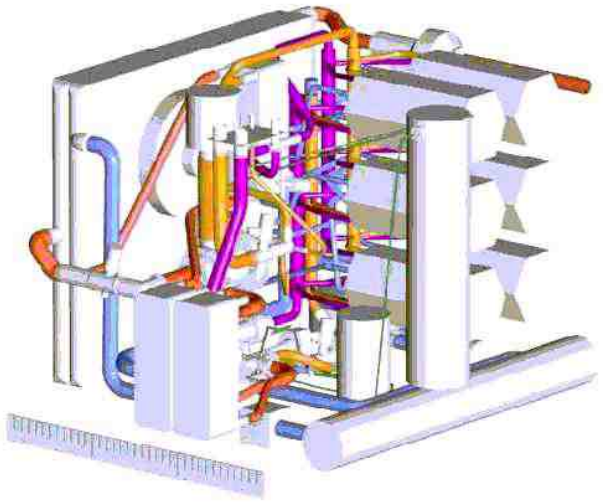

Figure 2. 50 kW Brassboard System Design

For air delivery, the fuel cell stack system is equipped with a Honeywell turbocompressor developed under separate DOE funding (see Figure 4). The turbocompressor delivers enough air for the fuel cell stack system and the fuel processor at an

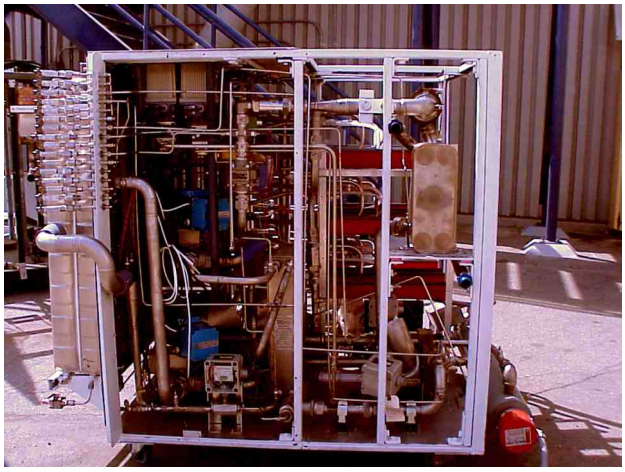

Figure 3. 50 kW Brassboard System

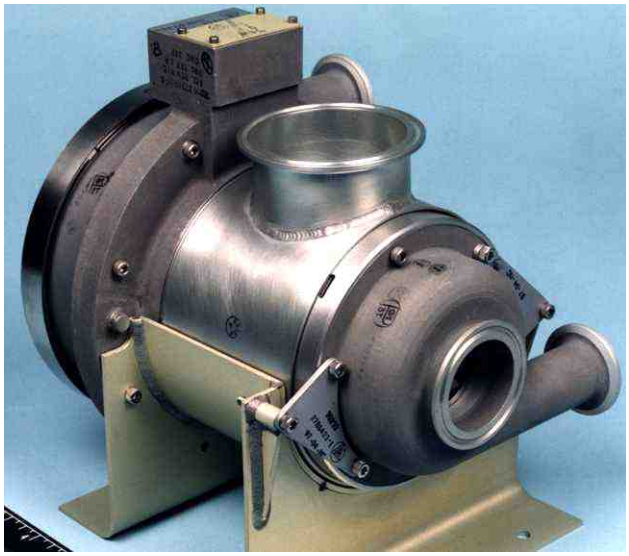

Figure 4. Honeywell Phase II Turbocompressor

operating pressure of up to 3 atmospheres at peak condition. During this reporting period the balance-of-plant with the integrated turbocompressor and its controller has been tested to verify adequate performance. Six 10-kW class PEM fuel cell stacks have been built using compression molded bipolar plates. These stacks have been integrated into the balance-of-plant for final system performance testing.

10-kW PEM Fuel Cell Stack With Molded Bipolar Plates

For the fabrication of the 50-kW PEM fuel cell stack, compression-molded composite bipolar plates have been employed. These plates are made in a single step, which will help to reduce the manufacturing cost substantially in the future. During this reporting period, Honeywell has received final delivery of all molded bipolar plates and has completed the assembly and testing of six 10-kW size PEM fuel cell stacks.

In order to test the performance of the compression-molded bipolar plates, a 63-cell subscale stack was built initially and tested. The performance of the subscale stack at the nominal power condition is shown in Figure 5. The test conditions are described in detail in Table 1. At a current density of 0.115 A/cm^2, the stack was able to stably operate at an anode stoichiometry of 1.15. The single cell voltage at this point was measured at 0.74 V. This results in slightly higher performance than previously seen with machined bipolar plates.

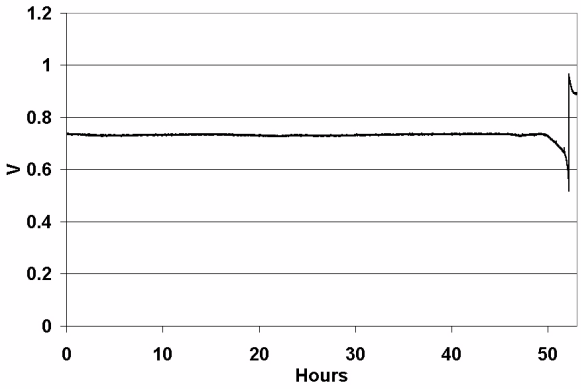

Figure 5. Performance of 63-cell PEM Fuel Cell Stack with Compression Molded Composite Bipolar Plates

	Anode	Cathode
Gas	Reformate	Air
Stoich	1.15	2.15
RH	100%	50%
Temperature	80°C	80°C
Pressure	1.25 atm	1.25 atm

Table 1. Test Conditions for 63-cell PEM FC Stack with Molded Composite Bipolar Plates

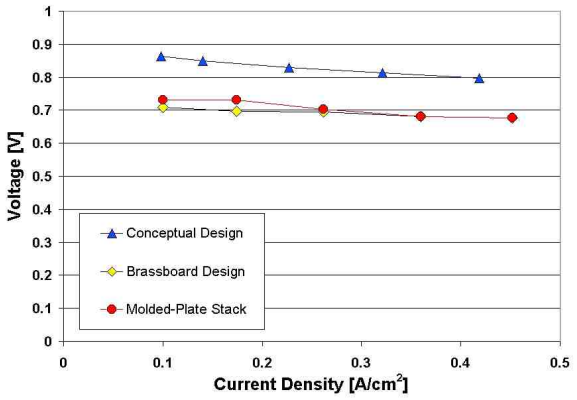

Figure 6. PEM Fuel Cell Stack Performance at Different System Operating Points

After completion of the testing of the 63-cell stack, the first 10-kW size stack was built and tested. Figure 6 compares the performance of this stack with the conceptual design performance and the originally predicted performance for the 50-kW brassboard system. The results show that the single-cell voltage remains slightly below the desired performance for the conceptual design, but has improved over the predicted brassboard performance for the lower power conditions. At the higher power conditions, including peak power, the voltage is identical to the prediction. In addition, the results show that the stack was able to operate at an anode stoichiometry of 1.25 for all power settings above 12.5 kW. At the nominal power setting, the overall pressure drop through the anode flowfield of the molded bipolar plates at flows below 1.35 stoichiometry is too low to remove liquid water. Anode stoichiometry below 1.25 at the nominal condition were demonstrated in later testing by reducing the anode relative humidity to 50%.

After successful testing of the first 10-kW size stack with molded bipolar plates, five more stacks were assembled and tested. Successively, all six stacks were integrated into the balance-of-plant, and the system is ready for performance testing.

Conclusions

In this reporting period Honeywell has completed the assembly and testing of the balance-of-plant with the turbocompressor and fuel cell stacks. Our attention is now focussed on the final performance testing of the 50 kW brassboard system and delivery to Argonne National Laboratories. Results from a 63-cell sub-scale PEMFC stack test with compression-molded composite bipolar plates demonstrated a low anode stoichiometric flow of 1.15 at nominal conditions. A full size 10-kW PEM fuel cell stack demonstrated stable performance at all system power points for an anode stoichiometric flow of 1.25.

The current projected brassboard system nominal efficiency is 45% (assuming 1.25X stoichiometric flow of reformate), and the projected power densities are ~0.2 kW/kg and ~ 0.15 kW/L, versus the CY 2002 DOE targets established for this project of 55%, 0.35 kW/kg and 0.35 kW/L. It should be noted that the above numbers include contributions from off-the-shelf components for the brassboard, i.e. oversized heat exchangers and valves. The main contributers to the loss of efficiency are increased flow stoichiometry and parasitic loads. Some of the key reasons for increased parasitic loads are compressor motor power and increased pressure drop for some components (heat exchangers, valves, etc.).

IV.D.2 Development of Comprehensive Computer Models for Simulation of Fuel Cell Systems

Hongtan Liu
Department of Mechanical Engineering
University of Miami, Coral Gables, FL 33214
(305) 284-2019, fax: (305) 284-2580, e-mail: hliu@miami.edu

DOE Technology Development Manager: Donna Lee Ho
(202) 586-8000, fax: (202) 586-9811, e-mail: Donna.Ho@ee.doe.gov

ANL Technical Advisor: William Swift
(630) 252-5964, fax: (630) 972-4473, e-mail: Swift@cmt.anl.gov

Objectives

- Develop comprehensive computer model for Polymer Electrolyte Membrane (PEM) fuel cells.
- Demonstrate the feasibility of unified model approach to eliminate errors due to approximate boundary conditions at various interfaces.
- Develop reliable tools for design and optimization of fuel cells, fuel cell stacks, and fuel cell energy systems (long-term).

Approach

- Develop general mathematical models valid in different elements of a fuel cell .
- Eliminate boundary conditions at the various interfaces between different elements of a fuel cell.
- Develop models with flexibility, adaptability and different levels of complexity, so that they can be used for different purposes. The model must be easy to update and revise to incorporate custom code.
- Develop independent packages (not based on any CFD package) that are economical, robust and high-speed.

Accomplishments

- Demonstrated the feasibility of the unified approach.
- Developed sub-model A: 2D single-phase flow model – down the channel and across the FC sandwich.
- Developed sub-model B: 2D single-phase flow model – across the channel and across the FC sandwich.
- Developed a 3-D model for hydrogen feed with constant over-potential across the catalyst layer.
- Developed a 2D two-phase flow model with variable over-potential across the catalyst layer.
- Substantially extended and improved the 3-D single phase model, including the variation of over-potential across the catalyst layers.
- Developed a 3-D single-phase model for reformate feed in the anode.
- Developed a preliminary fuel cell stack model.
- Performed systematic experimental tests to calibrate and improve the models.
- Worked closely with industry to customize and improve the models.

Future Plans

- Further develop the 3-D single-phase model: improve on reformate feed and for different flow fields.
- Improve the fuel cell stack model.
- Couple the stack model with a system model.
- Extend the models to other types of fuel cells.
- Further interactions with industry.

Introduction

A fast, reliable, and specialized CFD model for PEM fuel cell simulation can be very useful in fuel cell design optimization and operation control. In this project, a unified PEM fuel cell simulation model has been successfully established. This project started in FY 2000 with 2-D single-phase models. In FY 2001, the 2-D models were successfully transformed into a unified 3-D model for hydrogen feed. In FY 2002, this established 3-D model was extended to include reformate feed, accounting for the poisonous effect of carbon monoxide as well as the dilution effect of the reformate gas stream on the anode side. Based on this 3-D model with the geometry of a single fuel cell, a preliminary stack model was established. Extensive experiments in our lab and industry interactions were carried out to improve and calibrate the computation model.

Approach

The geometry of a single fuel cell is shown in Figure 1. The PEM fuel cell is divided into 9 regions according to the material properties and flow characteristics. In FY 2000, this project started with 2-D single-phase models that included 2 sub-models [1, 2]. One of the 2-D models has a geometry comprised of flow direction and the plane across the fuel cell sandwich (on the xy-plane). The other one includes the region across the channel and across the fuel cell sandwich (on the xz-plane).

In FY 2001, a general 3-D model was developed [3]. This general mathematical model consists of the equations of continuity, momentum, energy, and species concentrations in different elements of the fuel cell sandwich, as well as the equations for phase potential in the membrane and the catalyst layer. This set of governing equations is coupled with chemical reaction kinetics by introducing various

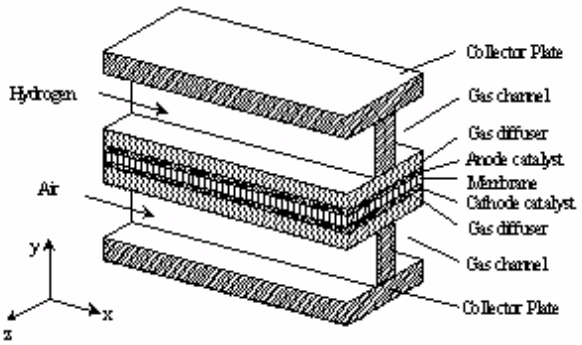

Figure 1. Single Fuel Cell Geometry

source terms. The generality of the model lies in its independence of chemical kinetic models, since the kinetics are incorporated in the source terms. One can choose any kinetics model, and any new development in the electrochemistry can easily be incorporated in this general model. To solve the mathematical model, an in-house computer code has been developed. Compared with some commercial CFD packages, this self-produced code was designed for a specific purpose so that the computation time could be significantly reduced. The output results from this 3-D model include oxygen concentration variations in different planes, local current density distributions, reaction rate, temperature distributions, water vapor distributions along anode and cathode, etc. Details about the model and results can be found in Zhou and Liu [3]. In FY 2001, a preliminary 2-phase, 2-D model was also developed [4]. It was found that a single-phase model is sufficient when the current density is low, when the current density is larger and approaching the current density limit, phase changing of water becomes significant.

In FY 2002, the 3-D single-phase model was significantly improved in several aspects. Specifically, instead of assuming constant overpotential across the catalyst layer, the variation

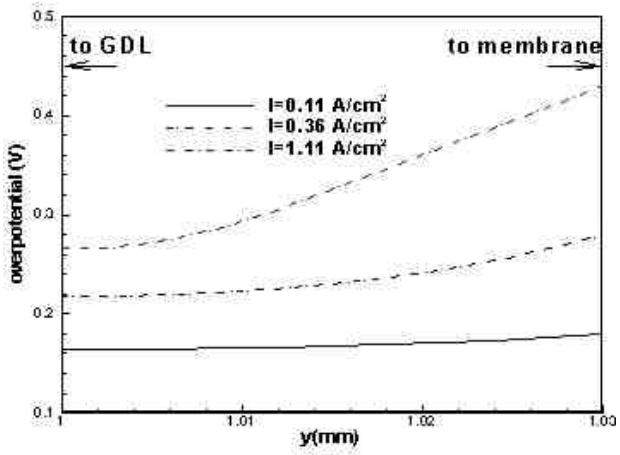

Figure 2. Variation of Overpotential Inside the Catalyst Layer

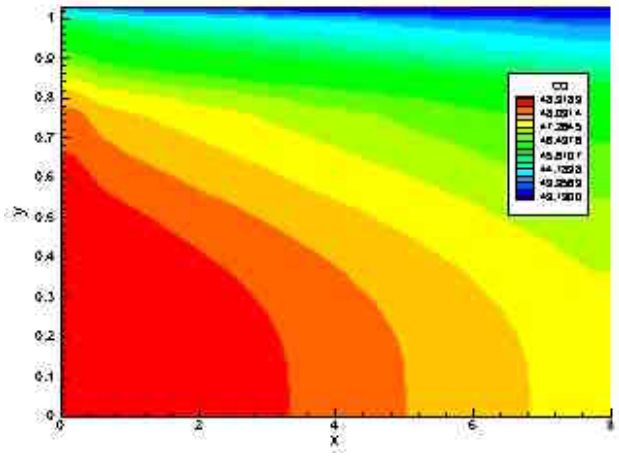

Figure 3. CO Concentration Along the Flow Direction

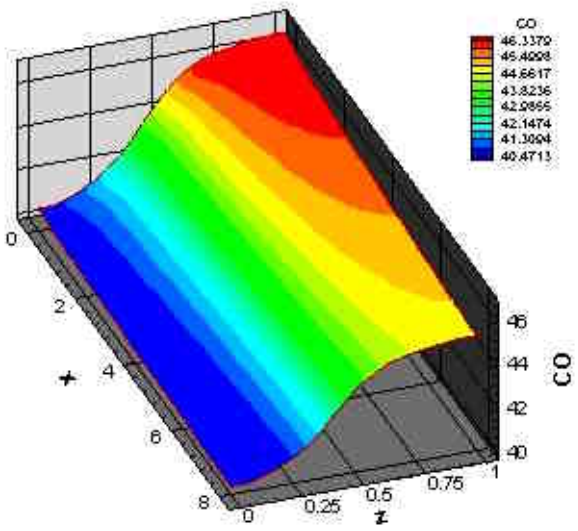

Figure 4. CO Concentration Across the Fuel Cell (Half of Z Over the Shoulder Plate)

of over-potential across the catalyst layer was added to the model [5]. Figure 2 shows the variation of the overpotential within the catalyst layer at different current densities. When the current density is low, variation of overpotential is not significant, but when the current density is high, the overpotential variation is significant and cannot be neglected. In order to reduce computation time and ensure the accuracy of the model, systematic analysis and reductions of the model have been conducted, some highlights of which can be found in [5].

Reformate feed is expected to be the viable intermediate fuel for fuel cell applications, and a PEM fuel cell operating on reformate gas has unique characteristics. Two of the characteristics are the dilution effect of the inert gases and the variation of hydrogen content at different locations of a fuel cell. The third is the poisoning effect of the carbon monoxide (CO) present in the reformate. The previous 3-D model has been extended and modified to account for these extra characteristics. The kinetic equations for CO poisoning effects that were presented by Springer et al. [6] were used. With those adjustments, the 3-D model now can successfully demonstrate some features not revealed by 1-D kinetic models in the literature [6]. The reduction of CO at larger current density due to reaction consumption is shown by the CO contours in Figures 3 and 4. The model results of CO affecting PEM fuel cell performance is shown in Figure 5. Figure 6 shows that the computation results compared very well with the test data available from the literature [7].

Based on the single fuel cell model, a preliminary stack model is set up as shown by Figure 7. This modeled region includes 5 channels and 3 cells. Cooling plates were inserted into the stack at an interval of 3 cells. (This choice is just used as an example.) The model can easily accommodate different numbers of cells and channels, and different stack designs can also be easily handled. With this stack model, computational investigations of the temperature distributions were carried out. Some sample temperature contours are shown in Figures 8

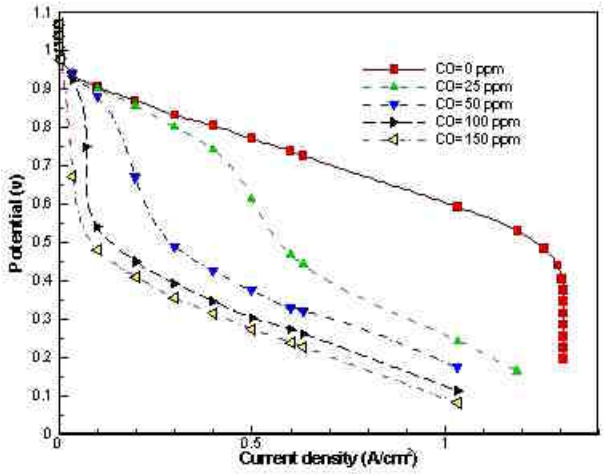

Figure 5. Polarization Curves at Different CO

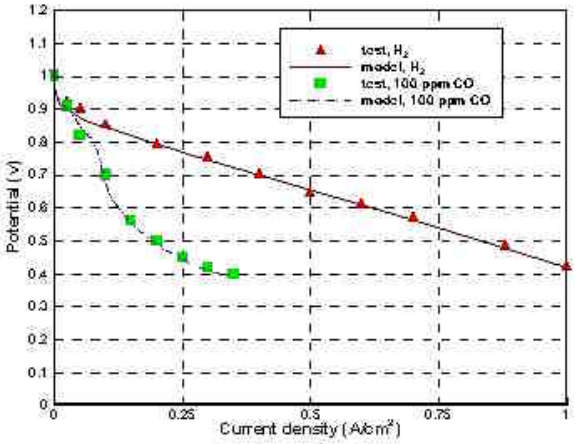

Figure 6. Comparison of Modeling Results With Experimental Data for CO Poisoning

and 9. While the cooling plates and the convection along the border cool the fuel cells, some locations of the fuel cells inside the stack can experience very high temperature. The modeling results can be used to devise better ways for fuel cell stack thermal management.

To calibrate the model, extensive experiments were conducted in our Fuel Cell Laboratory at the University of Miami [8]. Close interaction with the fuel cell industry was also carried out.

Conclusions

During the past 3 years, a generalized 3-D PEM fuel cell simulation model was developed at the

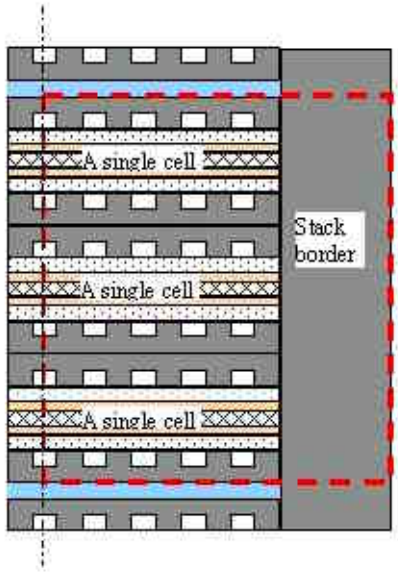

Figure 7. Geometry for the Fuel Cell Stack Model

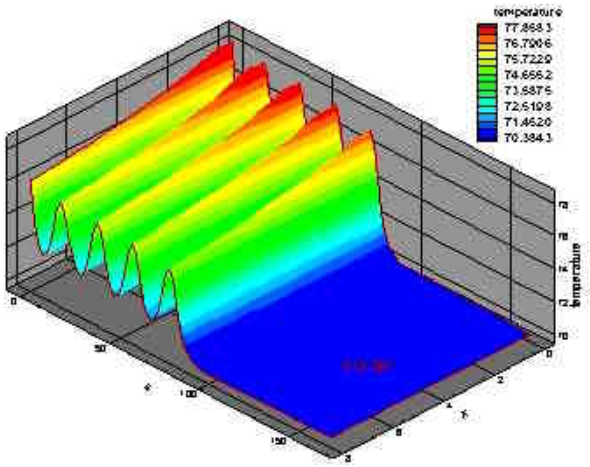

Figure 8. Temperature Contours Across the Flow Channels

University of Miami. This generalized model started from the basic fluid flow and electro-chemical principles. This generalization makes it easily adaptable to include choices of different flow fields, different fuel cell materials and flow design, and different fuels used. A computation code specifically designed for this mathematical model was produced and proved accurate and efficient. In FY 2002, the 3-D model has been significantly improved by adding the variation of overpotential across the catalyst layer. It was also extended to include the reformate feed at the anode. Extension of this single-cell model to study various stack design choices has also been

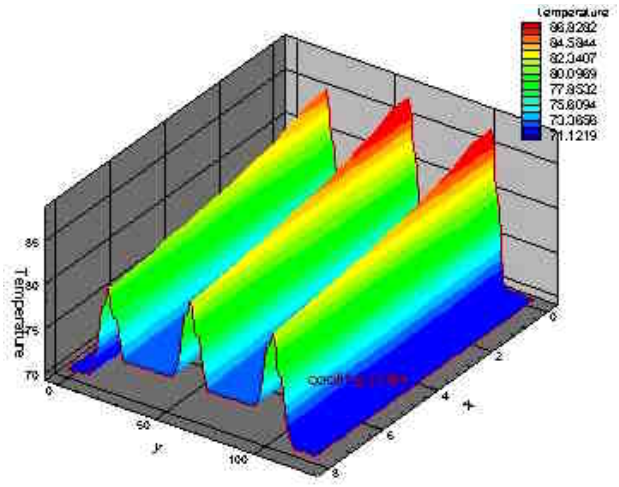

Figure 9. Temperature Distribution Within the 3 Cells Along the Flow Direction

proven feasible. The great potential of the models for industrial applications has been demonstrated, especially through the close collaborations with industry partners. Our future research plans include extending this generalized 3-D model to other types of fuel cells and coupling the stack model to a fuel cell system model.

References

1. Gurau, V., Liu, H.T. and Kakac, S., *AIChE*, Vol. **44**, pp. 2410-2422, 1998.

2. Kazim, A., Liu, H.T. and Forges, P., *J. Applied Electrochem.*, Vol. **29**, pp. 1409-1416, 1999.

3. Zhou, T. and Liu, H.T., *Int. J. Transport Phenomena*, Vol. **3** (3), pp. 177-198, 2001.

4. You, L. and Liu, H.T., *Int. J. Heat and Mass Transfer*, Vol. **45**, pp. 2277-2287, 2002.

5. Zhou, T. and H.T. Liu, *6th Biennial Conf. on Engineering Systems Design and Analysis*, Istanbul, Turkey, July 8-11, 2002.

6. Springer, T.E., Rockward, T., Zawodzinski, T.A., *J. Electrochemi. Soc.*, Vol.**148** (1), pp. A11-A23, 2001 .

7. Divisek, J., Oetjen, H.-F., Schmidt, V.M. and Stimming, U., *Electrochem. Acta*., Vol. **43**, pp. 3811-3815, 1998.

8. Wang, L., Husar, A., Zhou, T., and Liu, H., Zhou, T, "Parametric Study of PEM Fuel Cell Performances," to be presented at ASME Congress, New Orleans, November 17 – 22, 2002.

FY 2002 Publications and Presentations

1. Zhou, T. and Liu, H.T., "A General Three Dimensional Model for PEM Fuel Cells," in *Int. J. Transport Phenomena*, Vol. **3** (3), pp. 177-198, 2001.

2. You, L. and Liu, H.T., "A Parametric Study of the Cathode Catalyst Layer of PEM Fuel Cells Using a Pseudo-Homogeneous Model," *Int. J. Hydrogen Energy*, Vol. 26, pp. 991-999, 2001.

3. Liu, H.T., Zhou, T. and You, L., "CFD Modeling of Proton Exchange Membrane Fuel Cells," in *Proc. 9th Annual Conference of the CFD Society of Canada*, Kitchener, Ontario, Canada, May 27-29, 2001.

4. Zhou. T. and Liu, H.T., "Numerical Simulation Of Performance Of PEM Fuel Cells," in *Proc. of the 2nd Int. Conference on Computational Heat and Mass Transfer*, COPPE/UFRJ – Federal University of Rio de Janeiro, Brazil, October 22-26, 2001.

5. You, L. and Liu, H.T., "A Two-Phase Flow And Transport Model For The Cathode Of PEM Fuel Cells," *Int. J. Heat and Mass Transfer*, Vol. **45**, pp. 2277-2287, 2002.

6. Zhou, T. and Liu, H.T., "Heat Transfer Enhancement in Fuel Cells with Interdigitated Flow Field Design," *Int. J. Computer Applications in Technology*, in publication, 2002.

7. Zhou, T. and Liu, H.T., "Development and Simplification of a Three-Dimensional PEM Fuel Cell Model," *6th Biennial Conference on Engineering Systems Design and Analysis*, Istanbul, Turkey, July 8-11, 2002.

8. Zhou, T. and Liu, H.T., "Effects of Heat and Mass Transfer Enhancements on PEM Fuel Cell Performances," *12th International Heat Transfer Conference,* France, August 18-23rd, 2002.

9. Zhou, T. and Liu, H.T., "Simulation of Performance of PEMFC Operated by Reformed Gas," accepted for the *2002 Fuel Cell Seminar*, Palm Springs, California, November 18-21, 2002.

10. Wang, L., Husar, A., Zhou, T., Liu, H., and Zhou, T, "Parametric Study of PEM Fuel Cell Performances," accepted to the ASME Congress, New Orleans, November 17 - 22, 2002.

11. Higier, A., Husar, A., and Liu, H., "Design of a Fuel Cell Fixture with Precise Compression Control and Preliminary Experimental Results," accepted for the *2002 Fuel Cell Seminar*, Palm Springs, California, November 18-21, 2002.

IV.D.3 High Performance, Matching PEM Fuel Cell Components and Integrated Pilot Manufacturing Processes

Mark K. Debe (Principal Investigator), Judith B. Hartmann (Primary Contact)
3M Company
3M Center, Building 0201-01-C-30
St. Paul MN 55144-1000
(651) 736-1772, fax: (651) 575-1187, e-mail: jbhartmann@mmm.com

DOE Technology Development Manager: Valri Lightner
(202) 586-0937, fax: (202) 586-3237, e-mail: Valri.Lightner@ee.doe.gov

DOE Technology Development Manager: JoAnn Milliken
(202) 586-2480; fax: (202) 586-9811; e-mail: JoAnn.Milliken@ee.doe.gov

ANL Technical Advisor: Thomas Benjamin
(630) 252-1632, fax: (630) 252-4176, e-mail: benjamin@cmt.anl.gov

Subcontractor: GM - GAPC, Rochester, NY

Objectives

- Develop a set of high performance, matched proton exchange membrane (PEM) fuel cell components and pilot manufacturing processes to facilitate high volume, high yield stack production.
- Demonstrate the matched component performance in a 1-kW fuel cell stack.

Approach

- Phase 1
  - Increase surface area of the 3M-patented, nanostructured, thin film catalyst support system consistent with high volume manufacturing process.
  - Develop anode catalyst compositions and structures with higher reformate tolerance and/or a non-precious metal replacement for Ru, using a catalyst deposition process that easily generates new compositions and structures.
  - Investigate binary and ternary catalyst compositions and structures to produce higher activity cathodes.
  - Develop carbon electrode backing (EB) media, optimized for performance with the catalyst system and flow field.
  - Optimize the fuel cell flow field design for optimized water management and air bleed utilization with the catalyst and EB components.
  - Define pilot manufacturing scale-up of the processes for fabrication of catalysts, catalyst coated membrane (CCM) assemblies, and electrode backing media.
- Phase 2
  - Optimize pilot scale manufacturing of roll-good fabricated catalyst support films and catalyst deposition.
  - Specify membrane electrode assembly (MEA) component parameters and conduct final pilot scale runs to generate process statistics.

- Fabricate, test, and deliver a 1-kW stack to subcontractor for evaluation using optimized flow field and matched MEAs fabricated by pilot processes.

Accomplishments

- Developed a new Pt ternary cathode catalyst that gives the same performance with one-half the amount of Pt, producing 0.4 A/cm^2 at 0.8 V under 30/30 psig H_2/air with 0.2 mg/cm^2 total precious metal per MEA.
- Identified a non-precious metal replacement for Ru on the anode for reformate tolerance, which, with air bleed, gives equivalent performances within ±10-20 mV.
- Integrated multiple process steps for generating the nanostructured catalyst support films into a single pass, dry web-coating, pilot plant process. Completed MEA fabrication cost model based on existing pilot production process and equipment.
- Developed a unique flow field design via modeling and basic principles of gas transport that optimizes the uniformity of hydrogen and air mass flow velocities for the matched EB media and increases high current density performance over conventional designs.
- Developed a roll-good processed electrode backing/gas diffusion layer component having matched properties to the nanostructured thin film catalyst and flow field; generated pilot scale production quantities for statistical analysis of variance and demonstration of process capability.

Future Directions

- Complete pilot scale fabrication of multiple lots of roll-good, nanostructured support films, anode and cathode catalyst deposition on those substrates, and roll-good CCM fabrication to generate statistical process and performance data.
- Complete fuel cell testing of statistically sampled, roll-good fabricated, coated EB materials and CCMs having matched properties for optimum performance.
- Complete evaluation of roll-good fabricated MEAs from pilot processed material lots in 1-kW stacks at 3M and subcontractor facilities.

Introduction

The membrane electrode assembly (MEA) is the core component set of a PEM fuel cell (PEMFC) stack. An MEA consists of five basic components: anode and cathode catalysts, ion exchange polymer membrane, and anode and cathode gas diffusion layers. The functions of these basic components are intimately related, and their properties must be matched for optimum performance. For large-scale volume fabrication at the cost and quality targets required by transportation applications, very high yields and in-line process control of integrated processes based on cost effective materials are required. This project is directed towards demonstrating high performance, matching PEM fuel cell components manufacturable by integrated pilot processes, utilizing a patented nanostructured thin film catalyst support system.

Approach

Our approach to developing high performance, matching PEMFC components and integrated pilot manufacturing processes has several facets. These include optimization of the individual components, such as the anode and cathode catalysts and their supports, and electrode backing and gas diffusion layers, all made by processes consistent with high volume manufacturing methods.

For the anode and cathode catalyst development, the unique nanostructured support and catalyst coating methods offer many combinations of materials and process conditions to generate new

catalyst compositions and structures. The major focus areas have been generating higher surface area supports, fabricating and testing new Pt_xM_y binary and ternary constructions for anodes and cathodes, and reducing air bleed - all with goals of increasing performance and stability and reducing precious metal loading.

Development of carbon electrode backing (EB) media has included evaluation of different types of electrode backing materials, coatings, coating configurations, and coating processes. Evaluation involves measurement of a variety of physical properties and of fuel cell performance under a broad range of controlled conditions using nominally identical catalyst coated membranes (CCMs).

The flow field is an integral component of the MEA system. Matching it to the EB material is particularly important in order to obtain uniform gas flow velocity and pressure distributions that in turn will yield the most uniform current density distributions. The gas permeability properties of the various electrode backing and gas diffusion layers were key inputs for fluid dynamic modeling used to devise a unique flow field design that gives optimized mass flow uniformity while enhancing performance at high current densities and matching pressure drop specifications supplied by the subcontractor.

Scale-up and integration of the processes for producing the nanostructured catalyst support films via a single pass, dry web process with on-line monitoring has been a major focus during the past year to demonstrate process control, determine the pilot production equipment limits, increase material yields, and reduce costs. The catalyst coating processes have also been scaled up to give the required cross-web uniformities and apply the new multi-element catalysts. A detailed cost model for several different final integrated process scenarios was developed.

Results

Cathode Catalysts

In the past year, screening of a wide range of binary Pt_xM_y catalysts to find a cathode catalyst with greater mass activity and/or stability than pure Pt was completed. The process for fabricating the nanostructured catalysts allows a wide range of new constructions to be easily made and tested.

Figure 1 compares the performance of three different Pt binaries and two different Pt ternary constructions with the pure Pt cathode catalyst. The test uses high-pressure hydrogen/oxygen to best reflect the oxygen reduction reactivity of the cathode catalysts. As can be seen, all the combinations outperform the pure Pt catalyst. All the samples contained 0.1 mg/cm^2 of precious metal, except for the second ternary, PtAB-2, which contained 0.15 mg/cm^2. PtAB-2 was selected for scale-up during Phase 2 and became the focus for 50-cm^2 fuel cell testing.

As discussed in Reference 1, it is well documented that, with our standard nanostructured support particles, the baseline pure Pt catalyst has a mass specific surface area of about 7 m^2/g. For our standard loadings of 0.22 mg/cm^2, this corresponds to an effective surface roughness factor (or SEF, surface enhancement factor) of 12-15 cm^2/cm^2. Figure 2 shows duplicate measurements (Series A, Series B) of the SEF for the PtAB-2 ternary catalyst at three different loadings compared to the standard Pt at 0.22 mg/cm^2. It is seen that the ternary has the same surface area with half the amount of Pt as the standard pure Pt catalyst. This doubling of the mass

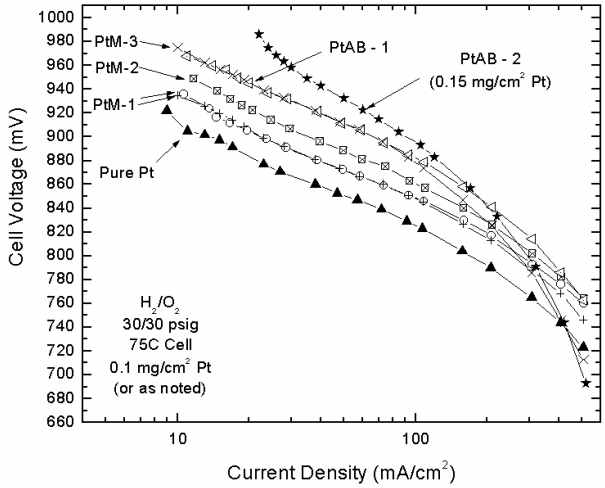

Figure 1. Comparison of the oxygen reduction activity of various binary and ternary catalysts with pure Pt, using 30-psig oxygen test conditions to enhance the differentiation.

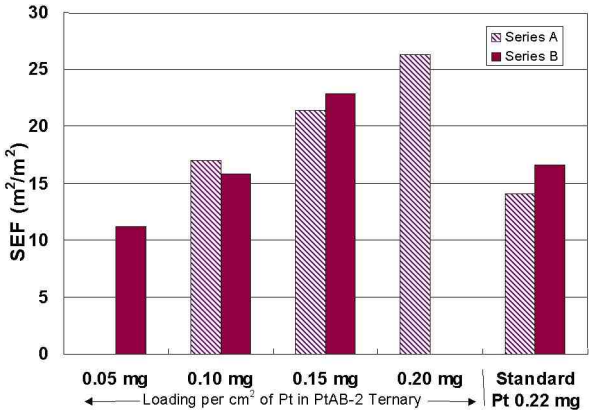

Figure 2. Comparison of the measured surface area, using hydrogen adsorption-desorption cyclic voltammetry, from pure Pt and the PtAB-2 ternary containing varying amounts of Pt.

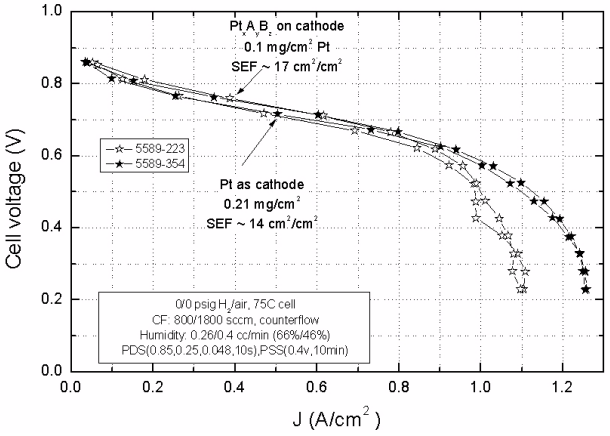

Figure 3. Comparison of PDS polarization curves from a single MEA tested in two orientations, first with the PtAB-2 ternary (with 0.1 mg/cm^2 Pt) as a cathode and the pure Pt (0.21 mg/cm^2) as the anode (5589-223), and second with the PtAB-2 as the anode and the pure Pt as the cathode (5589-354). The ternary with half the amount of Pt outperforms the pure Pt.

specific surface area to ~ 15 m^2/g allows the same fuel cell performance to be obtained with half the precious metal content.

This is best shown by comparing polarization curves for the same MEA, taken in two orientations. The first orientation has the PtAB-2 catalyst, with 0.1 mg/cm^2 Pt, as the cathode and the standard Pt catalyst, with 0.2 mg/cm^2, as the anode. In the

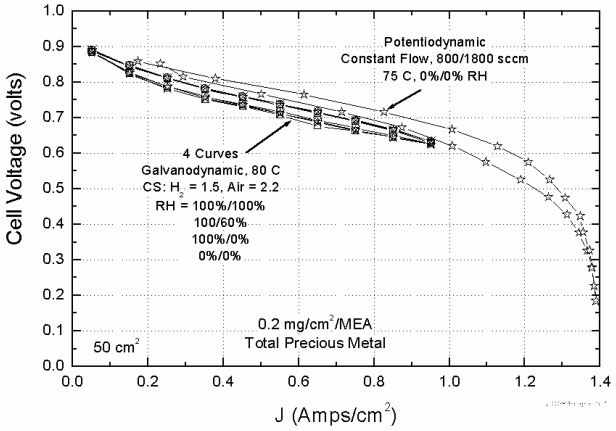

Figure 4. PDS-CF and GDS-CS polarization curves at 30 psig inlet pressure from an MEA having a total of 0.2 mg/cm^2/MEA of total precious metal (Pt).

second orientation, the hydrogen, air, and voltage leads are reversed so the ternary becomes the anode and the standard Pt is on the cathode. Figure 3 compares potentiodynamic (PDS) constant flow polarization curves at ambient pressure for these two MEA orientations and clearly indicates the improved kinetic behavior of the ternary over the standard Pt catalyst.

Figure 4 shows two types of polarization scans from an MEA having a total of 0.2 mg Pt/cm^2/MEA. This MEA has the same PtAB-2 catalyst on the cathode as in Figure 3, but the standard Pt on the anode reduced to 0.1 mg/cm^2. In Figure 4, the single potentiodynamic scan (PDS) polarization curve was obtained with constant flow (CF) conditions at 75ºC, while the lower four galvanodynamic scan (GDS) curves were obtained with constant stoichiometric flow (CS) conditions and varying humidification at 80ºC. All were obtained with H_2/air at 30/30 psig inlet pressures. The 30-psig constant flow conditions can achieve close to the DOE technical target of 0.4 A/cm^2 at 0.8 V for MEAs on hydrogen/air. This performance with this total loading of 0.2 mg/cm^2/MEA of Pt corresponds to the 2005 target of 0.6 g/kW at 0.8 V and 0.3 g/peak kW of precious metal.

Anode Catalysts

Screening for better or less costly anode catalysts is also a major task area. Finding a replacement for

Ru was a primary goal, along with reducing the amount of Pt required for adequate reformate tolerance. To facilitate the rapid screening of many new catalyst constructions having different compositions and structures, anode over-potential (AOP) and AC impedance measurements were used. Reference 1 discussed results from two new binary anode catalysts containing 0.1 mg/cm^2 of Pt and non-precious metal replacements for Ru, which had less AOP than the PtRu control. This past year led to development of still another PtM binary, where M is a non-precious metal replacement for Ru, which was down-selected for scale-up during Phase 2. Figure 5 compares 75ºC, 30 psig, constant flow polarization curves under H_2/air, reformate with 2% air bleed, and reformate with 4% air bleed from an MEA having this binary as the anode (0.20 mg/cm^2 Pt) and a standard Pt cathode (0.21 mg/cm^2). There is little difference between 2% and 4% air bleed and about a 35 mV loss compared to pure hydrogen at 0.5 A/cm^2. The curves suggest the DOE reformate target of 125 mA/cm^2 at 0.83 V and 9 psig are close to being met, but the rated power targets under reformate of 500 mA/cm^2 at 0.75 V and 30 psig fall short by about 35 mV.

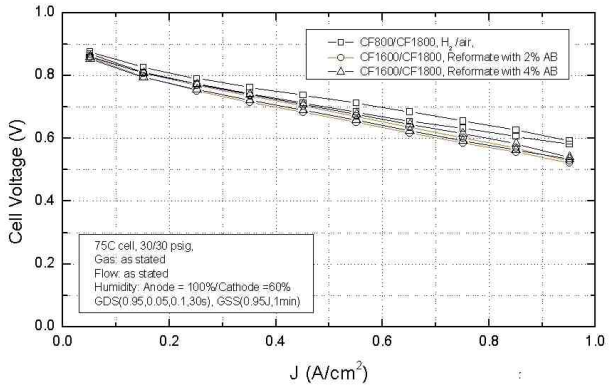

Figure 5. GDS-CF polarization curves under hydrogen and reformate with 2% and 4% air bleed, from an MEA having a PtM binary on the anode containing no Ru and 0.2 mg/cm^2 of total precious metal (Pt).

Roll-Good Electrode Backing Media

The EB materials and configurations demonstrating the highest potential for meeting project goals were selected for optimization. This past year, the work focused on demonstrating the EB/GDL process capability. Rolls of EB material were processed and the EB coatings applied in multiple pilot scale coating runs. Two types of on-line measurements were successfully used for characterization of two key physical properties. All lots were characterized off-line as well for these two plus a third critical property. All three parameters were demonstrated to be in process control. Analysis of variance within and between rolls did show some statistically significant differences, but total variability was small. Fuel cell characterization of MEAs having EB/GDL samples taken across all the produced rolls are underway using CCMs having standard Pt anodes and cathodes. Fuel cell tests of EB/GDL media sampled from one 450-lineal-yard roll are also underway with CCMs having the new PtAB-2 ternary cathode catalyst. This matched CCM/EB combination is giving the best performance to date and excellent statistical reproducibility, as shown in Figure 6. This shows the galvanodynamic, constant stoichiometry polarization curves from the first seven tested MEAs of 12 statistically sampled EB/GDLs from the fully processed 450-lineal-yard roll-good.

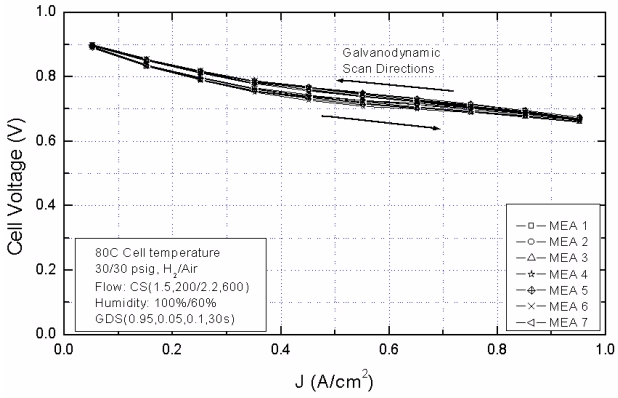

Figure 6. Seven GDS-CS polarization curves of EB/GDL samples taken from a pilot-scale processed 450-lineal-yard roll. The excellent reproducibility also reflects uniformity of the CCM. The galvanostatic (GSS) current density between scans was 0.95 A/cm^2.

Flow Field

The flow field and EB/GDL must be matched for optimum performance and durability. Designing for the most uniform gas flow distributions and effective water management should translate into the most

uniform current distributions. This year, computational fluid dynamics (CFD) modeling at 3M has led to a unique flow field design targeted for the EB roll-good materials discussed above. This design was refined as well to meet the desired in-cell pressure drops for the pressure-flow rate curves suggested by our subcontractor. Figure 7 shows a series of comparison polarization curves from different MEAs, each tested first in a cell having a commercially available quad-serpentine flow field, and then after transferring to a cell having the optimized flow field. By design, the gas flow distributions should be significantly more uniform in our new optimized flow field. As Figure 7 shows, there is also better performance in the high current density regime, as expected due to the operating principle of the new flow field.

Nanostructured Catalyst Process Scale-Up

A key aspect of demonstrating an integrated MEA manufacturing process has been development of a single pass, dry web coating process for generating the nanostructured catalyst support films with their catalyst coating. This overall process involves several separate sub-processes, which previously were done individually. Reduced cost and improved yields are greatly facilitated by sequentially carrying out these individual process steps during a single web coating run. This year significant progress was made on demonstrating a single pass pilot process with online control of the nanostructured support films. Scanning electron microscopy (SEM) imaging allows off-line characterization of the catalyst coated support films to document the nanostructured element feature dimensions, number density, and geometric surface area as a function of cross-web and down-web position. Figure 8 shows SEM cross-sectional and plan view images of Pt-coated nanostructured features at 50, 125, and 240 ft respectively, down-web of a single pass 250-lineal-ft coating run. The nanostructured support whiskers are essentially identical both cross-web and down-web. Twelve nominally identical coating runs have been completed for statistical characterization of this integrated process.

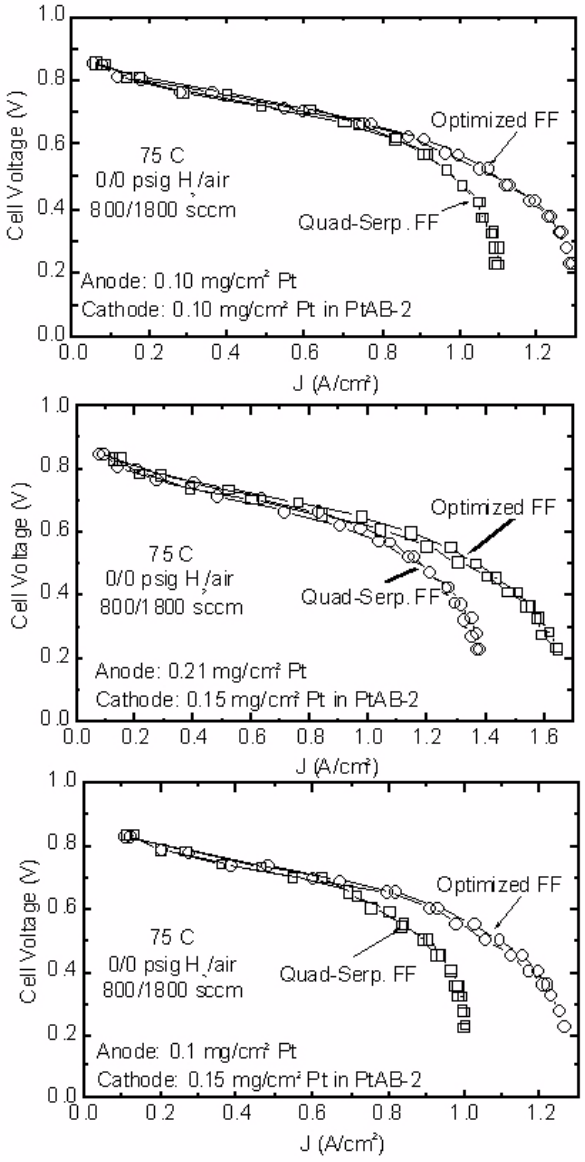

Figure 7. Comparison of PDS-CF polarization curves from three MEAs, each evaluated first in the standard quad-serpentine flow field, and

Stack Testing

The MEAs fabricated with the matched components and integrated manufacturing processes are to be evaluated in a 1-kW stack at the subcontractor's facilities. Development of the stack with the proprietary flow fields is being done at 3M

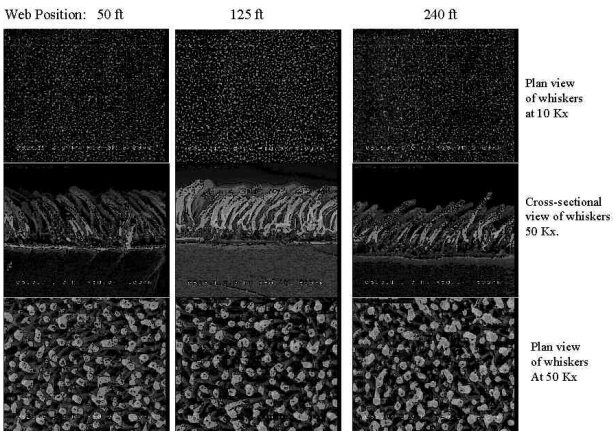

Figure 8. Scanning electron micrographs of the nanostructured catalyst support films at beginning (50 ft), middle (125 ft) and end (240 ft) locations of a 250-lineal-ft pilot scale run in which the support films were produced in a single pass, dry process.

with consultation from the subcontractor. The first H_2/air tests with 200-cm^2 MEAs incorporating the new cathode ternary catalysts and optimized EB/GDL were started on June 28, 2002, in this first stack and currently show excellent cell-to-cell uniformity.

Conclusions

Significant progress has been made in all aspects of the objectives of developing high performance, matched PEM fuel cell components and integrated pilot manufacturing processes. Results to date indicate that, with the new ternary cathode catalyst, the potential is good for meeting the project performance objectives on hydrogen air in a 1-kW stack while exceeding the precious metal loading targets. Similarly, the progress on development of the integrated manufacturing processes indicates the potential for meeting volume and quality objectives. Future work includes finishing the generation of multiple lots of roll-good fabricated CCM and subsequent characterization and fuel cell testing to determine the statistical variance of the processes, completion of a similar fuel cell evaluation of the EB/GDL roll-good media, and completion of the 1-kW stack development and testing of the pilot manufactured MEAs at the subcontractor facilities.

References

1. FY 2001 Progress Report for Fuel Cells for Transportation, page 113.

IV.D.4 Design and Installation of a Pilot Plant for High-Volume Electrode Production

James Arps (Primary Contact)
Southwest Research Institute
P.O. Drawer 28510
San Antonio, TX 78228-0510
(210) 522-6588, fax: (210) 522-6220; e-mail: jarps@swri.org

DOE Technology Development Manager: JoAnn Milliken
(202) 586-2480, fax: (202) 586-9811, e-mail: JoAnn.Milliken@ee.doe.gov

DOE Technology Development Manager: Valri Lightner
(202) 586-0937, fax: (202) 586-3237, e-mail: Valri.Lightner@ee.doe.gov

ANL Technical Advisor: Thomas Benjamin
(630) 252-1632, fax: (630) 252-4176, e-mail: Benjamin@cmt.anl.gov

Subcontractors: General Motors, Warren, MI; W.L. Gore and Associates, Inc., Elkton, MD

Objectives

- Demonstrate proofs of concept for the large-scale preparation of high performance electrodes for membrane electrode assemblies (MEAs) and assess electrode and MEA architecture against FreedomCAR cost targets.
- Design, build, and install equipment for a high-volume pilot plant capable of catalyzing tens of thousands of square meters of electrode material per year.
- Complete process development and qualification of the pilot plant.
- Benchmark MEAs fabricated at SwRI against commercially available products.
- Incorporate MEAs into two ”short stack” fuel cells built by General Motors and deliver to Argonne National Laboratory for testing and evaluation.

Approach

- Prepare MEAs using ultra-low load Pt and Pt-alloy deposition technologies that exceed DOE 2005 precious metal loading targets, and test the MEAs under hydrogen-air and reformate-air operating conditions.
- Determine the impact of large-scale catalyzation methods on MEA performance, if any, and develop approaches to minimize them.
- Establish *in situ* process control methods for catalyst deposition and demonstrate high-efficiency metal recovery approaches.
- Complete equipment shakedown and initiate regular operations at the pilot plant.
- Fabricate sufficient ultra-low load MEAs from catalyzed electrode material for incorporation into two short stacks.

Accomplishments

- Completed construction, acceptance testing, installation, and shakedown of pilot manufacturing system at SwRI.
- Catalyzed several thousand square feet of anode and cathode electrode materials at feed rates up to 40 feet per minute using the pilot system.
- Confirmed that materials manufactured using the pilot system exhibit similar performance to electrodes catalyzed on a laboratory scale.
- Developed robust, off-line methods for spot-checking loading and uniformity of catalyzed material.
- Fabricated more than fifty 800-cm^2 MEAs to date as part of the development effort for the GM stacks.

Future Directions

- Complete trials to optimize electrode catalyzation rates, catalyst utilization, material throughput, and production yield.
- Continue efforts to optimize catalysts for improved CO tolerance and long-term durability.
- Complete fabrication of hydrogen-air and reformate-air MEAs for GM stacks.
- Assemble, test, characterize, and deliver stacks to Argonne National Laboratory.

Introduction

Broad commercial acceptance of fuel cell technology for use in automotive applications is expected to require a fuel cell stack that meets FreedomCAR target costs of $35/kW by 2010. One of the most critical components impacting overall system performance and economics is the membrane electrode assembly (MEA). It is anticipated that the MEA must be available for less than $10/kW in order to meet these overall cost targets. Central to achieving these economics is the reduction of the amount of precious metal catalyst in the MEA, specifically platinum (Pt) and related alloys such as Platinum Ruthenium (Pt-Ru), without degrading power density or system longevity. To this end, a target of 0.2 g per rated kW or approximately 0.1 mg/cm^2 total platinum loading in the MEA has been established for 2010.

Work at Southwest Research Institute (SwRI) has been directed at addressing this issue through the development of large-area, high-throughput, vacuum-based coating technologies to reduce the overall precious metal content of finished electrodes. Specifically, "ultra-low" Pt and Pt-Ru catalyzed electrodes with loadings of 0.10 mg/cm^2 or less have been fabricated using state-of-the art electrode substrates procured from W.L. Gore and Associates. A pilot manufacturing facility has now been completed which has the capability to catalyze more than 100,000 square meters of electrode material per year on a two-shift basis – enough to allow the fabrication of MEAs for potentially several thousand fuel cell-powered vehicles.

Approach

The centerpiece of this project, a highly automated system for catalyzing fuel cell electrode materials, was installed in April; acceptance testing was completed in May 2002. A photograph of the system in operation is shown in Figure 1. In general, the system has performed to design specifications, with material feed rates up to 40 feet per minute having been demonstrated in recent trials at precious metal deposition rates of ~0.02 mg/cm^2/sec. Cycle time from loading of a roll of electrode material to catalyzation and removal is typically less than 2 hours. Additional features of note include the ability to account for and adjust to changes in the material such as splices, wrinkles, and edge shifts, and the incorporation of removable, recyclable shielding that should allow for the recovery of more than 90% of any unused catalyst.

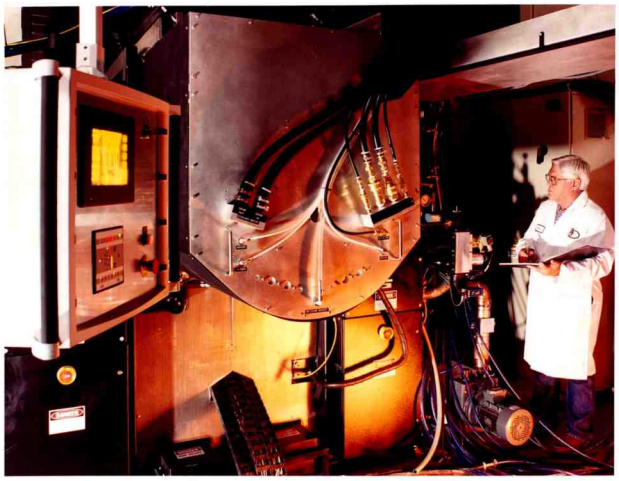

Figure 1. Photograph of Pilot System

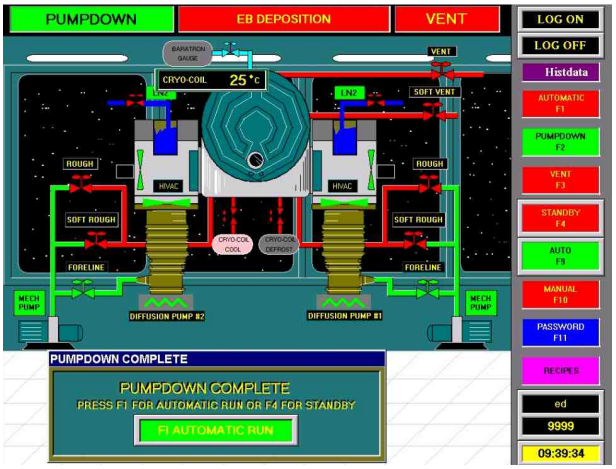

Figure 2. Sample Control Screen

One of the control screens developed for the system is illustrated in Figure 2. Notable data acquisition and control features include fully computerized, touch-screen control of the entire process sequence, including one-touch pump down, automated run, and vent cycles.

Data logging of all critical deposition and vacuum system parameters is available to ensure optimal run-to-run quality control, correlate material and system performance, and assess long term machine stability.

Several thousand linear feet of additional intermediate electrode material has been supplied by Gore over the past year for use with this system

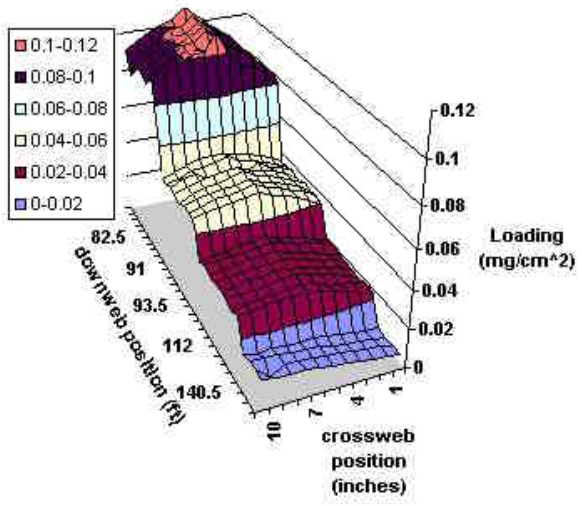

Figure 3. Catalyst Loading Contour Plot at Different Deposition and Feed Rates

during extensive production optimization trials. Pilot quantities of catalyzed electrode material, up to 500 linear feet per run, have been prepared and evaluated using standardized test methods. A hand-held spectrophotometer has also been implemented for rapid inspection of catalyst loading and uniformity (few seconds per point). A section of electrode material intentionally catalyzed at different platinum loadings from approximately 0.01 to 0.10 mg/cm^2 is presented in Figure 3. The catalyst uniformity is better than +/-10% both parallel and perpendicular to the machine direction.

Small scale (25-100 cm^2 active area) MEAs have been fabricated using electrode materials with the pilot system. Sample MEAs have been test evaluated in both hydrogen-air and simulated reformate-air with 10-50 ppm CO at H_2/air stoichiometries of 1.2/2.0 and 2.0/3.5 at pressures ranging from ambient to 30 psig. MEAs tested on hydrogen-air have produced beginning-of-life performance in the range of ~200 mA/cm^2 at 0.8 V and ~700 mA/cm^2 at 0.7 V at a total loading of ~0.1 mg Pt/cm^2. MEAs tested on reformate (40% H_2)-air have generated initial current densities in the range of up to ~150 mA/cm^2 at 0.8 V and ~500 mA/cm^2 at 0.7 V at a total loading of ~0.2 mg Pt/cm^2. Given the particularly good performance on neat H_2 at ultra-low loadings, it was agreed that two smaller stacks, ~10 kW each, optimized to run on neat hydrogen and

Figure 4. Photograph of a General Motors "Short" Stack that Will Utilize SwRI-Manufactured MEAs

reformate, respectively, would be constructed with MEAs fabricated at SwRI as the final deliverables for the project. Figure 4 is a photograph of a GM stack similar to the ones scheduled for construction.

Conclusions

The primary objective, construction and demonstration of a pilot-scale system for catalyzing ultra-low load electrodes for polymer electrolyte fuel cells, has been achieved. The system has nominally met major design targets for material feed rates and catalyst deposition rates. It is estimated that, in two-shift operation, the system is capable of catalyzing sufficient electrode material to fabricate stacks for as many as 10,000 vehicles. MEAs fabricated with electrodes produced by this system significantly exceed 2005 FreedomCAR targets for catalyst loading and approach the requirements set for 2010. Continued work is planned to further optimize material throughput, yield, and catalyst utilization on the pilot system. Additional efforts to evaluate the performance of SwRI-manufactured MEAs at higher CO concentrations and over longer durations are also anticipated.

IV.D.5 Integrated Manufacturing for Advanced Membrane Electrode Assemblies

Emory S. De Castro
De Nora N.A., E-TEK division
39 Veronica Ave
Somerset, NJ 08873
(732) 545-5100 ext 114, fax: (732) 545-5170, e-mail: emory.decastro.etek@denora.com

Mark G. Roelofs
DuPont Company
Chestnut Run
Wilmington, DE
(302) 695-7342, fax: (302) 695-2503, e-mail: mark.g.roelofs@usa.dupont.com

DOE Technology Development Managers:
Valri Lightner: (202) 586-0937, fax: (202) 586-3237, e-mail: Valri.Lightner@ee.doe.gov
JoAnn Milliken: (202) 586-2480, fax: (202) 586-9811, e-mail: JoAnn.Milliken@ee.doe.gov

ANL Technical Advisor: Thomas Benjamin
(630) 252-1632, fax: (630) 252-4176, e-mail: Benjamin@cmt.anl.gov

Subcontractors: DuPont Company, Wilmington, DE; Nuvera Fuel Cell, Cambridge, MA; Northeastern University, Boston, MA

Objectives

- Create improved cathode structures and catalysts for proton exchange membrane fuel cells (PEMFCs) at temperatures <100°C that allow a significant reduction of precious metal without loss in performance
- Discover and develop proton exchange membranes (PEMs) capable of extended fuel cell operation at higher temperatures of 120 to 150°C, at low relative humidity (RH), and without leachable components
- Incorporate the advances of the efforts described above with advanced MEA fabrication processes that are amenable to mass production

Approach

- Fabricate highly controlled gas diffusion layers through fine gradient machine coating methods; exploit a new structure-function approach to designing improved catalysts and catalyst alloys
- Investigate additives to extend the stable performance of Nafion® membranes to 120°C; create a new class of ionizable materials that enable proton transport in the absence of water (150°C operation)
- Develop new machine-based or ion beam coating methodologies to create very low loaded precious metal MEAs

Accomplishments

- Identified a preparation for platinum on carbon black catalyst that provides ~60% reduction in precious metal grams/kW compared to current commercial preparations
- Established “proof of principle” for catalyst structure-function approach

- Set up basis for constructing fine-gradient ELAT® materials
- Developed a new base material into a gas diffusion layer (GDL) with lower resistance and improved mass transport at high current density
- Synthesized and screened approximately twenty electrolyte and monomer compounds for high temperature membranes
- Identified several model liquid electrolytes with >100 mS/cm conductivity at 150°C and low RH
- Fabricated a candidate composite membrane with 60% increase in conductivity vs. Nafion® N117 at 120°C and low RH

Future Directions

- Further develop catalyst structure-function approach and implement to create designed catalysts with anticipated reduced metal loads
- Link ink morphology to GDL structure; establish relationship between GDL structure and FC performance; build fine gradient ELAT® with increased precious metal (PM) utilization
- Continue exploration of alternate polymeric backbones and acid groups (high temperature membrane)
- Create and test hypotheses as to required functionality and utilize these to narrow and focus the synthetic effort (high temperature membrane)
- Evaluate FC lifetime and performance of benchmark Nafion® and candidate membranes (high temperature membrane)

Introduction

A significant challenge for PEMFC technology is precious metal thrift and creating new ion exchange membranes that are capable of stable operation at temperatures exceeding 120°C and preferably 150°C. The greatest barrier to reduction of platinum metal in the MEA is due to the cathode half reaction. For membranes to operate at over 120°C, a new class of materials employing alternative proton transport mechanisms is necessary. Current platinum or alloy catalysts have a distribution of crystal facets, and some of these crystal planes exhibit higher activity for oxygen reduction. If one could selectively synthesize catalysts with a greater number of the desired planes, a more potent catalyst would result. However, advances in catalyst structure are not enough; the utilization of the catalyst and also proton and oxygen transport must improve to realize the full potential of the activity and ultimately reduce PM loading. Proton and oxygen transport may be improved through the realization of a fine gradient structure for the GDL. A satisfactory answer to these technical challenges would reduce the barrier to commercialization by reducing precious metal cost, allow a significant reduction in heat exchangers, and provide a vast simplification for systems operating with hydrogen derived from hydrocarbon sources.

Approach

A series of innovative catalyst preparation techniques has been identified. Each technique is surveyed, and the resulting catalyst is subjected to electrochemical and spectroscopic evaluation. Spectroscopic data are reintegrated in a sophisticated computer model that allows detailed bulk structural information to be derived. For this modeling, the methods are ranked according to the likelihood of selectively fabricating highly active crystal faces. Thus, the model provides a link to design catalysts based on a structure-function approach.

For the fine-gradient ELAT®, we first establish the relationship between ink formulation parameters and how they impact key architectural quantities such as pore size distribution and hydrophobicity. Next, the architectural quantities are linked to actual fuel cell test results. Finally, fine gradients of porosity and hydrophobicity are constructed using the relationship(s) previously established.

For high temperature membranes, three avenues are being pursued: a) synthesis of new ionomers, b) covalent modification of Nafion®, and c) polymer-inorganic composites. Some of the approaches aim to increase the attractive forces holding water within the membrane, enabling operation at low RH. Others seek to embody Brønstead bases as an alternative to water, which allow for proton mobility in the absence of water. This mechanism is exemplified by proton conductivity in e.g. H_3PO_4 or $CsHSO_4$, in which the protons hop and the protonated base need not move macroscopic distances.

Results

A summary of catalyst synthesis methods investigated for both activity and potential to control the crystal face population(s) is shown in Table 1. Of these, the methodology indicated as "Shows Promise" appears to provide a wide range of structures over only a moderately small range of tested parameters. Due to this unexpected result, additional efforts were directed to this method.

Catalyst	Pt on carbon	Alloys on carbon
Organic Method	XXX	XX
Controlled Environment	⊕	---
Simultaneous vs. Sequential	NA	XX
New Carbons	⊕	---
Temperature	⊕	---

Key	Symbol
Preliminary Evaluation	⊕
Shows Promise	XXX
Interesting Results	XX
No Potential	X
Not Evaluated to date	---
Not Applicable	NA

Table 1. Methods Evaluated to Control Crystal Face Population

Table 2 summarizes some preliminary results in testing these new platinum catalysts. Using our rapid catalyst screening protocol (70°C, 43 psig cathode, 36 psig anode), we record a reduction in precious metal usage of around 60% as measured by power.

Preparation Method	"High Efficiency Hydrogen" at 0.8V	"Reformate Target" at 0.75V
Commercial	4.25 g/kW	2.84 g/kW
Organic Method	1.76 g/kW	1.02 g/kW
Percent Reduction in PM	59%	64%

Table 2. Comparison of "Organic Method" Platinum on Carbon Black vs. Commercial Catalyst (cathode metal only)

In developing the fine-gradient ELAT®, one activity is incorporating new carbon cloth or paper materials as the support web for the microporous carbon black/catalyst coatings. Figure 1 shows the consequences of converting a new type of web to the ELAT® configuration. We were able to build an assembly with lower overall electrical resistances that can facilitate transport at high current density.

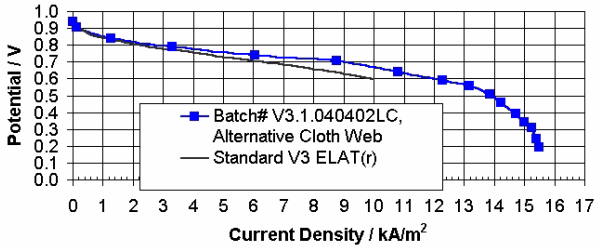

Figure 1. Evaluation of Alternative Web (Cathode/ Anode: 1.5 Bar A, 70°C; Anode hydrator T = Cathode hydrator T = Cell: 70°C)

An example of the process behind building a GDL is shown in the metrics of Figure 2. Here we are evaluating a 2 x 2 matrix of formulation (1 and 2) vs. coating method (A and B), and plotting the total solids deposited on the web versus the position of the layer. In addition to the differences in deposition rate listed here, most notable is the instability induced at the fifth position for Formulation 1, Coating method

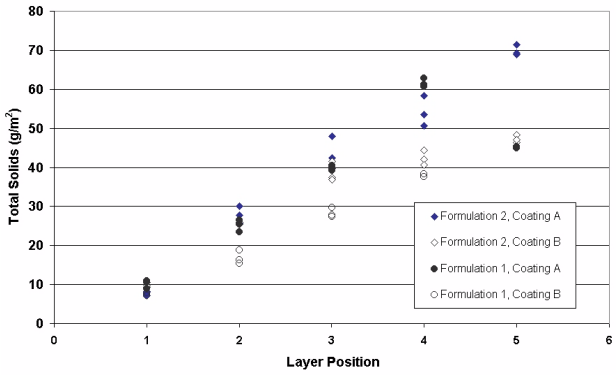

Figure 2. Comparison of Formulations and Coating Parameters

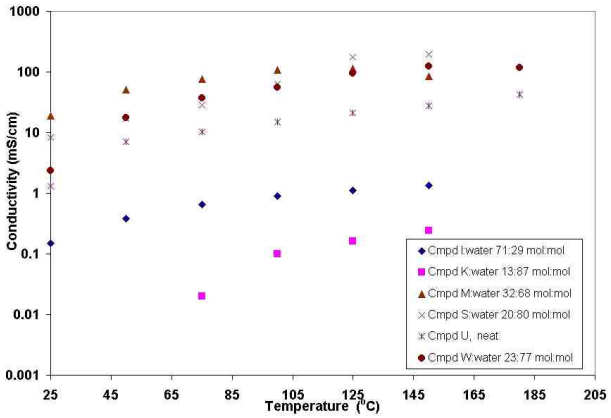

Figure 3. Conductivity vs. Temperature

A: instead of a linear increase in solids, we actually start to remove solids under these conditions. In addition to solids, we also measure through-plane conductivity, permeability, and numerous other characteristics as a function of the position in the gradient. The correlation of these characteristics to the formulation morphology is the goal of these experiments.

A series of model electrolyte compounds and monomers has been synthesized with the aim of understanding which functionalities can engender conductivity at low RH for high temperature membranes. The working hypothesis is that ionomers are in general less conductive than their constituent monomers, so that chemistries may be screened using model compounds prior to investment in polymer synthesis and membrane fabrication. A cell was constructed of quartz, ceramic, PTFE, and Pt materials, allowing measurement of the conductivity of 800 microliter liquid samples at temperatures up to 200°C. Conductivities of several liquid organic electrolyte model compounds are shown in Figure 3, with a few samples attaining 50 to 200 mS/cm at 150-180°C. The water contents indicated are the starting compositions and are chosen to correspond to significantly lower water contents (acid:water mole:mole) than is required by Nafion®. Though water vapor pressure was not explicitly controlled, the cell was not pressurized and the water vapor partial pressure was less than 1 atm. The maximum conductivity, followed by a decrease in conductivity at higher temperatures, observed for some samples is believed to be due to evaporation of water.

Compound U is one of the very few electrolytes investigated in which the neat liquid without added water generates appreciable conductivity. For comparison, the conductivity of Nafion® 117 membrane was measured as 7 mS/cm at 150°C and a water vapor partial pressure of 1.1 atm (23% RH).

The electrolytes investigated so far cover a range of aliphatic and aromatic compounds, fluorinated and non-fluorinated, with sulfonic and non-sulfonic acid groups. Our challenge now is to learn to incorporate these acid functionalities into ionomers without losing the conductivity as they are diluted and immobilized with polymer scaffolding.

Another potential method for achieving a high temperature membrane utilizes composites of ionomers with hydrophilic inorganic compounds. The desire is for the inorganic compounds to alter the microstructure of the ionomer, perhaps by holding open the ionic pores or by increasing the attractive force with which the water is held in the membrane. A further function of the filler is to decrease the creep of the ionomer and prolong membrane life. The most promising results have been obtained with an ionomer/inorganic composite membrane, where the conductivity at 120°C, 23% RH has been increased from ~5 mS/cm for N117 to ~9 mS/cm (Table 3). The goal resistance of 0.1 ohm cm^2 would, however, require 50 mS/cm, assuming a 50 micron thick membrane. Thus, we still need a much larger increase in conductivity to achieve very thin membranes.

Conclusions

Although quite early in our program, the use of the structure-function approach for catalyst design has yielded great improvements to the platinum on carbon black design. The further development of this methodology, when combined with the anticipated increase in performance of the fine-gradient ELAT®, should result in greatly enhanced cathode structures for normal temperature operation (up to 100°C).

For the high temperature membrane, achieving high conductivity at low relative humidity is one of the most challenging requirements. However, given that low resistance is the germane need, low conductivity may be ameliorated with very thin membranes. If such a compromise proves necessary, it will then place the onus back on achieving excellent puncture, creep, and fuel permeation properties. Our future path includes work to further increase conductivity and to incorporate the existing liquid electrolyte leads into ionomers without losing the conductivity as they are made into solid membranes.

Membrane	Conductivity (mS/cm)		
	@ 80°C, 95% RH	@ 80°C, 20% RH	@ 120°C, 23% RH
N117, sample 1	86	3.3	4.5
N117, sample 2	85	5.5	6.1
Candidate V, sample 1	89	5.8	10.0
Candidate V, sample 2	105	4.3	8.4

Table 3. Conductivities measured with AC-impedance, 4-point probe for N117 and a candidate composite membrane. Metered dry air and water are mixed in a vaporizer then fed to a pressurized flow cell in an oven. The 80°C, 95% RH data are for membranes which had been previously exposed to low RH. Freshly-boiled expanded membranes which have not been exposed to low RH give much higher conductivities of the order of 180 mS/cm @80°C, 95% RH.

IV.D.6 Development of High Temperature Membranes and Improved Cathode Catalysts

Dr. Shari Bugaj (Primary Contact)
UTC Fuel Cells
195 Governor's Highway
South Windsor, CT 06074
(860) 727-2808, fax: (860) 727-2750, e-mail: Shari.Bugaj@utcfuelcells.com

DOE Technology Development Manager: Valri Lightner
(202) 586-0937, fax: (202) 586-3237, e-mail: Valri.Lightner@ee.doe.gov

Main Subcontractors:
High Temperature Membrane
Virginia Polytechnic Institute and State University (Virginia Tech), Blacksburg, Virginia
Pennsylvania State University, University Park, Pennsylvania
Stanford Research Institute International, Menlo Park, California
IONOMEM, Marlborough, Connecticut
Princeton University, Princeton, New Jersey
Cathode Catalysts
Northeastern University, Boston, Massachusetts
University of South Carolina, Columbia, South Carolina
United Technologies Research Center, East Hartford, Connecticut
Case Western Reserve University, Cleveland, Ohio

Objectives

- Develop and demonstrate an advanced polymeric membrane able to operate at near ambient (1-1.5 atmospheres) pressure in the temperature range of 120~150^{o}C and able to meet DOE's program goals for performance.
- Develop and demonstrate improved high-concentration platinum (Pt) cathode catalysts that will enable the reduction of Pt loading to 0.05 milligrams per centimeter squared (mg/cm^2) and meet DOE's goals for performance.

Approach

- Phase 1: High Temperature Membranes (HTMs) and improved Pt catalysts will be synthesized, characterized and compared with issued specifications.
- Phase 2: Laboratory-scale catalyst-coated membranes (CCMs) will be fabricated, optimized and tested using the Phase 1 down-selected membranes and catalysts.
- Phase 3: Full-size CCMs with the down-selected and optimized HTMs and catalysts will be fabricated and tested in two individual multi-cell stacks.

Accomplishments

- This project was initiated during the first quarter of 2002. Eight out of the nine subcontractors have initiated membrane and catalyst synthesis. Technical accomplishments for the four months since the initiation are given below.
- At Virginia Tech., high yields (>80%) of 3,3'-disulfonate, 4,4'-dichlorodiphenylsulfone were obtained by sulfonating commercially available monomers. Films (>40,000 molecular weight) drawn from these co-monomers showed negligible degradation in boiling water and acceptable proton conductivity at room temperature in water.
- United Technologies Corporation Fuel Cells (UTCFC) has developed and applied a new and novel in-situ electrochemical technique to quantify hydrogen crossover in membranes.
- High-concentration (40 weight percent [wt%]) ternary Pt alloy samples prepared using the carbothermal technique have yielded surface area and activity values comparable to commercial Pt samples. Platinum/Carbon (Pt/C) prepared by pulse-electrodeposition showed superior surface area and activity when compared to direct current deposited Pt/C electrodes.

Future Directions

- Continue polymer synthesis and evaluation of the fabricated films per membrane screening specifications. Initiate the fabrication of initial promising candidates into CCMs.
- Continue evaluation of Pt catalysts being synthesized using the colloidal sol, carbothermal and the electrodeposition techniques and compare results against catalyst screening specifications. Debug rotating disk electrode technique.

Introduction

Two main challenges in the PEMFC arena are the reduction of cathode Pt loading and development of membranes that can operate over 120^{o}C. Surmounting these two challenges will directly affect the cost, performance and the size of PEMFC stacks. On the HTM project, new polymeric materials with negligible thermal degradation and acceptable proton conductivity in the 120-150^{o}C range are required. On the improved catalyst project, a combination of higher activity catalysts and thinner catalyst layers is required to achieve the aggressive DOE performance targets.

Approach

To develop HTMs, UTCFC has teamed with research groups that possess competencies in the fields of polymer chemistry and engineering. The subcontractors on the HTM project are investigating modified Nafion® and new non-Nafion® based membrane systems (see Table 1). The subcontractors on the improved catalyst project and their individual approaches are given in Table 2.

Table 1. High Temperature Membrane Program Approach

Group	Principal Investigator	Approach
IONOMEM	Mr. Leonard Bonille	Hygroscopic solid ion conductor (e.g., zirconium phosphate, etc.) filled Nafion®
Penn State University	Prof. Digby Macdonald	Sulfones and sulfoxides of aromatic PPBP and aliphatic PVA. Covalent sulfonic acid bonded PEEK, PBI and PPBP
Princeton University	Prof. Andrew Bocarsly	Layered sulfonated Polystyrene/Fluoropolymer system
Stanford Research Institute	Dr. Susanna Ventura	Sulfonated PEEK-PBI-PAN
Virginia Tech	Prof. James McGrath	Sulfonated Poly(arylene ether sulfone)

Results

This project was initiated during the first quarter of 2002. Since then, all the subcontractors have hired appropriate personnel and initiated membrane/catalyst synthesis. A majority of the required processes are in place, and eight of the nine

Table 2. Advanced Cathode Catalyst Program Approach

Group	Principal Investigator	Approach
North Eastern University (NEU)	Prof. Sanjeev Mukerjee	Micellar Pt nano cluster synthesis, colloidal sol synthesis of binary Pt alloys
University of South Carolina (USC)	Prof. Branko Popov	Pulse electro-deposition of Pt and Pt alloys on Carbon [Pt and Pt-X, X=Fe, Ni, Co, Mn, Cu]
UTC Fuel Cells	Dr. Shari Bugaj	Carbothermal synthesis of ternary Pt alloys [Pt-Ir-X and Pt-Rh-X, [X=Ni, Co and V]]
Case Western Reserve University (CWRU)	Prof. Al Anderson	Quantum chemical modeling of Pt alloys and ORR
UT Research Center (UTRC)	Dr. Ned Cipollini	Reproducible and stack size CCM fabrication

subcontractors have reported preliminary results. At Case Western, the catalyst modeling work will start in September 2002, when Dr. Jerome Roques will start as a post doctoral associate. Some of the preliminary results obtained during the past four months are presented here.

High Temperature Membranes

To measure the gas crossover in HTMs, UTCFC developed a new in-situ electrochemical test. The test involves oxidizing the hydrogen that is transported across the membrane and measuring the limiting currents. Typical crossover limiting currents for two membranes of different thicknesses are depicted in Figure 1.

At VirginiaTech, 3,3'-disulfonate, 4,4'-dichlorodiphenylsulfone co-monomers with varying degrees of sulfonation were prepared from commercially available monomers. Nuclear magnetic resonance (NMR) spectroscopy was conducted on selected polymeric films to investigate the level of sulfonation. The NMR results showed that the sulfonation levels could be quantified very accurately. The water uptake of bi-phenol sulfone (BPSH) films increased with an increase in the degree of sulfonation. The membrane samples drawn from BPSH40 with 20, 30 and 40 K molecular

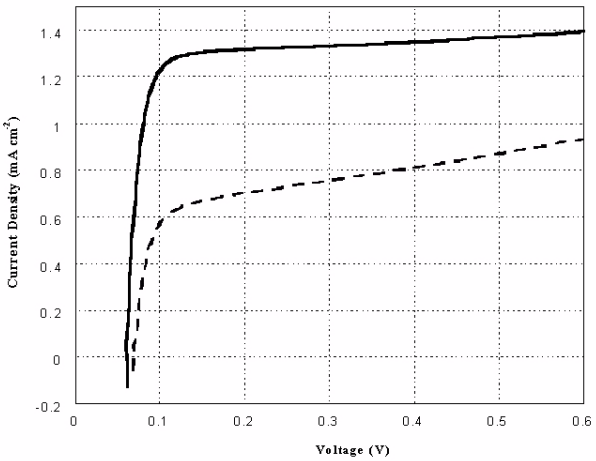

Figure 1. In-situ Limiting Hydrogen Crossover Currents for Two Membranes of Different Thicknesses

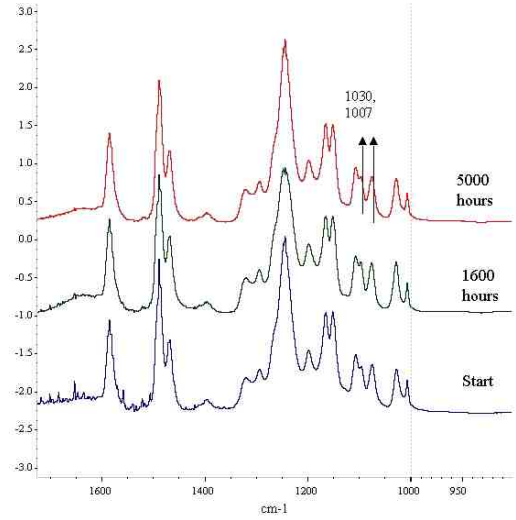

Figure 2. Influence of Hot Water Soxhlet Extraction on the FTIR of Sulfonated Poly(arylene ether) Copolymers BPSH40

weights showed proton conductivity values on the order of 0.09 S/cm. To evaluate the thermal degradation of the polymers, BPSH40 films were exposed to boiling water extractions using the Soxhlet technique in conjunction with Fourier transform infrared (FTIR) spectroscopy. The spectra were collected as a function of exposure time (see Figure 2). As seen from the figure, there is negligible change in the spectra up to 3,500 hours,

indicating that the hydrolytic stability of the films is excellent. No noticeable change in the nature or the ion exchange capacity of the membrane was noted during the Soxhlet experiment.

Penn State has modified electrochemical instrumentation that operates above 100°C. The accuracy of the instrumentation was confirmed by Nafion® 117 characterization. Princeton has initiated the synthesis of laminar membranes and anticipates initial characterization results on these materials over the next quarter. IONOMEM possesses a HTM that was shown to operate at 120°C prior to the start of this program. Since the initiation of this program, IONOMEM's efforts have been focused on electrode structure and catalyst modifications to establish a performance base.

Advanced Cathode Catalysts

UTCFC has modified the carbothermal synthesis process (U.S. Patent 4,677,092, US 4,806,515, US 5,013,618, US 4,880,711, US 4,373,014, etc.) to prepare 40 wt% ternary Pt alloy catalysts. Various high-concentration Pt catalyst systems were synthesized and the electrochemical surface area (ECA) and electrochemical activity values compared to commercially available catalysts (see Table 3). The UTCFC catalysts showed ECA and activity values comparable to the commercial catalysts. A rotating disk electrode technique for catalyst activity measurements has been developed and is currently being debugged at UTCFC.

Table 3. Preliminary ECA and Activity Data of Synthesized Pt Alloys

Catalysts	Catalysts ECA (m^2/Pt)	Catalyst Activity (A/gPt)
Commercial 50% Pt/C	98	25.1
Comercial 50% PTFE/C alloy	63	37.7
40% PT/Carbon C	110	27
40% $Pt_{50}Ir_{23}Co_{25}$	75/62	33
40% $Pt_{50}Ir_{23}Ni_{25}$	60	23

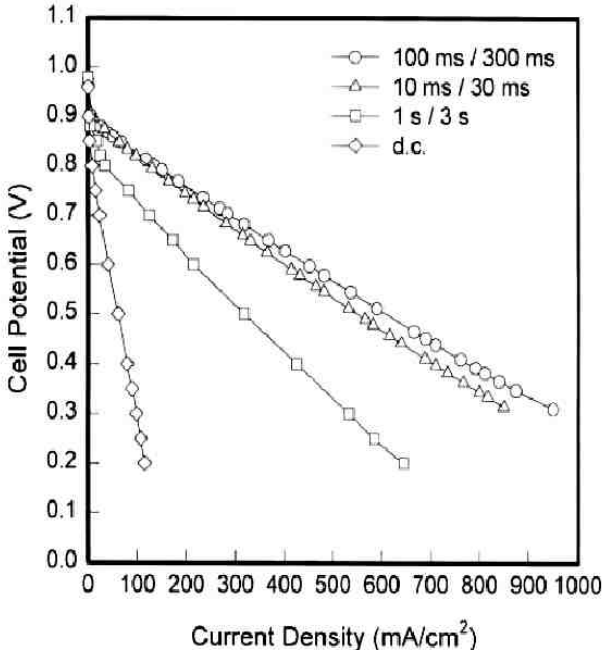

Figure 3. Polarization Curves at 50 milliamps/cm^2 and Duty Cycle of 0.25

At the University of South Carolina, Pt/C electrodes were fabricated by using direct current (DC) and pulse current electrodeposition methods. With the use of current pulses rather than DC, a higher deposition current density could be used and Pt deposits with a higher surface area were possible. Figure 3 compares the polarization performance of electrodes prepared by pulse electrodeposition (current density=50 mA/cm^2 and duty cycle=0.25) and DC deposition. Electrodes fabricated under pulse deposition conditions display better performance than the DC-plated electrode. The best performance is obtained when the ON time is 100 ms and OFF time is 300 ms.

At NEU, a series of electrocatalysts were synthesized based on classical colloidal sol synthesis techniques. These included platinum nickel/carbon (PtNi/C), platinum chromium/carbon (PtCr/C), and platinum cobalt/carbon (PtCo/C) together with the control Pt/C. All of the above electrocatalysts were prepared with 20% metal loading on carbon support (Vulcan XC-72, Cabot Corp). Ohmic corrected Tafel

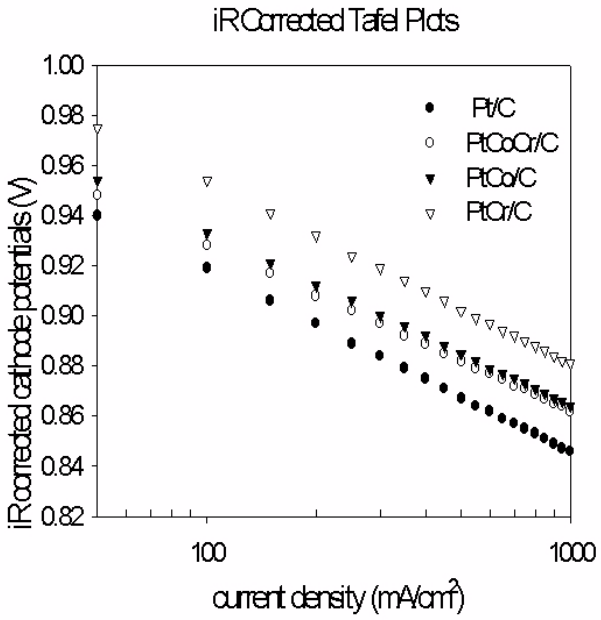

Figure 4. Ohmic Corrected Tafel Plots for Oxygen Reduction on Pt and Pt Alloy Electrocatalysts Prepared at Northeastern (note that PtCr/C is a system being considered only for ORR fundamentals; it will not be under consideration for down-selection)

plots for PtCr/C, PtCo/C, PtCoCr/C and PtNi/C are shown in Figure 4. As seen from the figure, the alloy catalysts are inherently more active than the Pt/C control. The data shows a lowering of the overpotential for oxygen reduction by up to 50 millivolts. At a potential of 0.9 volts, this translates to an eight-fold enhancement in oxidation-reduction reaction (ORR) activity. Stability and surface analysis of the Pt alloys was also performed using x-ray techniques.

Conclusions

The project is in its early stages and processes are in place for making progress. Preliminary results show that the HTM team is ramping up by initiating polymer synthesis processes and also by modifying instrumentation to perform high temperature measurements. On the advanced catalyst program, Pt and Pt alloys prepared using the colloidal sol, carbothermal and pulse electrodeposition processes are being characterized and compared with commercial Pt catalysts.

References

1. S. Kocha, P.Plasse, L.Onishi, D. Wheeler, J. Bett, AIChE Spring Meeting Proceedings- Fuel Cell Technology: Opportunities and Challenges, March 10-14, 2002, New Orleans.

IV.D.7 High-Temperature Membranes

Thomas A. Zawodzinski (Primary Contact), Hayley Every
Department of Chemical Engineering
Case Western Reserve University
Cleveland, OH 44106
(216) 368-5547, fax: (216) 368-3016, e-mail: taz5@po.cwru.edu

Michael Eikerling, Lawrence Pratt, Antonio Redondo, Tom Springer, Judith Valerio, Francisco Uribe, Michael Hickner and Tommy Rockward
Los Alamos National Laboratory
Electronic and Electrochemical Materials and Device Research Group
Los Alamos, NM 87545

DOE Technology Development Managers:
JoAnn Milliken: (202) 586-2480, fax: (202) 586-9811, e-mail: JoAnn.Milliken@ee.doe.gov
Nancy Garland: (202) 586-5673, fax: (202) 586-9811, e-mail: Nancy.Garland@ee.doe.gov

Objectives

- To develop new membranes and membrane electrode assemblies (MEAs) for operation at temperatures substantially in excess of 120°C

Approach

- Simultaneously carry out R&D on:
  - Physical chemistry of polymer electrolytes
  - New polymeric electrolytes
  - New approaches to proton transport in polymer electrolytes
  - Development of MEAs based on new polymer electrolytes

Accomplishments

Physical Chemistry

- Computational studies revealed key intermediate states in proton transfer processes; showed that water plays a role in 'bridging' and organizing acid groups to facilitate proton transfer

New Membranes

- Synthesized new polymers with higher acidity
- Developed several strategies targeting 'water replacements'

Catalyst-Coated Membranes (CCMs)/Electrodes

- Successfully fabricated MEAs for one class of new membrane materials; achieved performance comparable to that of Nafion-based MEAs

Industrial and Other Collaborative Interactions

- Worked directly with several university partners in developing and testing high-temperature membranes
- Assisted DOE industry partners in CCM development for high-temperature membranes

- Developed draft Roadmap for High Temperature Polymer Membranes
- High-Temperature Polymer Membrane Working Group (HTPMWG) was expanded and strengthened through several meetings

Future Directions

- Perform more extensive computational studies on novel systems
- Continue to develop methods for screening new membrane concepts at a higher rate; test new electrolytes in fuel cells on a 4 month cycle starting in the fall of 2002
- Expand initial tests on enhancing electrode performance; develop capability for probing oxidation reduction reaction (ORR) at temperature ex situ; develop understanding of interactions at buried interfaces within electrodes
  - Develop reliable CCM fabrication approaches
  - Continue to develop means for scale-up of polymers, film-making and CCM production to modest scale
- Industry and Other Collaborations
  - Continue to make industrial and academic contacts from Case Western Reserve University (CWRU) to enable technology transfer and dissemination of ideas
  - Organize the HTMWG (streamline funding mechanism, improve meeting scheduling); evolve toward a discussion group format, idea exchange

---

Introduction

The need to operate at temperatures exceeding 100°C presents difficult new challenges for the polymer electrolytes used in fuel cells. This difficulty stems from the decrease in water content of the polymer electrolytes in the desired temperature range. There is a need for detailed understanding of the impact of poor or zero hydration on membrane and electrode processes in the fuel cell. Water plays a key facilitating role in proton transport; thus, lower water content leads to lower conductivity. Lack of water also has important negative consequences for electrode behavior.

Approach

At this point, we do not know which of several approaches is most promising. Thus, our membrane development efforts involve (1) a full-fledged effort to explore approaches involving polymer synthesis and development, as well as implementation of new "carrier" media to replace the function of water in Nafion, and (2) a study of proton transfer dynamics. We are using theoretical approaches to explore specific possibilities for new acid group types or for acid-base interactions that could lead to progress in proton transfer media. We are also working to establish better understanding of the energetics of proton transfer to inform synthetic efforts. We also are working to incorporate new polymers in fuel cells by developing catalyst-coated membranes from the new materials. Finally, we have assisted DOE in setting up a range of polymer electrolyte development efforts, involving several universities and with significant industrial input.

Results

Physical Chemistry

As a starting point for our efforts, proton solvation and transfer in water-containing polymer electrolytes will provide some clues on critical steps in the approach. We are studying the energetics and dynamics of these processes. The tools we develop allow us to compare strengths of various target acids and assess the efficacy of water 'replacements.' We continue to expand the range of acid types studied as hydrates using density functional computational methods. These studies give us insight into the relative importance of solvation and dissociation

processes for various highly delocalized anions. The most interesting work this year used a sophisticated *ab initio*/molecular dynamics method to identify some surprising aspects of the proton transport dynamics. Specifically, we found that sidechain-to-sidechain hopping of protons could occur, albeit with the 'cooperation' of certain water configurations bridging between sidechain groups. This finding is highly suggestive regarding possible water replacements and their structural requirements for facilitating proton transport.

Additional work is underway to use computational methods to (i) tailor bases to mimic water, perhaps using substituted imidazoles or other proton carriers; (ii) understand proton transport in phosphoric acid/basic polymer systems; and (iii) augment other experiments on new polymers and additives of various types.

New Membranes

Three classes of membrane materials are presently in preparation and testing. These are (i) polymers and inorganic materials with controlled pore size to be modified with acid groups lining pores, (ii) polymeric systems with intrinsically stronger acid groups, and (iii) polymer systems swollen or imbibed with tailored proton acceptors. These are useful both intrinsically and as test or model systems. At least two more types of materials are 'on the drawing board.' Details of our ideas and approaches will be provided as the materials are tested later this year.

CCMs

We are forming CCMs from new polymers, often with radically different properties than those to which we are accustomed. Observed difficulties in achieving good performance with new CCMs stem from processes occurring at several different length scales:

- Macro scale (CCM level): adhesion phenomena, polymer segregation in catalyst layer, mechanical properties of electrode and membrane
- Meso scale (agglomerate level): mass transport of gases, continuous proton and electron conducting pathways
- Nano scale (local level): proton accessibility to site, electrocatalysis, polymer adsorption, polymer mobility

We have successfully catalyzed the Virginia Tech membranes and obtained performance comparable to that obtained with Nafion membranes of comparable thickness. Results are shown in Figures 1 and 2. The importance of these results lies in our ability to overcome difficulties inherent in catalyzing many of the emerging new membranes. Achieving good performance required some treatment of the CCM under operating conditions in the cell. The cells thus prepared appear to be robust in lifetests over hundreds of hours.

A more fundamental problem that arises in the high temperature regime is the necessity of good proton accessibility to electrodes. Many new polymer types proposed involve a sulfonated aromatic polymer. Microelectrode studies of the ORR on such materials indicate a significant loss of activity with decreasing water content in the polymer, far exceeding that observed with Nafion. This is likely due to the lower acidity of the aromatic sulfonates compared with that of the perfluorinated material. Our best results to date have been obtained using Nafion as the ionomer in the cathode catalyst layer.

We are actively studying the impact of the range of environments local and corresponding different

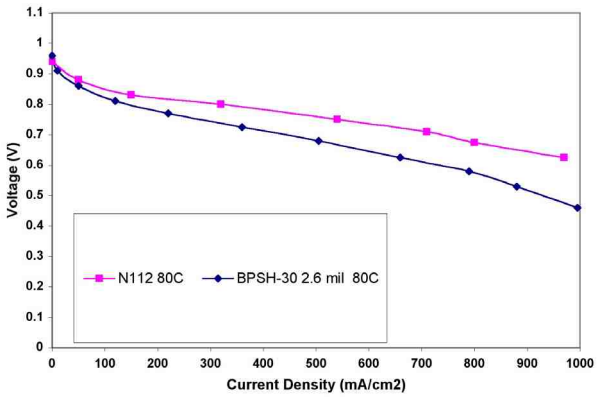

Figure 1. Polarization curves showing comparison of performance at 80°C of CCMs prepared from Nafion 112 and biphenyl sulfone (BPSH-30, 2.6 mil thick) membranes. Catalyst loading: 0.2 mg/cm^2 Pt anode, 0.4 mg/cm^2 cathode.

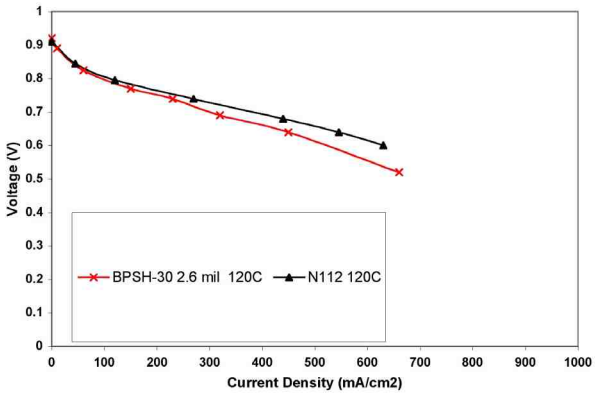

Figure 2. Polarization curves showing comparison of performance at 120°C of CCMs prepared from Nafion 112 and BPSH-30 (2.6 mil thick) membranes. Catalyst loading: 0.2 mg/cm^2 Pt anode, 0.4 mg/cm^2 cathode.

degrees of proton access to surface. Given the constrained dynamics of the polymer system, acid access to the catalyst surface is a key issue. Various additives, such as low molecular weight acids, have been and are being used to augment catalyst layer acidity and the mobility of acidic groups. Results to date have been inconclusive.

Industrial and Other Collaborative Interactions

We are engaged in a series of collaborative efforts with industry, national laboratories, and universities to facilitate efforts to achieve the targets for high-temperature polymer membranes. We have organized the High-Temperature Polymer Membrane Working Group, which has met four times to date. Bi-annual meetings allow us to assess progress and to communicate issues and needs to the high-temperature membrane community at large.

Conclusions

The development of new polymer electrolytes for operation at elevated temperature is under way. However, this is a long-term project. Replacement of water is the most difficult problem, but adequate stability and cathode activity are not trivial objectives to achieve. We have developed several different approaches to address this problem. Fundamental work, including computational and experimental studies of new acid-functionalized materials, can provide useful insights into the conduction process to guide synthetic efforts. The first polymers geared for temperatures in excess of 100°C are emerging, and testing is showing that, although promising, there are definite shortcomings. Work on making viable new materials continues.

IV.D.8 Bacterial Cellulose Membranes

Hugh O'Neill (Primary Contact), Barbara R. Evans, and Jonathan Woodward
Chemical Sciences Division, Oak Ridge National Laboratory
P.O. Box 2008
Oak Ridge, TN 37831-6194
(865) 574-5004, fax: (865) 574-1275, e-mail: oneillhm@ornl.gov

DOE Technology Development Managers:
JoAnn Milliken: (202) 586-2480, fax: (202) 586-9811, e-mail:JoAnn.Milliken@ee.doe.gov
Nancy Garland: (202) 586-5673, fax: (202) 586-9811, e-mail: Nancy.Garland@ee.doe.gov

ORNL Technical Advisor: David Stinton
(865) 574-4556, fax: (865) 241-0411, e-mail: stintonp@ornl.gov

Objectives

- To synthesize a low cost proton conductive membrane from bacterial cellulose for polymer electrolyte membrane (PEM) fuel cells.
  - This membrane must be stable at temperatures greater than 120^{o}C.
  - It must maintain the conditions conducive to proton conductance from the anode to the cathode through the polymeric medium, while operating at high temperatures. The area specific resistance must be no greater than 0.1 ohm-cm^2.

Approach

- Bacterial cellulose has several properties that have been identified as useful for PEM fuel cell development, including thermal stability and low hydrogen crossover characteristics.
- Bacterial cellulose membranes were modified with acid groups to produce a proton conductive membrane without compromising the structure of the cellulose membrane.

Accomplishments

- Different strategies to confer ion-exchange properties on bacterial cellulose were investigated. The synthesis of a cellulose phosphate membrane was the most successful.
- Several properties of the cellulose phosphate membrane were evaluated, including hydrogen crossover, ion-exchange capacity and thermal stability.

Future Directions

- Complete the characterization of phosphate membranes, especially the determination of the proton conductivity of the membranes.
- Test the performance of ion-exchange membranes in a membrane electrode assembly (MEA).
- Revisit and evaluate other strategies for chemical modification of cellulose.
- Modify cellulose *in vivo* by using activated glucose monomers.

Introduction

Bacterial cellulose is produced by *Gluconoacetobacter sp*. bacteria during growth on carbohydrate sources. Nascent cellulose strands, synthesized by the bacteria, are secreted and form layers at the air-liquid interface (Figure 1A, 1B). This network of cellulose fibrils resembles a sponge and is called a pellicule. After cleaning to remove cellular debris, the pellicule typically contains greater than 99% H_2O, the remainder being cellulose. On drying the pellicules to remove water, the layers of cellulose collapse on top of each other to produce a very thin membrane (< 50 μm thick).

Of particular interest to the DOE fuel cell program is the development of thermostable membranes that will facilitate the transfer of protons from the anode to the cathode during operation of a PEM fuel cell at high temperatures (>120^{o}C). At higher operating temperatures, the electrode kinetics is improved, resistance to poisoning by carbon monoxide is increased, and the catalyst cost is minimized. In addition, higher operating temperatures would facilitate the thermal management of the system and stack.

Bacterial cellulose has several unique properties that potentially make it a valuable material for the development of PEM fuel cells (Reference 1): (1) it is an inexpensive and non-toxic natural resource; (2) it has good chemical and mechanical stability; (3) it is very hydrophilic; and (4) it doesn't re-swell after drying. Additionally, its thermal stability and gas crossover characteristics are superior to Nafion 117®, a material currently widely used as a proton conductive membrane in PEM fuel cells.

Approach

There is a wealth of data, both in the scientific and patent literature, on the chemical modification of plant cellulose. All of these methods are equally applicable to bacterial cellulose given that the two types of cellulose are chemically identical. However, it is the physical structure of bacterial cellulose membranes that make them a potential material for PEM fuel cells. Therefore, the aim is to modify bacterial cellulose pellicules in a manner that retains the structure of the cellulose and does not compromise the physical properties, such as thermal stability, gas crossover characteristics, and resistance to re-swelling after drying.

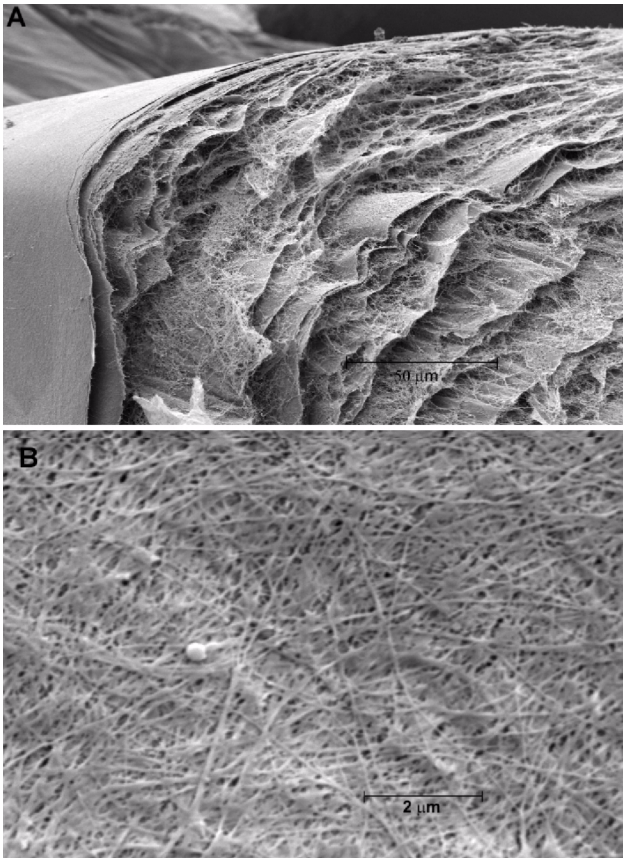

Figure 1. SEM Micrographs of Freeze Dried Bacterial Cellulose (A: transverse section, B: top view)

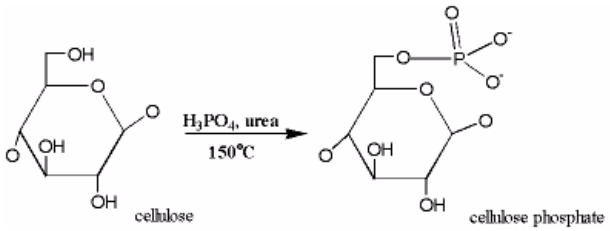

Figure 2. Synthesis of Cellulose Phosphate

Results

Several different strategies were employed to modify bacterial cellulose with ion-exchange groups. Of the methods attempted, modification of native bacterial cellulose with phosphate groups was the most successful (Figure 2). The properties of the

Membrane Characteristics		Native Cellulose	Cellulose Phosphate	Nafion 117®
Physical Properties	Dry membrane thickness (mm)	0.010	0.023	0.199
	Wet membrane thickness (mm)	0.032	0.081	0.225
	H_2O content / g dry membrane (g/g)[1]	3.47	3.16	0.31
	Thermal stability (^oC)	130	245	<90
	Ion exchange capacity (mequiv/g)	0	1.3	0.9
	H_2 crossover (nmol.mil/h.cm^2.atm)[2]	n.d.	267.2	2039.4
Mechanical stability	Resistance to crease/crack: dry	Yes	No	Yes
	hydrated	Yes	Yes	Yes
	Resistance to tearing: dry	No	No	Yes
	hydrated	Yes	Yes	Yes
	Resistance to gas pressure (dry)	n.d.	30 psi	>50 psi
Chemical stability	Acid stability (% weight loss)[3]	12	39	2.5

Table 1. Comparison of the Properties of Cellulose Phosphate with Native Bacterial Cellulose and Nafion 117®

native and modified membrane compared with Nafion 117® are presented in Table 1.

Thermogravimetric analysis of cellulose phosphate in an oxygen atmosphere indicated that it started to degrade at 245°C, compared to less than 90°C for Nafion 117®. This marked increase in the thermal stability of cellulose phosphate over native cellulose was not unexpected given that this material was first developed as a flame retardant. Cellulose phosphate has only 13% of the H_2 permeability of Nafion. Unlike Nafion, cellulose phosphate is prone to swelling in H_2O. However, at temperatures greater than 120^{o}C this may not pose a problem during operation of the fuel cell. The density of ion-exchange groups available for proton transport is similar in both materials. The superior mechanical properties of Nafion are most probably due to the difference in thickness between the materials.

The acid stability of the cellulose phosphate membrane was determined at 95^{o}C in 1N sulfuric acid. After 45 hours cellulose phosphate lost 39% of its original weight. This increase in sensitivity to acid attack is most probably an artifact of the reaction conditions employed in the synthesis. Modifications on the reaction procedure will be investigated to minimize this unwanted side reaction.

Conclusions

Several properties of cellulose phosphate have been evaluated. The material has good thermal stability and low hydrogen crossover, two requirements that are important to meet DOE fuel cell program targets. Further characterization of the material is required, especially the determination of proton conductivity. In addition, testing of the material in an MEA will allow the effect of acid stability and swelling properties of cellulose phosphate be evaluated under typical PEM fuel cell operating conditions.

References

1. O'Neill, H., Evans, B.R., and Woodward, J. (2001) in Fuels Cells for Transportation Annual Progress Report pp 141-145

Publications/ Presentations

1. Evans, B.R., O'Neill, H., Malyvanh, V.P., Woodward, J. "Palladium-bacterial cellulose membranes for fuel cells" Biosensors and Bioelectronics, submitted

2. O'Neill, H., Evans, B.R., and Woodward, J. (2002) "Bacterial Cellulose in Energy Conversion Applications" A poster presentation at the 24th Symposium on Biotechnology for Fuels and Chemicals, April 28th to May 1st, Gatlinburg, TN.

3. O'Neill, H., Evans, B.R., and Woodward, J. (2002) "Micro-fuel cell development based on bacterial cellulose" An oral presentation at the 14th World Hydrogen Conference, June 9th- 13th, Montréal, Canada.

Special Recognitions & Awards/Patents Issued

1. Evans, B.R., O'Neill, H., Malyvanh, V.P., and Woodward, J. (2001) "Metallization of bacterial cellulose for electronic and electrical devices" Patent Pending ID 0869, S-96, 631

2. O'Neill, H., Evans, B.R., and Woodward, J. (2002) "Synthesis of a novel ion-exchange/ proton conductive membrane" Invention disclosure, submitted ID 1099, S-99, 279

IV.D.9 Nano-particulate Porous Oxide Electrolyte Membranes (POEMs) as Proton Exchange Membranes

M. Isabel Tejedor, Marc A. Anderson, and Walt Zeltner
Environmental Chemistry and Technology Program, University of Wisconsin
Room 109, 660 North Park Street, Madison, WI 53706
(608) 262-2674, fax:(608) 262-0454, e-mail: nanopor@facstaff.wisc.edu

Mark A. Janney and James O. Kiggans
Metals and Ceramics Division, Oak Ridge National Laboratory
P.O. Box 2008, MS 6087, Oak Ridge, TN 37831-6087
(865) 574-8863, fax:(865) 574-8271, e-mail: kigganssjo@ornl.gov

DOE Technology Development Manager: JoAnn Milliken
(202) 586-2480, fax: (202) 586-9811, e-mail: JoAnn.Milliken@ee.doe.gov

ORNL Technical Advisor: David Stinton
(865) 574-4556, fax: (865) 241-0411, e-mail: stintondp@ornl.gov

ANL Technical Advisor: Thomas Benjamin
(630) 252-1632, fax: (630) 252-4176, e-mail: benjamin@cmt.anl.gov

Objectives

- Develop microporous inorganic oxide-based membranes of TiO_2 with high proton conductivity that can operate at above 100°C with minimal water management problems.
- Develop processes to fabricate porous nickel or graphite paper electrodes that support the membrane.
- Demonstrate fuel cell behavior in porous oxide electrolyte membrane- (POEM-) based membrane electrode assemblies (MEAs).

Approach

- Phase 1: (a) Determine conditions under which nanoparticle sols of candidate oxides yield microporous gels; (b) Measure proton conductivities of these gels as a function of temperature and relative humidity; (c) Chemically adsorb anionic or cationic functional groups onto oxide particles contained in xerogels or membranes in order to enhance proton conductivity.
- Phase 2: (a) Develop methods for depositing platinum on asymmetric mesoporous electrodes; (b) Deposit crack-free films of POEMs on mesoporous electrodes; (c) Characterize permeabilities of H_2 and O_2 through the resulting supported membranes under desired conditions of relative humidity and temperature; (d) Fabricate and test an entire inorganic MEA containing a POEM deposited on mesoporous electrodes.

Accomplishments

- Demonstrated proton conductivity of 0.022 S/cm in POEMs (membranes <1 μm thick) at temperatures up to 135^{o}C at a relative humidity (RH) of 81%.
- Better defined the effects of pore size and pH on proton conductivity in POEMs.

- Collected initial data concerning open circuit potential and current-voltage relationships for an oxide-based anode/POEM configuration (i.e., 2/3 of an MEA). (Pt loading in anode = 0.003 mg/cm^2)

Future Directions

- Develop a better understanding of the relationships and interactions among the various layers in the MEA (particularly the cathode layer) and how they control the performance of the overall fuel cell system.
- Characterize and subsequently optimize the performance of fuel cells that contain POEMs.
- Develop testing techniques for measuring proton conductivity at temperatures approaching 150°C at ≥ 40% RH.
- Investigate POEMs using the nickel substrate as the support for the cathode instead of the anode in an inorganic MEA.
- Further develop graphite fiber paper supports as a potential substitute for nickel substrates.

Introduction

Nano-particulate porous oxide electrolyte membranes (POEMs) are being developed as a radical alternative to polymeric proton exchange membranes (PEMs) for fuel cells. These new membranes can operate at temperatures over 100°C, retain water at these elevated temperatures, and provide proton conductivities of the same order of magnitude as the presently employed Nafion membranes. In addition, inorganic membrane electrode assemblies (MEAs) that incorporate POEMs should reduce the cost of fuel cells by substantially reducing the amount of Pt catalyst required to operate the fuel cell, and by minimizing CO poisoning of the Pt and facilitating heat rejection when operating at elevated temperatures.

One constraint in using POEMs is that they must be supported on a structural substrate because the membranes are thin (≤ 500 nm), porous (~40 vol% void space), and brittle (an inherent property of ceramic membranes). The porous substrate provides both electrical conductivity and gas distribution. Because the POEM itself is composed of 5-10 nm particles, an intermediary sandwich layer (particle diameter 50 to 500 nm) is required to provide geometric compatibility.

These membranes are made of nanoparticle oxides, which represent hydrophilic, higher temperature alternatives to polymeric proton exchange membranes (PEMs). These membranes are supported on either tape cast porous nickel or porous graphite paper electrodes – to date, we have only examined the porous nickel supports.

Approach

The objective of this effort is to develop MEAs for H_2 fuel cells based on POEMs. These membranes are made of nanoparticle oxides such as TiO_2, SiO_2, ZrO_2, or Al_2O_3 that are hydrophilic and offer higher temperature stability and operation than polymeric PEMs. These membranes are supported on tape cast porous nickel.

The POEM MEA is a complex materials system, not just a collection of individual components. This oxide-based MEA (anode / membrane electrolyte (separator) / cathode) is a composite material that simultaneously performs a variety of operations. One cannot consider any particular aspect of this materials system in isolation; all functions must operate in concert with one another. The anode must conduct electrons and at the same time convert hydrogen gas to protons at one interface with the POEM. The POEM itself must conduct protons but not electrons, which would cause a short, while also preventing crossover of hydrogen and oxygen across the POEM. Lastly, the cathode must convert gaseous oxygen to O^{-2} ions that then combine, at the other interface with the POEM, with protons that have migrated through the POEM. This cathode reaction is

a four-electron-transfer reaction that is quite difficult to perform efficiently. More will be said about the cathode layer and reasons for improving its performance later in this report.

Results and Discussion

Membrane Development – pH Effects

Proton conductivity in fluid-filled, hydrophilic, mesoporous, inorganic membranes such as these POEMs derives from the movement of H^+ ions (1) by hopping along surface sites from particle to particle, (2) by migrating through the electrical double layer in the pores near the surface of the particles, or (3) by migrating through the bulk pore fluid. As shown in Figure 1, proton transport and the resulting conductivity drastically change with the pH at which the membrane is equilibrated. Note that "Nafion" type membranes are often soaked in strong acids to protonate their acid groups. In this regard POEMs are similar, although full protonation of the surfaces of these inorganic membranes may be reached at higher pH values than required for Nafion.

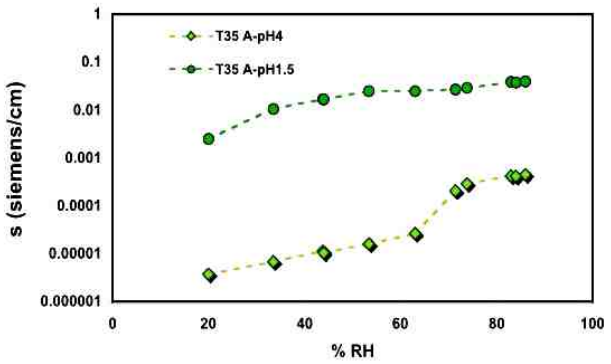

Figure 1. Dependence of Proton Conductivity on pH at 40°C

This behavior also greatly depends upon the nature of the oxide as shown in Figure 2. Note that at lower relative humidities, TiO_2/ZrO_2 and Al_2O_3 membranes have conductivities that are two to three orders of magnitude higher than SiO_2 even though the silica membranes are more acidic. The reason for this behavior is that these membranes were preequilibrated at pH 1.5. This pH is very close to the isoelectric pH (i.e., the pH at which the surface of the oxide is electrically neutral) of SiO_2, which is ≈ 2-3, but 4 to 7 pH units more acidic than the isoelectric

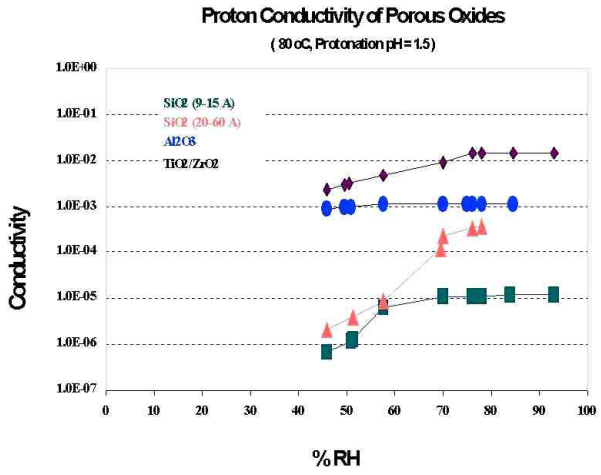

Figure 2. Proton Conductivity (in S/cm) for Various Oxides as a Function of Relative Humidity at 80°C [diamonds are TiO_2/ZrO_2, ovals are Al_2O_3, triangles are SiO_2 (20-60 A), squares are $Si0_2$ (9-15 A)]

pH values of TiO_2/ZrO_2 and Al_2O_3, respectively. As a result, the SiO_2 membranes are NOT highly protonated at pH 1.5 whereas the other two membranes have almost achieved maximum charging and therefore maximum proton conductivity.

Membrane Development – Pore Size Dependence

The conductivity of a particular membrane depends on the conditioning of the surfaces within the pores as well as the relative humidity. These two factors interact to determine how much water resides inside the pores. In the as-fired condition, the pore surfaces are poorly protonated. Conditioning the membrane material by exposing the membrane to an aqueous solution tends to increase the degree of protonation depending on the pH of the solution, as noted above. However, as can be seen in Figure 3, proton conductivity for TiO_2 at 40°C also depends upon pore size, increasing one order of magnitude at low RH values as pore diameter decreases from 35 to 25 Angstroms. We can lower the pore size in this membrane even further to ca. 15 Angstroms, which may further enhance its proton conductivity.

Initial Evaluation of an Inorganic MEA

Because these POEMs are not self-standing materials like organic polymer membranes such as

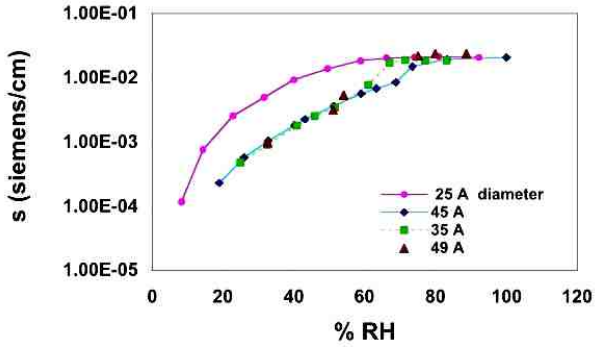

Figure 3. Dependence of Proton Conductivity on RH for Various Pore Size TiO_2 Membranes

Nafion, an MEA cannot be fabricated unless the membranes are cast on a rigid but porous support. Furthermore, the support must be electrically conducting and must already be coated with a porous catalyst layer before the membrane is cast. The resulting composite MEA will be activated by imbibing an acid solution into the MEA before it is used.

Enable Fuel Cell Corp. (Middleton, WI) fabricated a passive test chamber to evaluate the performance of the materials. For these initial room temperature tests, we fabricated 2/3 of an inorganic MEA (i.e., porous nickel support / nanoparticle TiO_2 membrane loaded with Pt catalyst to serve as one electrode / TiO_2 POEM). We used a carbon fabric loaded with Pt as the second electrode. We ran the inorganic MEA as either an anode or a cathode depending on the polarity of the test circuit. When hydrogen contacted the inorganic MEA (i.e., the MEA was operated as a working anode), we achieved open circuit voltages between 0.74 and 1.02 V. When the inorganic MEA was operated as a cathode, we obtained slightly lower voltages (0.76 – 0.88 V).

Unfortunately, it was difficult to seal the cell to prevent hydrogen leaks. In addition, it was difficult to test individual layers of the MEA system because the carbon fabric glued itself to the inorganic MEA and could not be detached without delaminating the MEA. To resolve these issues, we built a new test cell, as shown in Figure 4. As shown, the MEA is now sealed in a metal "O" ring using ceramic cement. This cell proved to be easily sealed without

Figure 4. Teflon Test Cell and the Inorganic MEA System

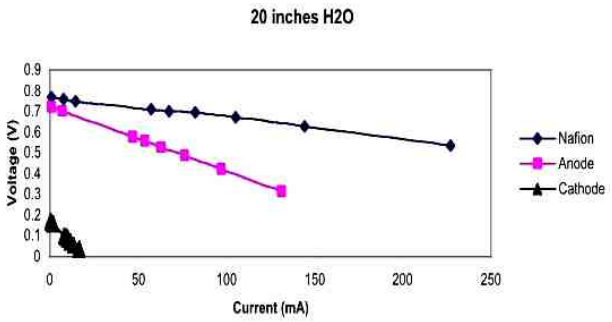

Figure 5. Current-Voltage Curves for the Inorganic MEA versus a Nafion System

hydrogen leaks and, furthermore, it could be readily disassembled. However, we still need to improve the ohmic contacts to the anode and cathode layers. We utilized copper wool to provide contacts in this apparatus. However, copper wool easily oxidizes when in contact with acids and does not provide a uniform contact with the electrodes.

Test Performance

Shown in Figure 5 are initial current-voltage curves for the 2/3 of an inorganic MEA system described above versus a similar Nafion-based system in tests at room temperature. As can be seen, the Nafion system performs somewhat better than our initial prototype when the inorganic MEA operates as an anode. When we invert the contacts so that the inorganic MEA operates as a cathode, the inorganic MEA system performs much worse. A positive side to this performance is that the Pt content of the inorganic MEA is 0.003 mg/cm^2.

Cathodes and the Total MEA

Shown in Figure 6 is a diagram of a nickel support and a Pt-loaded nanoparticulate oxide acting as a porous cathode. Organic-based fuel cell cathodes often have some Nafion added to improve proton conductivity but at the cost of electrical conductivity. However, we have the reverse problem – we have excellent proton conductivity in the inorganic cathode, but the oxides are electrical insulators. We need to boost the electrical conductivity of the cathode in order to fabricate a total inorganic MEA. This is a major objective of our future work.

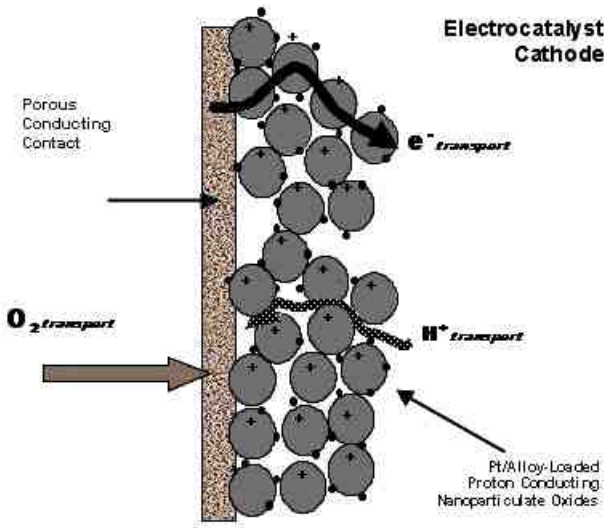

Figure 6. Diagram of an Inorganic Fuel Cell Cathode

Conclusions/Future Directions

- We have successfully fabricated and tested 2/3 of an inorganic MEA consisting of a porous nickel support, a nanoparticle TiO_2 membrane containing platinum catalyst that served as an effective anode, and a nanoporous TiO_2 porous oxide electrolyte membrane. A novel test cell was built to facilitate testing, but additional modifications are needed. Although the performance of this prototype inorganic MEA was not as good as a corresponding Nafion-based system at room temperature, the inorganic MEA required only a small amount of platinum to function. In order to prepare this inorganic MEA, a novel method had to be developed for applying a ceramic sandwich layer to the porous, electrically conducting nickel substrate. This method should be useful in other membrane applications.
- Efforts will continue to fabricate a full inorganic MEA and to test these systems at high temperatures. It appears that a functional inorganic MEA will require a cathode with higher electrical conductivity than available in our initial tests. In addition, we are attempting to develop a graphite fiber-based substrate having the requisite chemical compatibility with the PEM environment. As part of this development, POEM fuel cell assembly using standard, multilayer manufacturing technologies will be investigated.

FY 2002 Publications/Presentations

1. Results were presented at the national meeting of the American Institute of Chemical Engineers in New Orleans in March 2002.

IV.D.10 Low-Platinum Catalysts for Oxygen Reduction at PEMFC Cathodes

Karen Swider Lyons (Primary Contact), Gregory B. Cotten, and Jason A. Stanley
Naval Research Laboratory
Code 6171
4555 Overlook Ave, SW
Washington, DC 20375-5342
(202) 404-3314, fax: (202) 767-3321, e-mail: karen.lyons@nrl.navy.mil

Wojtek Dmowski and Takeshi Egami
Department of Materials Science and Engineering
University of Pennsylvania
3231Walnut Street
Philadelphia, PA 19104

DOE Technology Development Managers:
JoAnn Milliken: (202) 586-2480, fax: (202) 586-9811, e-mail: JoAnn.Milliken@ee.doe.gov
Nancy Garland: (202) 586-5673, fax: (202) 586-9811, e-mail: Nancy.Garland@ee.doe.gov

Objective

- Decrease the platinum content of the oxygen reduction reaction catalysts in fuel cell cathodes to meet the DOE 2010 precious-metal-loading goals of 0.2 g/rated kW.
- The new catalysts must cost less than $35/kW and be stable for at least 5000 hours.

Approach

- Low-platinum catalysts are prepared in combination with amorphous, hydrous transition-metal oxides. The catalysts are dispersed in carbon inks, and their electrocatalytic activity is screened in half-cell measurements.
- The physical properties of the catalysts are determined from thermal analysis, surface-area measurements, X-ray photoelectron spectroscopy, and transmission electron microscopy.
- Atomic pair-density function analysis of X-ray diffraction patterns is used to resolve the local structure of the catalysts from 0.15 to 2 nanometers (nm).
- Catalyst performance is confirmed by testing in fuel cells in collaboration with Los Alamos National Laboratory (LANL).

Accomplishments

- Half-cell measurements on catalysts of a Pt-doped iron-oxide phase have approximately 20 times the activity of the standard 10 weight % Pt on Vulcan carbon.
- Pair-density function analysis of X-ray diffraction patterns shows that active iron oxide (FeO_x) catalysts are disordered at the nanoscale by the platinum and also have micropores, while inactive catalysts do not share these features.
- Platinum supported on niobium oxide phases also exhibits high activity for oxygen reduction, despite a 50 to 150 fold decrease in platinum compared to the standard 10 weight % platinum on Vulcan carbon.
- The Pt-loading goals for the DOE 2008 program will be met if the half-cell performance of the new catalysts is matched in fuel cell measurements and the catalysts prove to be stable.

Future Directions

- Correlate the half-cell catalysis results to fuel cell performance.
- Improve corrosion resistance of catalysts.
- Improve activity and test stability of platinum-niobium oxide catalysts.
- Develop Pt-free catalysts by using transition-metal oxide mixtures that mimic Pt performance.
- Develop fuel-cell testing capabilities at the Naval Research Laboratory (NRL).

Introduction

State-of-the-art proton exchange membrane fuel cells (PEMFCs) contain high loadings of Pt, making the fuel cells costly and subject to fluctuations in the market availability of the noble metal. The cost of the fuel cells and imports of noble metals can be drastically reduced by using little or no Pt in fuel cell cathodes. This would improve the commercialization potential of fuel cells.

The catalytic activity of the oxygen reduction reaction (ORR) at the fuel cell cathode is known to be relatively slow, presumably because it is a 4-electron (e^-) mechanism:

$$O_2 + 4H^+ + 4e^- = 2\ H_2O$$

*Note: O_2 = Oxygen gas, H^+ = proton, H_2O = water

The cathode must be catalytically active, and the catalyst site must have a supply of oxygen, protons, and electrons, and must be able to transport away water. The reaction above becomes limited when the transport of any of these four species is slow.

We are designing new low-Pt electrocatalysts for oxygen reduction at PEMFC cathodes. Catalysts are targeted based on their ability to transport the following species: (1) molecular oxygen, (2) protons, (3) electrons, and (4) water. We have selected "amorphous" hydrous oxides with low amounts of platinum to fulfill these transport criteria. All catalysts are transition-metal oxide based, because hydrous transition-metal oxides are good proton and water conductors. Oxides are also less prone to poisoning (electro-chemical activity degradation) than metals, and some mixed-oxide catalysts also have the ability to mimic Pt. Some oxide catalysts may also be resistant to dissolving under the highly corrosive conditions at the PEMFC cathode.

Although the catalysts are termed amorphous, they can have nanoscale order in their atomic structures that can have a significant bearing on their activity and transport properties. These nanoscale structural properties are not easily discerned with conventional materials science tools, but can be elucidated using an emerging technique: atomic pair-density function analysis of X-ray diffraction (PDF-XRD).[1,2]

We analyzed the physical and structural properties of hydrous oxide materials having high ORR activity to determine the factors leading to high-performance PEMFC cathode catalysts. Last year, we reported 20 times the ORR activity per weight Pt when Pt-iron oxide (Pt-FeO_x) catalysts are compared to 10 weight % Pt/Vulcan carbon standards. The nanoscale structural properties that lead to this high activity are reported here.

Approach

Catalyst powders are prepared from aqueous solutions in ambient conditions and then heated at various temperatures to adjust their water contents. The water content of the final materials is determined via thermal analysis.

The catalytic activity of the catalysts for the ORR is screened using a rotating-disk electrode (RDE) method.[3] The activity of the new transition metal oxide catalysts is estimated by comparison to a standard RDE of 10 weight % platinum/Vulcan carbon, XC-72 (Pt/VC) catalyst (Alfa). The electrocatalytic activity of the catalysts are compared in Tafel plots of potential vs. current, calculated from the electrochemical data as described in the literature.

Because conventional structural analysis methods (e.g., X-ray diffraction and transmission electron microscopy) are not effective on amorphous

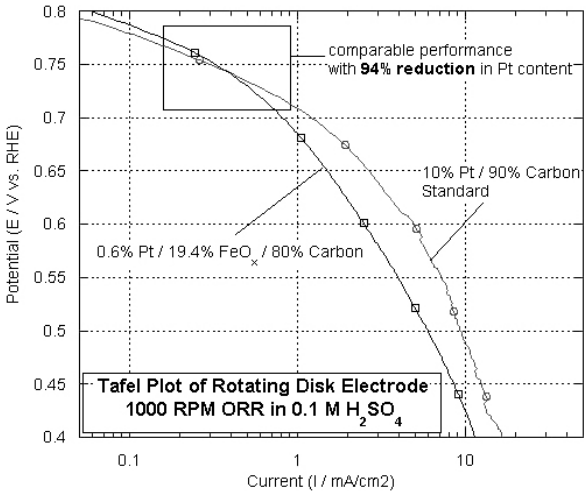

Figure 1. Tafel plot of standard 10% Pt on Vulcan carbon compared to the new catalysts of 20% Pt (~5% Pt-Fe_x) on Vulcan carbon (0.6 weight % Pt total).

Conditions: sweep rate = 10 millivolts; electrolyte: 0.1 M sulfuric acid (H_2SO_4); rotation rate = 1000 rpm; temperature = 60°C. Data from argon gas sweep subtracted from that of O_2 sweep.

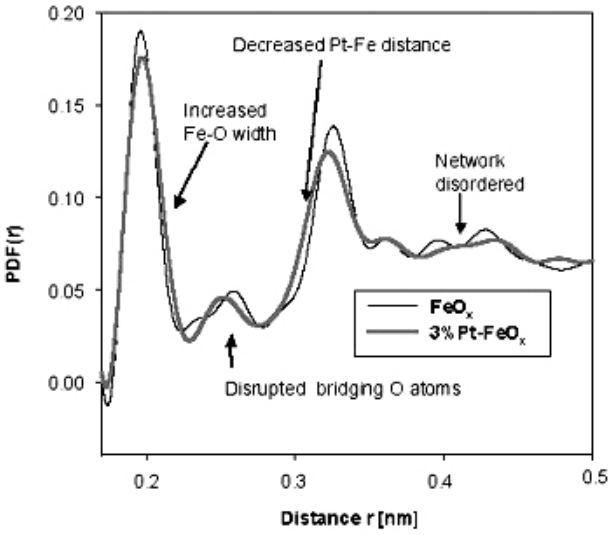

Figure 2. PDF-XRD of 3% Pt-FeO_x vs. FeO_x. The addition of 3% Pt to the FeO_x structure causes four significant changes: (1) an increase in the distance between the iron and oxygen atoms, (2) a decrease between the platinum and iron atoms, (3) disruption of the bridging oxygen, and (4) disorder to the network beyond 0.4 nm.

materials, the nanoscale structures are best resolved via atomic pair-density function (PDF) analysis of the X-ray diffraction patterns of the catalysts. High-energy X-ray diffraction is carried out at beamline X7-A of the National Synchrotron Light Source.

Results

As reported last year, Pt-FeO_x catalysts have the same ORR activity with 20 times less Pt than a 10 weight % Pt/VC standard. These results of an active catalyst are shown in a Tafel plot of current vs. voltage in Figure 1.

The Pt-FeO_x samples with the highest ORR activity are heated at 150°C in air. Samples heated at higher or lower temperatures, or under oxygen, argon or hydrogen have lower electrocatalytic activity. The procedures for adding the Pt to the FeO_x also have a significant impact on their activity.

Conventional XRD measurements show that all of the active and inactive samples are strongly disordered (i.e, amorphous solids or dispersed nanocrystals). However, the PDF-XRD measurements show significant differences between the active and inactive catalysts. When 3% Pt is added to the FeO_x, it distorts the entire FeO_x structure. The PDF-XRD data for a 3% Pt-FeO_x sample is compared to a pure FeO_x sample in Figure 2. The atomic structure of the best performing Pt-FeO_x sample is best described as glassy corner linked polyhedral (CLP) network. A schematic of this structure is shown in Figure 3. The iron (Fe) atoms are coordinated in a tetrahedral oxygen cage. In comparison, the inactive samples do not have this nanoscale structure and are partially crystalline.

The most active samples have only local order (to 1.0 nm) and also have cage-like structures, or ones with micropores. The micropores (sized on the order of 0.4 to 1.0 nm) are likely filled with water or hydroxyl groups and are therefore conducive for proton conduction. The iron in the active samples also exists in mixed valence states, which is likely to contribute to the electrochemical activity of the Pt-FeO_x. Furthermore, the Pt atoms are uniformly distributed throughout the structure.

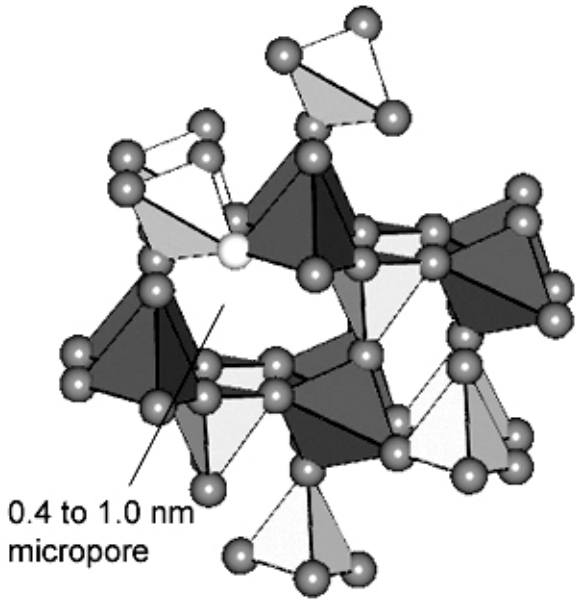

Figure 3. Schematic of a CLP framework. The micropores in the structure are ideal for proton conduction.

The Pt-FeO_x catalysts are not stable to corrosion, as has been confirmed in our laboratory and during fuel cell testing at LANL.

However, we can use our understanding of the Pt-FeO_x materials to design new, stable catalysts. Pt-niobium oxide (Pt-NbO_x) catalysts are currently under development. Preliminary studies show that despite having 150 times less Pt than the 10% Pt/VC standard, the Pt-NbO_x samples have high activity. NbO_x is a more stable oxide than FeO_x, and studies are underway to confirm its long-term activity.

Conclusions

The ORR activity of Pt is greatly enhanced by dissolving it in a matrix that is a good protonic conductor. PDF-XRD structural measurements show that the addition of low amounts of Pt (~3%) to FeO_x can lead to a material with high ORR activity and a unique structure. Active materials are disordered beyond ~1.0 nm and also have micropores. Disruption of the microporous structure causes a decrease in catalyst activity. Although the Pt-FeO_x catalysts are not stable to corrosion, new niobium-based catalysts are being investigated and already show higher stability.

Other transition-metal oxide systems having little or no Pt will continue to be developed. A fuel cell test station is also being acquired by NRL, so that new materials can be tested rapidly and effectively.

If the results from the half-cell measurements are matched in the actual fuel cell operation, the DOE goals to reduce the Pt loading of the fuel cell by 10X by 2008 will be met. The decreased amount of Pt in the fuel cell will also result in a significant decrease in the cost of the PEMFCs.

References

1. K. E. Swider-Lyons, K. M. Bussmann, D. L. Griscom, C. T. Love, D. R. Rolison, W. Dmowski, and T. Egami, in *Solid State Ionic Devices II Ceramic Sensors*, E. D. Wachsman, W. Weppner, E. Traversa, P. Vanysek, N. Yamazoe, M. L. Liu, Editors, The Electrochemical Proceedings Series, Pennington, NJ , 2000, PV2000-32, p. 148.

2. T. Egami, *Mater. Trans.,* 31 (1990) 163.

3. S. Lj. Gojkovic, S. K. Zecevic, and R. F. Savinell, *J. Electrochem. Soc.,* 145 (1998) 3713.

FY 2002 Publications/Presentations

1. K. E. Swider-Lyons, "Mixed-Conducting Oxides in Electrochemical Power Sources," in High Temperature Materials In Honor of the 65th Birthday of Professor Wayne L. Worrell, ed. S. Singhal, The Electrochemical Proceedings Series, 2002, PV 2002-5, p. 124.

2. K. E. Swider-Lyons, "Mixed-Conducting Oxides in Electrochemical Power Sources," Symposium on High Temperature Materials In Honor of the 65th Birthday of Professor Wayne L. Worrell, 100th Meeting of the Electrochemical Society, 12-17 May 2002, Philadelphia, PA.

3. W. Dmowski, T. Egami, K. E. Swider-Lyons, and C. T. Love, "Nanocrystalline or Amorphous? Structure of Hydrous RuO_2 from X-ray Scattering" Conference on Crystal Chemistry of New Materials and Soft Matter Studied by

Synchrotron and Neutron Diffraction and Scattering. August 2002, Grenoble, FRANCE.

4. Karen E. Swider-Lyons, Jason A. Stanley, Gregory B. Cotten, Wojtek Dmowski, and Takeshi Egami, "Low-Platinum Oxide-Based Electrocatalysts For Oxygen Reduction In Proton Exchange Membrane Fuel Cells," Symposium on Recent Advances in Fuel Cells and Fuel Processing, 224th National Meeting of the American Chemical Society,18-22 August 2002, Boston, MA.

IV.D.11 Low Platinum Loading Catalysts for Fuel Cells

Radoslav Adzic (Primary Contact), Jia Wang, Stanko Brankovic, Kotaro Sasaki
Brookhaven National Laboratory, Bldg. 555
Upton, NY 11973-5000
(631) 344-4522, fax : (631) 344-5815, e-mail: adzic@bnl.gov

DOE Technology Development Managers:
JoAnn Milliken: (202) 586-2480, fax: (202) 586-9811, e-mail: JoAnn.Milliken@ee.doe.gov
Nancy Garland: (202) 586-5673, fax: (202) 586-9811, e-mail: Nancy.Garland@ee.doe.gov

Objectives

- Develop a new catalyst with a considerably lower Pt loading, to reach the 2004 DOE target of 300 μg/cm^2 total noble metal loading (150 μg/cm^2 for anode) and improved carbon monoxide (CO) tolerance compared with the commercial platinum Ruthenium (Pt-Ru) catalysts.
- Characterize Pt/Ru electrocatalysts prepared by a new method involving a spontaneous deposition of Pt on Ru nanoparticles.

Approach

- Synthesize electrocatalysts having a submonolayer Pt loading on Ru nanoparticles by spontaneous deposition of Pt on a Ru surface.
- Determine the catalytic properties of the new catalyst for hydrogen (H_2) and H_2 + CO oxidation and improve the thin layer rotating disk electrode method.
- Characterize new electrocatalysts by high-resolution transmission electron microscopy (HRTEM), in-situ fourier transform infrared (FTIR) spectroscopy and extended x-ray absorption fine structure (EXAFS) techniques.
- Test the new electrocatalyst in the membrane electrode assembly (MEA) at Los Alamos National Laboratory.
- Explain the catalytic activity and function of the new electrocatalyst.

Accomplishments

- Electrocatalysts with a 1/8 of monolayer Pt loading on Ru nanoparticles have been synthesized by spontaneous deposition of Pt on a Ru surface, each of which have at least three times larger mass-specific activity for H_2 oxidation than two commercial catalysts and a larger CO tolerance, as determined by thin film rotating disk electrode measurements.
- The carbon-supported catalysts with 1% Pt on 10% Ru (18 μg Pt/cm^2) tested in the MEA at Los Alamos National Laboratory by Dr. Francisco Uribe exhibited a high CO tolerance and the same activity for H_2 oxidation as commercial catalysts with 10 times larger Pt loadings. This catalyst has the noble metal loading close to the 2004 DOE target (200 vs. 150 μg/cm^2), which can be reached by a small decrease of Ru content.
- The possibility of having a catalyst for diatomic oxygen (O_2) reduction with a monolayer of Pt on Ru that approaches the activity of carbon-supported Pt has been demonstrated.
- A method of synthesizing carbon-supported W nanoparticles has been developed with D. Mahajan from Brookhaven National Laboratory (BNL). These nanoparticles will be tested as the *core* for new catalysts containing low coverages of noble metals in the shell.

Future Directions

- Further optimization of the catalyst prepared by spontaneous deposition of Pt and further catalyst characterization with electrochemical and EXAFS techniques.
- Further testing of the catalyst in the MEAs.
- Investigation of possibilities to reduce or replace Ru in the catalyst by non-noble metals.
- Investigations of low Pt loading catalysts for O_2 reduction.

Introduction

In June 2001 we initiated this project to explore the possibilities of decreasing the Pt loading in Pt-Ru catalysts for H_2/CO oxidation in the polymer electrolyte membrane fuel cells (PEMFCs). We have demonstrated a new method for the preparation of the Pt-Ru catalysts involving spontaneous deposition of Pt on Ru nanoparticles that we explored first with single crystal Ru surfaces. The resulting catalysts have a high CO tolerance with considerably lower Pt loading than the commercial catalysts.

Approach

Pt is deposited only at the surface of Ru nanoparticles rather than throughout the Pt-Ru nanoparticles. The method facilitates tuning of the electronic and catalytic properties of Pt-Ru catalysts by controlling the Pt cluster size. In contrast to the Pt-Ru alloy catalysts, this structure has all the Pt atoms available for the catalytic reaction, which decreases the Pt loading.

Results

Characterization of the Electrocatalyst

HRTEM has been used to investigate the type of Pt deposited on Ru nanoparticles. For the $PtRu_{20}$ catalyst, the dominant features, both in symmetry and lattice spacing, are consistent with the hexagonally close-packed Ru single crystal structure. An example of the images with different resolutions obtained with the help of Y. Zhu (BNL) is shown in Figure 1. Figure 1e is a pattern Fourier transferred from the boxed area in Figure 1d, where the particle is viewed along the $(\bar{1}01)$ direction.

The distribution of the lattice spacing and the lattice fringes obtained from 170 particles fit well with the low index spacings of the hexagonally close-packed Ru single crystal. Pt is selectively deposited

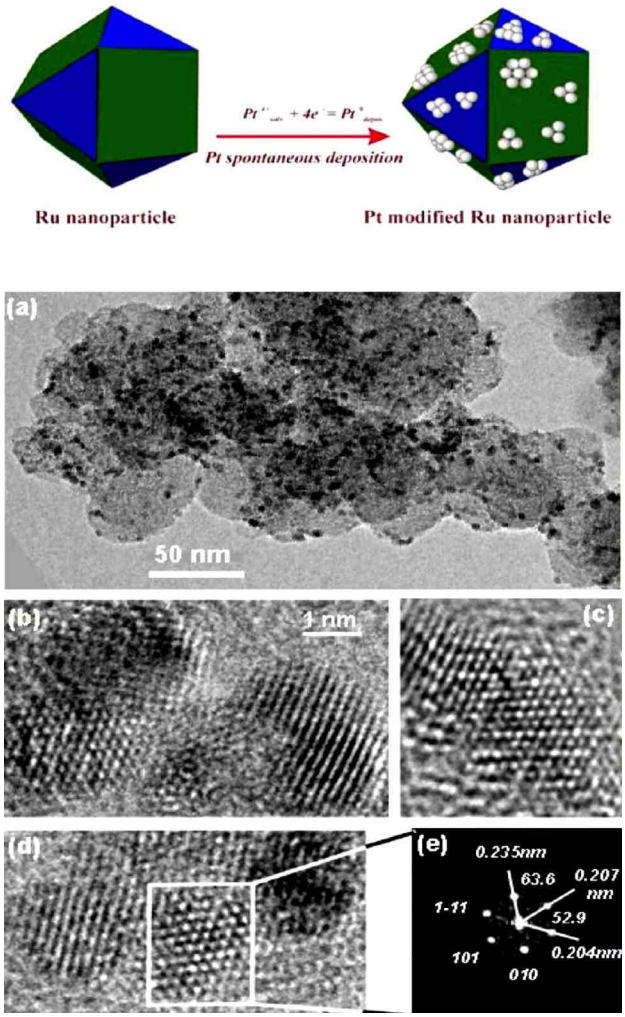

Figure 1. Upper panel: model of Pt islands on a Ru cubooctahedron nanoparticle. Lower panel: Electron micrographs of the $PtRu_{20}$ catalyst. (a) Low magnification morphology of the metal particles (black dots, average size 2.5 nm) on carbon spheres (average size 50 nm). (b-d) High-resolution images showing atomic resolved lattice structures. (e) Diffractogram obtained from the high-resolution image shown in (d).

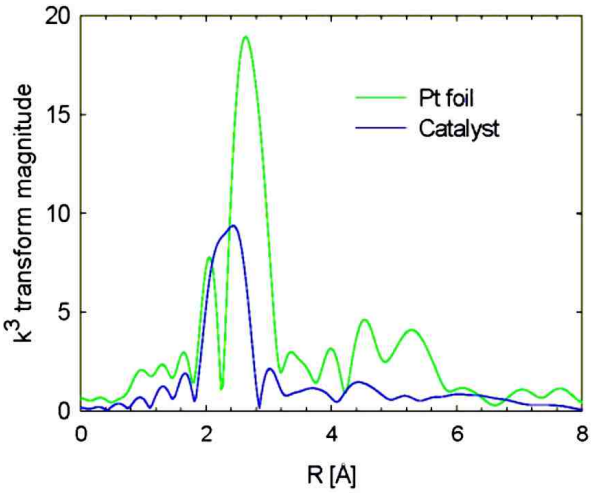

Figure 2. In situ EXAFS data for the $PtRu_{20}$ electrocatalyst at 0.05 V vs. reversible hydrogen electrode in 0.5 M H_2SO_4 solution. The curve for a Pt foil is given for comparison.

on Ru nanoparticles and not on carbon because a metallic Ru surface acts as a reducing agent for Pt deposition. For low Pt:Ru atomic ratios the small Pt clusters are expected, and these probably acquire the Ru lattice spacing upon small contraction.

In-situ EXAFS data obtained with the help of M. Subramanian and J. McBreen (BNL) are shown in Figure 2. The radial structure functions of Pt foil and Pt/Ru catalysts are compared. The spectrum for the Pt/Ru catalyst is dominated by Ru. The analysis shows that the smaller peak can be fitted by the one Pt atom coordinated to four Ru atoms. The Pt-Ru bond length is 2.69Å, as in the Pt-Ru alloys. The Pt-Pt coordination is being analyzed. First results indicate that the Pt islands on Ru are very small, which is consistent with the HRTEM data.

Catalytic Activity

The thin-film rotating disk electrode has been used for determination of the catalytic activity. The catalyst was attached to the glassy carbon electrode by careful deposition from aqueous dispersion and *no Nafion® film was used* to cover the deposit. This can significantly improve the tests of supported electrocatalysts. Kinetic parameters for the oxidation of H_2 and H_2 + CO have been determined by

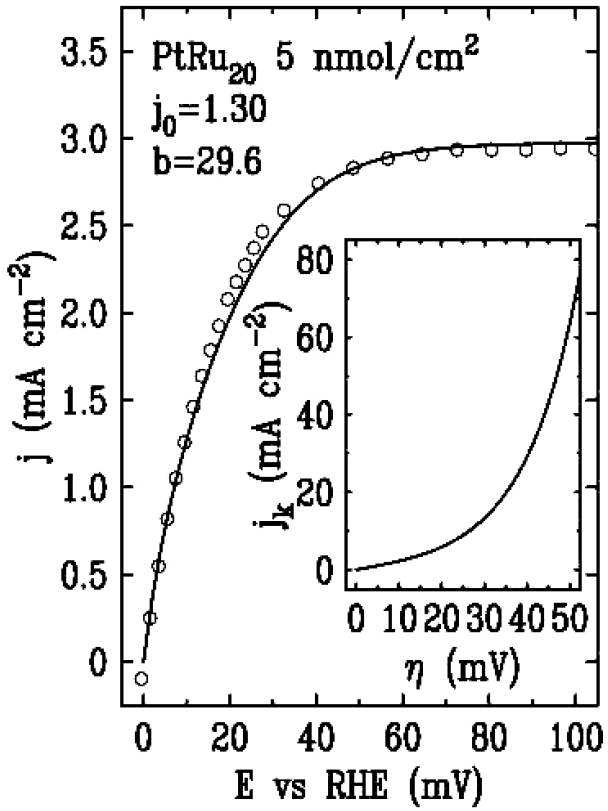

Figure 3. Polarization curves for H_2 oxidation on $PtRu_{20}$/C prepared by spontaneous Pt deposition in 0.5 M H_2SO_4 solution. The parameters of the best fits are given in the graph. Insert: Calculated kinetic current vs. potential with b=29.6 mV and j_0=1.30 mA/cm^2.

nonlinear fitting of the entire polarization curve. Mass-specific activities of the catalysts were determined by finding the minimum Pt loading needed to obtain the Tafel slope, exchange current density, and the Levich slope comparable to those found for the polycrystalline Pt electrode. In this way, a full utilization of the catalyst is verified. Figure 3 shows H_2 oxidation on the $PtRu_{20}$ catalyst; the curve is the fit to the experiment (points) for j_0 = 1.3 millamps per centimers squared (mA/cm^2) and b = 29.6 millivolt (mV), which are the values for polycrystalline Pt. The insert shows the calculated kinetic current in the absence of diffusion control.

For the $PtRu_{20}$, $PtRu_{10}$, and $PtRu_5$ samples prepared by spontaneous deposition of 1/9 to 4/9

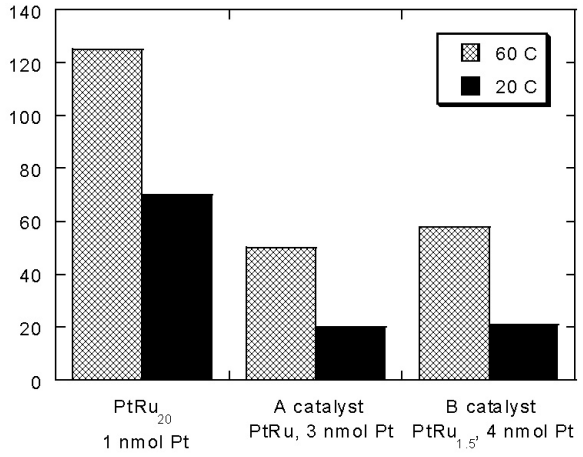

Figure 4. Mass-specific activities of the three electrocatalysts for the oxidation of H_2 at 0.05 V in 0.5M H_2SO_4 at 25 and 60º C at 2500 rpm.

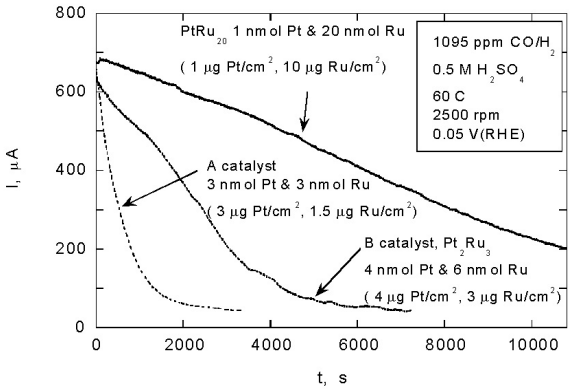

Figure 5. CO tolerance of the three electrocatalysts from a time dependence of the current for the oxidation of H_2 with 1095 ppm CO in 0.5M H_2SO_4 at 60º C at 2500 rpm.

monolayer Pt on Ru, the minimum Pt loading is 5 nmol/cm^2 (1 μg Pt/cm^2). This is only 1/3 of that for Pt or PtRu (Commercial A) catalysts and only twice of the atomic density of a Pt(111) surface, indicating that the high activity of Pt metal for hydrogen oxidation is retained when the atomic assemblies are reduced to submonolayer levels on Ru. The enhanced CO tolerance was studied at low potentials by correlating the loss of activity in 0.1% CO/H_2 and the CO coverage on Pt and Ru sites.

Figure 4 displays a mass-specific activity of $PtRu_{20}$ catalyst in comparison to Commercial A's PtRu 1:1 alloy and Commercial B's Pt_3Ru_2 electrocatalysts for the oxidation of H_2 in 0.5M H_2SO_4. A considerably higher mass-specific activity of the $PtRu_{20}$ electrocatalyst has been observed.

CO Tolerance

Figure 5 displays a comparison of the CO tolerance of three catalysts based on the current as a function of time for the oxidation of H_2 with 1095 ppm of CO at 60º C for the $PtRu_{20}$, Commercial A's PtRu and Commercial B's Pt_3Ru_2 catalysts with the loadings indicated in the graph obtained with rotating disk electrode at 2500 rpm. A considerably larger CO tolerance is seen for the $PtRu_{20}$ electrocatalyst.

Conclusions

The new electrocatalyst has higher mass-specific activity and CO tolerance than commercial electrocatalysts with several times larger Pt loadings. The Pt islands on Ru have lower CO coverage than that of the Pt-Ru alloy, as inferred from the CO stripping charges. Lower Pt-CO bond strength and an efficient CO spillover to RuOH are the likely causes of enhanced CO tolerance. The new catalyst facilitates reaching the limiting value for Pt dispersion, and thus, full catalyst utilization becomes possible.

For Pt, the loading of the new catalyst is below the DOE target (150 μg/cm^2) for precious metals for 2004. For Ru, it is at the present level of the state-of-the-art catalysts.

Preliminary data for O_2 reduction on ½ monolayer of Pt on Ru nanoparticles (not shown) indicates that a very active catalyst for O_2 reduction can be designed with low Pt loadings.

FY 2002 Publications

1. S. R. Brankovic, J.X. Wang, and R.R. Adzic, 2. Pt submonolayers on Ru nanoparticles - a novel low Pt loading, high CO tolerance fuel cell electrocatalyst , Electrochem. Solid State Lett., 4, A217-A220 (2001).

3. S.R. Brankovic, J McBreen, R.R. Adzic, Spontaneous Deposition of Pt on a Ru(0001) Surface, J. Electroanal. Chem., 503, 99-104 (2001).

4. S.R. Brankovic, J. McBreen, R.R. Adzic, Spontaneous deposition of Pd on a Ru(0001) Surface, Surf. Sci., 479, L363-L368 (2001).

5. S.R Brankovic, J.X Wang, R.R. Adzic, Metal monolayer deposition by replacement of metal adlayers on electrode surfaces, Surf. Sci., 477, L173- L179 (2001).

IV.D.12 Development of High-Performance, Low-Pt Cathodes Containing New Catalysts and Layer Structure

Paolina Atanassova (Primary Contact), David Dericotte, Paul Napolitano, Rimple Bhatia, Jim Brewster, Mark Hampden-Smith (SMP), Cynthia Lundgren, Lin Wang (DuPont) and Sandip Mazumder (CFDRC)
Superior MicroPowders, LLC
3740 Hawkins Dr. NE
Albuquerque, NM 87109
(505) 342-1492, fax: (505) 342-2168, e-mail: paolina@smp1.com

DOE Technology Development Managers:
JoAnn Milliken: (202) 586-2480, fax: (202) 586-9811, e-mail: JoAnn.Milliken@ee.doe.gov
Valri Lightner: (202) 586-0937, fax: (202) 586-3237, e-mail: Valri.Lightner@ee.doe.gov

Contractor: Superior MicroPowders, LLC, Albuquerque, NM
Subcontractors: DuPont, Wilmington, DE; CFDRC, Huntsville, AL

Objectives

- Develop and apply combinatorial powder synthesis platform based on spray pyrolysis for discovery of high-performance low-Pt cathode electrocatalysts.
- Develop engineered cathode layer structures containing the new electrocatalysts.
- Demonstrate enhanced performance of membrane electrode assemblies (MEAs) with low Pt content towards the DOE goals of 0.6 g Pt/kW in automotive applications for the year 2005.

Approach

- Design and build a combinatorial powder synthesis system (CPSS) capable of generating a large number of electrocatalyst powders with variable composition and microstructure.
- Test benchmark catalysts with half-cell rapid screening technique for their activity in the oxygen reduction reaction (ORR) and compare ranking of catalysts with their performance in polymer electrolyte membrane MEAs.
- Synthesize binary and ternary Pt-alloy electrocatalysts by spray pyrolysis and test their performance in MEAs.
- Optimize the MEA structure with benchmark Pt-based supported catalysts with various Pt loadings in the catalysts and in the cathode layer.
- Improve the software for modeling the operation of fuel cells to account for the effect of liquid water on the performance of the cell, and perform validation studies.

Accomplishments

- Combinatorial Powder Synthesis System (CPSS) designed and assembled on schedule.
- Half-cell rapid screening technique for screening electrocatalysts for their ORR activity in place and benchmarked for various Pt-based electrocatalysts.

- Various binary and ternary Pt-alloy catalysts synthesized by spray pyrolysis and improved performance demonstrated in terms of lower g Pt/kW at 0.8 V – up to 40% reduction of Pt loading demonstrated for ternary Pt-alloy catalysts compared to supported Pt catalysts.
- Strategy and workflow for future combinatorial synthesis in place.
- MEA structure and printing approach improvements demonstrated in comparison with initial test data.
- Improvements in the fuel cell performance modeling developed and validation studies in progress.

Future Directions

- Install and apply the CPSS for production, in a combinatorial mode, of a large number of electrocatalyst powders with variable composition and microstructure.
- Increase capacity of half-cell rapid screening technique to match the screening needs of CPSS powder generation capability.
- Continue to improve the structure and performance of the cathode layer and test the performance of newly discovered electrocatalyst compositions in MEA configuration that are identified by the rapid screening technique to have enhanced kinetic performance.
- Use modeling to predict trends in the MEA performance as a function of variables in the electrode structure and operating conditions.
- Demonstrate the performance of combined features derived from the best performing low-Pt electrocatalyst and the optimal MEA structure in a short stack fuel cell.

Introduction

One vital issue delaying mass production of PEMFCs is the availability of a low-cost, high-performance oxygen reduction catalyst. Superior MicroPowders (SMP) has developed a spray-based process for low-cost, high-volume manufacturing of high-performance, highly reproducible electrocatalyst powders for PEMFC applications (1). This powder production process serves as the platform for this project to achieve the aggressive low-Pt DOE targets of 0.6 g Pt/kW by the year 2005.

The project goals are to significantly improve both the kinetic performance of the electrocatalyst powder at low noble metal loading and its utilization in the cathode layers through layer structure development. Limitations in the catalyst performance will be addressed through combinatorial discovery of supported catalyst compositions and microstructures. The discovery of these new catalyst formulations will be carried out under conditions that have been scaled for commercial powder production. A large variation of binary, ternary and quaternary noble metal - transition metal alloys and mixed metal-metal oxide catalyst compositions will be screened. To improve the utilization/performance of the catalyst in MEAs, the electrocatalyst-containing formulations will be applied to proton-conductive membranes where the chemical composition of the formulation and the nature of the coating will be varied to uncover the optimum cathode layer performance.

Approach

Effort 1: *Combinatorial discovery of low Pt compositions with microstructure optimization using spray based catalyst manufacturing.* This effort is focused on the combinatorial discovery of new low Pt electrocatalyst formulations. A large variation of multi-component catalysts will be produced by SMP in a combinatorial discovery mode. Initially, the powder synthesis will be performed with existing equipment and then on a new system designed and built at SMP. Samples generated at SMP, will be tested by DuPont in a half-cell rapid screening device for their electrochemical performance. The optimum compositions will be scaled up for testing in single MEAs and stacks.

Effort 2: *Development of engineered particles and layers.* This effort is focused on the ability of the spray-based generation approach to tailor electrocatalyst structure to minimize polarization

losses. SMP will engineer and produce novel composite particles and MEA structures and test them in single 50 cm^2 cell MEA configuration to optimize the cathode layer structure and performance. In parallel, Computational Fluid Dynamics Research Corporation (CFDRC) will model MEA processes on microscopic (primary and secondary particle structure) and macroscopic (layer, MEA) scales. Using the results from the single cell testing and the data from the CFDRC model, SMP will further optimize the MEA structure to obtain maximum performance with a focus on high-throughput manufacturing and cost reduction.

Stack testing. Ultimately, MEAs designed and fabricated by SMP that combine the best scaled up novel catalysts (Effort 1) and the optimal cathode structure (Effort 2) will be tested in full scale short stack operation modules. The stack building and testing will be performed by leading automotive PEMFC developers, such as General Motors. The end-users will also provide valuable feedback in terms of performance and cost targets from a perspective of commercial implementation in the market.

Results

In order to execute a combinatorial approach for discovery of novel electrocatalyst materials, several key workflow components need to be in place, including the ability to generate a large number of electrocatalyst powders with variation in the composition and microstructure and to test their activity in the ORR by a rapid screening technique.

Combinatorial Synthesis. The conceptual design of the CPSS was completed during the current report period and its installation is on schedule. Figure 1 illustrates the overall configuration of the CPSS, which is based on current R&D scale unit at SMP.

Rapid screening of the electrochemical performance. DuPont has developed rapid half-cell screening techniques to evaluate catalyst activity for methanol oxidation, CO tolerance and oxygen reduction. These measurements are performed in liquid sulfuric acid electrolytes, and up to 32 electrodes can be screened in parallel using a variety of electrochemical techniques in a 3-electrode

Figure 1. Combinatorial Powder Synthesis System

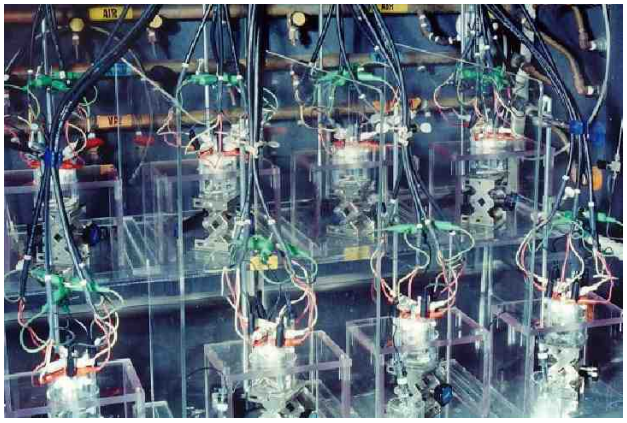

Figure 2. DuPont's Experimental Set-Up for Rapid Half-Cell Screening of Electrocatalysts

configuration. A picture of the experimental setup is shown in Figure 2. With this capability, DuPont can rapidly evaluate many electrocatalyst samples and map their activity for electrochemical reactions. Using this set-up, DuPont evaluated a series of benchmark Pt-based catalysts supplied by SMP for the oxygen reduction reaction using linear polarization techniques in a sulfuric acid medium. The catalysts were tested at various loadings in the electrodes, and the normalized currents at various voltages were compared to the current densities observed in the kinetic region for MEAs made and tested at SMP. We have been able to correlate the ranking of the activity by the rapid screening approach and the MEA performance for different classes of catalysts. Further optimization of the electrode formulation is needed for accurate ranking of catalysts supported on different types of carbons.

Binary and ternary Pt alloys. A large variety of Pt-based catalysts were tested for their performance in test conditions relevant to automotive applications and to benchmark their performance for further comparison with the newly discovered electrocatalyst compositions. Significant effort was placed on finding alternative platinum precursors to support the synthesis of complex alloy and metal-metal oxide electrocatalyst compositions, where metal precursor compatibility becomes important. Several platinum precursors were identified as yielding high performance Pt-based catalysts and being compatible with a variety of alloying metal precursors. The precursors are also more cost-effective for large-scale production.

In order to establish a baseline for our systems and methodologies, several binary and ternary compositions supported on Vulcan XC-72 were evaluated. Among these were Pt_xRu_y, Pt_xCo_y, Pt_xCr_y, Pt_xPd_y, $Pt_xCr_yCo_z$, and $Pt_xNi_yCo_z$. Initial efforts were directed towards variation of the spray conversion processing conditions to ensure conversion of metals, crystallite size and alloying. Post processing of the powders was attempted in several cases and consisted of annealing the electrocatalysts in varying H_2/N_2 atmospheres, temperatures and times. Conversion of the metal precursors and alloying of different species were monitored via x-ray diffraction (XRD). Figure 3 illustrates the effect of various processing conditions on the structural characteristics of $Pt_xNi_yCo_z$/Vulcan XC-72 electrocatalysts. A selected ternary alloy, 20 and 40 wt.% PtNiCo/Vulcan XC-72 electrocatalysts were tested in MEAs at identical total metal loadings and test conditions and compared to pure Pt supported catalyst. Improvement of up to 40% in terms of g Pt/kW at 0.8 V was observed when alloyed catalysts were compared to pure Pt ones. Figure 4 compares the performance of 40 wt.% PtNiCo/Vulcan XC-72 catalysts prepared at different conditions and 40 wt.% Pt/Vulcan XC-72 catalyst deposited at the same total metals loading of 0.45 mg Me/cm^2 (Me – total metals loading) in the MEA.

Test conditions. For the evaluation, 50 cm^2 test MEAs with Nafion 112 (DuPont) membrane were used. The MEAs were tested at 80°C, with flows corresponding to 1A/cm^2 at 1.5 stoichiometry for hydrogen and 2.5 stoichiometry for air on the anode

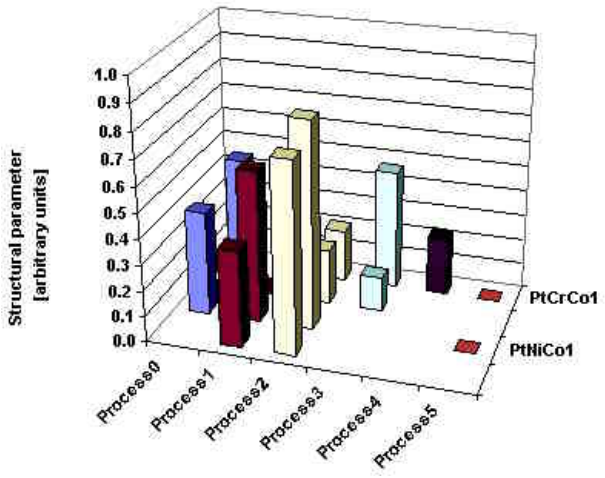

Figure 3. Synthesis of Ternary Pt-alloy Electrocatalysts: Effect of Composition and Processing Conditions on Structural Parameters

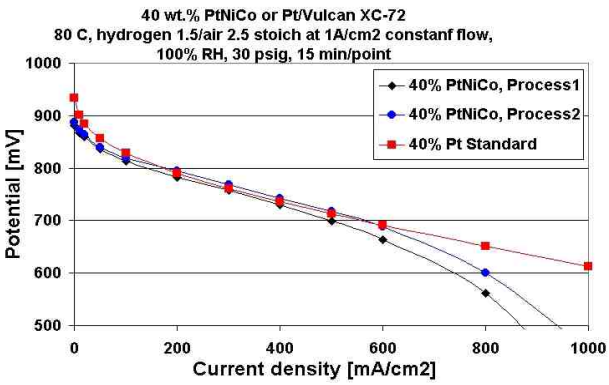

Figure 4. Performance Comparison of Ternary 40 wt.% $Pt_xNi_yCo_z$/Vulcan XC-72 and 40 wt.% Pt/ Vulcan XC-72 Electrocatalysts

and cathode, respectively. Humidified H_2 (100%) and air were used, at 30 psig pressure on both the anode and cathode sides.

MEA structure development. The development of the electrode structure was focused on finding optimal combinations of electrocatalyst loadings, layer thicknesses and ionomer-to-catalyst ratios. Figure 5a shows the polarization curves for MEAs with 60 wt.% Pt/Carbon used as cathode catalyst at Pt loadings in the range of 0.25 to 0.65 g Pt/cm^2. Figure 5b compares the performance of these MEAs in terms of g Pt/kW at 0.8 V. For all these benchmark Pt loadings, a performance around 2 g Pt/ kW was demonstrated.

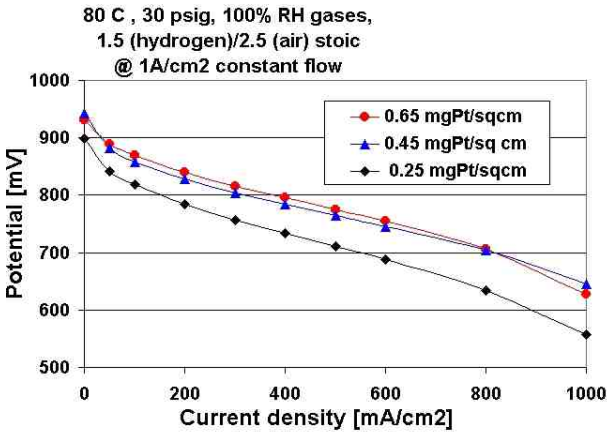

Figure 5a. Effect of Pt Loading on Performance Using 60 wt.% Pt/Carbon as Cathode Catalyst

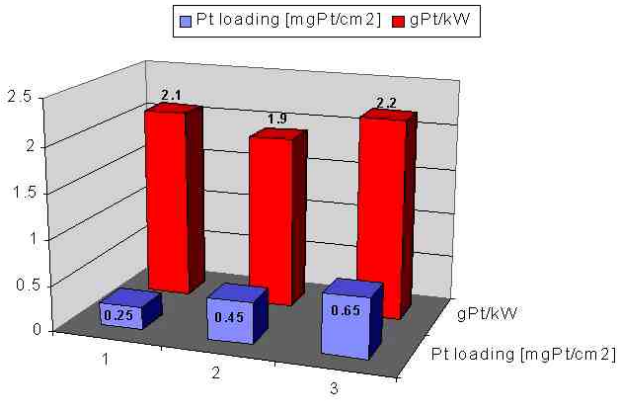

Figure 5b. Performance of MEAs with 60 wt.% Pt/ Carbon Cathode Electrocatalyst at 0.8 V

Various types of Nafion membranes and gas diffusion layers were compared as well. The electrode deposition technique was optimized to achieve performance comparable to the "state-of-the-art" for ink deposition approach. Several deposition techniques were investigated for printing the electrode layers, Figure 6 compares the performance achieved with two MEAs, printed by method A and method B with otherwise identical composition. Improved Method B yields performance of 1.9 g Pt/ kW at 0.8 V and the above stated test conditions. Further optimization of the electrode structure is in progress for catalysts with various loadings on high-surface-area carbon supports.

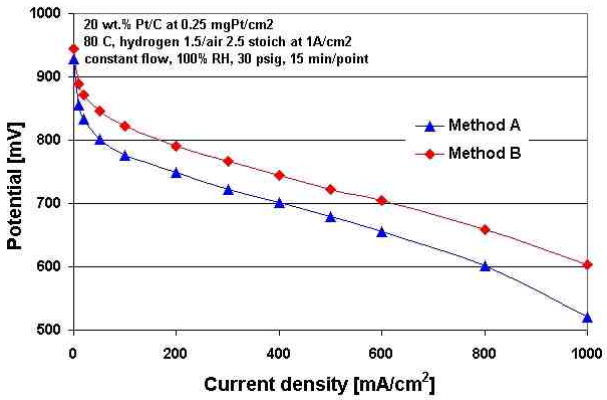

Figure 6. Effect of Deposition Method on the MEA Performance

Modeling effort. CFDRC has made several generic improvements to their existing software for modeling fuel cells and performed several validation studies. These are listed below:

- A comprehensive water transport model was developed to account for effect of liquid water on the performance of the cell. This involved solution of an additional transport equation for liquid water saturation. Effects of convection, surface tension, electro-osmotic drag, gravity and surface tension are taken into account in this model.
- Several new models to compute effective diffusivity in porous regions were implemented.
- Several validation studies were performed against data reported in the literature.

Validation of the code against data generated in-house at SMP is underway. Upon completion of these validation studies (expected by September, 2002), much of the focus will be on using the model as a predictive tool to identify better MEA designs. Further development of the model to account for variables in the structure on a microscopic level is in progress.

Conclusions

Significant progress has been made in implementing all necessary components for successful execution of both the combinatorial

discovery approach and electrode structure optimization. Results on the synthesis of benchmark alloy catalyst compositions demonstrate the ability of the SMP's spray approach to generate complex electrocatalyst formulations with improved electrochemical performance. Future work will expand on the compositions screened according to a combinatorial strategy in place. The advances in the two parallel efforts, i.e. improvements in kinetic performance and MEA structure optimization, will be combined to reveal the overall achievements in performance at reduced Pt loadings.

References

1. Kodas, T.T., M.J. Hampden-Smith, J. Caruso, D.J. Skamser, and Q.P. Powell, *Metal-carbon composite powders, methods for producing powders and devices fabricated from same*. 2000, Superior MicroPowders: US 6,103,393.

IV.D.13 New Electrocatalysts for Fuel Cells

Philip N. Ross, Jr. (Primary Contact), Nenad Markovic
Lawrence Berkeley National Laboratory
Materials Sciences Division
1 Cyclotron Rd., MS 2-100
Berkeley, CA 94720
(510) 486-6226, fax: (510) 486-5530, e-mail: pnross@lbl.gov

DOE Technology Development Managers:
JoAnn Milliken: (202)586-2480, fax: (202)586-9811, e-mail: JoAnn.Milliken@ee.doe.gov
Nancy Garland: (202) 586-5673, fax: (202) 586-9811, e-mail: Nancy.Garland@ee.doe.gov

Objectives

- Conduct research on the kinetics and mechanism of electrode reactions in low temperature fuel cells. Develop new electrocatalysts using a materials-by-design approach.

Approach

- Study the kinetics of fuel cell electrode reactions on well-characterized model electrodes and high surface area fuel cell electrocatalysts using modern electroanalytical methods. Study the mechanisms of the reactions using state-of-the art in-situ spectroscopes.
- Use ultra-high vacuum methods of surface preparation and surface analyses to form tailored surfaces. Synthesize nanoclusters to have the tailored surface.
- Characterize the microstructure of the nanoclusters by high-resolution electron microscopy.
- Transfer technology to catalysts developers/vendors.

Accomplishments

- Proof-of-principle experiments demonstrated that a Au-Pd alloy with <50 wt. % Pd can replace Pt as the hydrogen electrode catalyst without any loss in performance.
- Proof-of-principle experiments demonstrated that “Pt skin” structures with a non-precious metal core can be stable under PEMFC air cathode operating conditions

Future Directions

Cathode side

- Create “skin” nanostructures of Pt on non-noble substrates and determine their activity and stability as novel low-Pt air cathode electrocatalysts. Select the most promising substrate for synthesis as high surface area catalyst.
- Develop and optimize a new class of non-Pt model catalysts. Synthesize and test new non-Pt high surface area catalysts at fuel cell conditions.

Anode side

- Synthesize and characterize Pd-Au bimetallic nanoparticles and conduct preliminary testing of these nanoparticles as anodes in PEMFC hydrogen-air cells.
- Determine CO-tolerance of tailored electrodes consisting of thin films (1-10 monolayer) of Pd on the close-packed single crystal surfaces of Ta, Re, and W.

Introduction

It is known from the theory of surface segregation in bimetallic alloys that, in certain systems, preferential surface enrichment in one element is so strong that it leads to a "skin" structure, i.e. the outermost layer is a "skin" of one element. Theoretically, for nanoparticles, such a segregating alloy system could form particles having a "grape" microstructure, a skin of one element over a core of the other. In principle, one could use this thermodynamic property to replace the "buried" atoms in Pt nanoparticles with a non-precious metal, e.g. Fe or Co, resulting in 100% Pt dispersion (all Pt atoms are surface atoms) without the need to create extremely small particles, e.g. <2 nm. For example, if a standard pure Pt catalyst consists of particles having on average a dispersion of 20%, replacement of the buried atoms in those particles with a base metal would enable the Pt loading to be reduced by a factor of 5, all other factors being the same. This is the basic strategy we are currently pursuing to reduce Pt loading in PEMFC cathodes.

Approach

Pt_3Ni and Pt_3Co are classical examples of alloys of Pt having a skin surface structure, a pure Pt skin. In this case, enrichment occurs by interchange of Pt and Co atoms between the first two atomic layers, the subsequent layers having the bulk composition (75% Pt). The thermodynamic driving force in this case is for the larger atom to be at the surface, since, in face-centered cubic metals, the surface is generally relaxed outward and the second layer contracted. The Pt_3Ni and Pt_3Co systems do not represent cases of extreme segregation we need for replacing buried Pt atoms, but they do serve as a useful test case for the concept of a skin structure, and there may be, by serendipity, a beneficial electronic effect. The most important aspect of the study of this system was the stability of the skin structure when used as an oxygen reduction electrode under PEMFC conditions.

Results

Cathode Catalysts

Pt_3Ni and Pt_3Co solid electrodes were prepared using conventional metallurgy and pre-treated in a surface analytical vacuum chamber equipped with various instruments for surface preparation and analysis. For each alloy, either a pure Pt skin or a 75 at.% Pt surface was prepared and tested as an oxygen reduction catalyst. The resulting activity for oxygen reduction as a function of composition is shown in Figure 1. The Pt skin structure is both more and less active than the pure Pt reference surface, depending on whether the subsurface is Co or Ni, suggesting there is an electronic effect that can be either beneficial or deleterious. The most important result represented in Figure 1 is the stability of the skin structure under the conditions of use as an oxygen reduction electrode, e.g. continuous cycling between 0.1 – 1.0 V under 1 bar O_2 in acid electrolyte (1 M trifluoromethane sulfonic acid) at 60^{o}C produced no change in the curves.

Anode Catalysts

The catalytic activity of Pd for the hydrogen oxidation reaction (HOR) can be modified by preparing the Pd in the form of an ultrathin film, e.g. 1 monolayer (ML). This result is summarized in Figure 2. A 1 ML film of Pd on Pt(111) has about 5 times the catalytic activity of a multilayer of Pd. Pt(111) was chosen for the substrate because of the lattice match with Pd. Preliminary results with a Re(0001) substrate look equally promising. According to thermodynamic predictions, Pd should form a pure monatomic skin on the surface of a Re_3Pd (25% Pd) alloy. If this Pd skin has the same catalytic activity as the monolayer shown in Figure 2, then the Pd loading in the hydrogen anode of a H_2-air PEMFC can be as low as 0.05 g per kW, e.g. about the same as in current conventional gasoline vehicle catalytic converters.

Conclusions

Proof-of-principle experiments indicate that synthesis of Pt as surface enriched nanoparticles could enable Pt loadings in the PEMFC air cathode to be lowered by as much as a factor of 5 from present (optimized) levels, e.g. from 1 g per kW to the DOE target of 0.2 g per kW. Comparable experiments with Pd thin films indicate an even greater reduction in Pt Group Metal (PGM) loading is possible for the hydrogen electrode, comparable to the PGM content of the catalytic converter in current conventional gasoline vehicles.

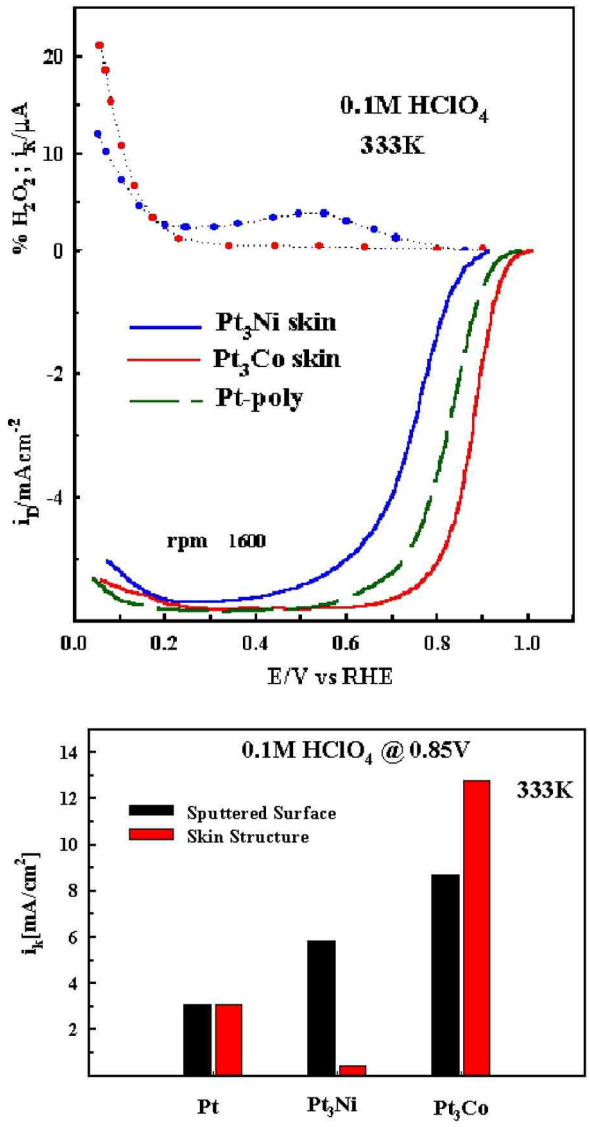

Figure 1. (top) Current-potential curve for a rotating disk electrode (1600 rpm) under 1 bar O_2 in 0.1 M $HClO_4$ for different disk electrodes: Pt skin on Pt_3Ni, Pt skin on Pt_3Co, and pure Pt. (bottom) Steady-state current densities (per unit geometric area) at 0.85 V (vs. reversible hydrogen electrode [RHE]) for the five different electrodes: pure Pt, Pt skin on Pt_3Ni and Pt_3Co, the 75% Pt surfaces on Pt_3Ni and Pt_3Co. 333 K.

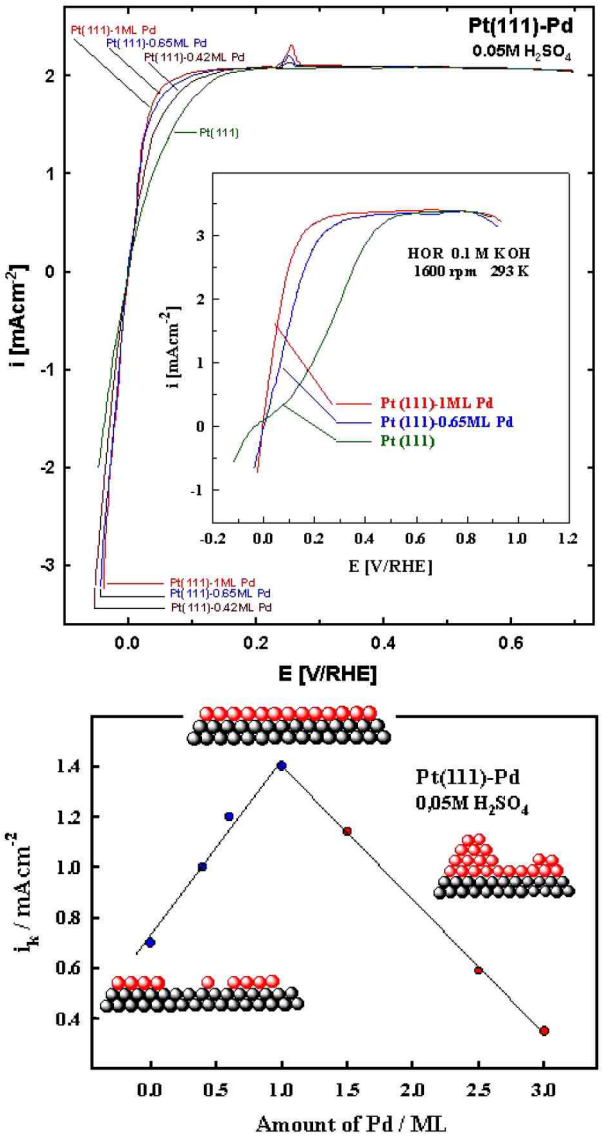

Figure 2. (top) Current-potential curve for a rotating disk electrode (1600 rpm) under 1 bar H_2 in 0.1 M $HClO_4$ for different disk electrodes as indicated in the labels. (bottom) Exchange-current densities in acid electrolyte (pH = 1) for the hydrogen oxidation reaction as a function of Pd coverage on the Pt(111) substrate. 293 K.

Publications

1. Markovic, N. M. and P. N. Ross, "Electrocatalysts by Design: From the Tailored Surface to a Commercial Catalyst", *Electrochim. Acta*, **45**, 4101, 2000.

2. Markovic, N. M. and P. N. Ross, "New Electrocatalysts for Fuel Cells: From Model Surfaces to Commercial Catalysts", *CATTECH* **4** (2000) 110.

3. V. Stamenkovi_, N. M Markovi_, P. N. Ross, "Structure-Property Relationships in Electrocatalysis: Oxygen Reduction and Hydrogen Oxidation Reactions on Pt(111) and Pt(100) in Solution Containing Chloride Ions", *J. Electroanal. Chem.* **500** (2001) 43.

4. T.J. Schmidt, B. N. Grgur, N.M. Markovi, and P.N. Ross, "Oscillatory Behavior in the Electrochemical Oxidation of Formic Acid on Pt(100): Rotation and Temperature Effects", *J. Electroanal. Chem.* **500** (2001) 43.

5. N. M Markovic, T.J. Schmidt, V. Stamenkovic, P.N. Ross, "Oxygen Reduction Reaction on Pt and Pt Bimetallic Surfaces: A Selective Review", *Fuel Cells-From Fundamentals to Systems* , **1** (2001)105-116.

6. T.J. Schmidt, V. Stamenkovic, C.A. Lucas, N.M. Markovi, and P.N. Ross, "Surface Processes and Electrocatalysis of the Pt(hkl)/Bi –Solution Interface", *Physical Chemistry Chemical Physics* **3** (2001)3879.

7. T.J. Schmidt, P.N. Ross, N.M. Markovi, "Temperature-Dependent Surface Electrochemistry of Pt Single Crystal Surfaces in Alkaline Solution" Part I. CO Oxidation", *J. Phys. Chem*, B **105** (2001)12082.

8. U.A. Paulus, A. Wokaun, G.G. Scherer, T.J. Schmidt, V. Stamenkovic, V. Radmilovic, N.M. Markovi, and P.N. Ross, "Oxygen Reduction on Carbon Supported Pt-Ni and Pt-Co Alloy Catalysts", *J. Phys. Chem. B* **106** (2002) 4181.

IV.D.14 Electrodes for Polymer Electrolyte Membrane Fuel Cell Operation on Hydrogen/Air and Reformate/Air

Francisco A. Uribe (Primary Contact), Tom Zawodzinski, Judith Valerio, Guido Bender, Fernando Garzon, Andrew Saab, Tommy Rockward, Peter Adcock, Jian Xie, Wayne Smith
Los Alamos National Laboratory
PO Box 1663, MS D429
Los Alamos, NM 87545
(505) 667-3964, fax: (505) 665-4292, e-mail: uribe@lanl.gov

DOE Technology Development Managers:
JoAnn Milliken: (202) 586-2480, fax: (202) 586-9811, e-mail: JoAnn.Milliken@ee.doe.gov
Nancy Garland: (202) 586-5673, fax: (202) 586-9811, e-mail: Nancy.Garland@ee.doe.gov

Objectives

- Optimize existing polymer electrolyte membrane (PEM) fuel cell technology for use with H_2 and reformed hydrocarbons.
- Improve overall PEM fuel cell operating efficiency.
- Improve the efficiency of the fuel cell cathode while lowering the dependence on precious metal loading.
- Achieve 0.4 amps per centimeters squared (A/cm^2) @ 0.8 volt (V) on hydrogen (H_2) with <0.25 milligrams platinum per centimeters squared (mg Pt/cm^2) on cathode
- Demonstrate 0.4 A/cm^2 @ 0.8 V on Reformate with <0.40 mg Pt/cm^2 on cathode
- Initiate Cooperative Research & Development Agreement with Donaldson for studying the effect of ambient air impurities on fuel cell performance.
- Establish the effect of 50 parts per billion hydrogen sulfide on anode performance

Approach

- Investigate the use of a reconfigured anode to improve fuel cell performance in the presence of trace levels of carbon monoxide (CO) impurities.
- Evaluate new anode catalysts for CO tolerance.
- Study the effect of other potential reformate impurities on fuel cell performance.
- Evaluate new cathode catalyst and materials for higher operating efficiencies at lower precious metal loadings.
- Evaluate new membrane electrode assembly (MEA) fabrication protocols to enhance catalyst utilization and overall fuel cell efficiency.

Accomplishments

- Demonstrated the effectiveness of using the reconfigured anode in reformate fuel streams containing up to 250 parts per million (ppm) CO impurity with air bleed.
- Obtained good performances with a new CO tolerant 90:10 ruthenium:platinum anode catalyst.
- Determined the effects of hydrogen sulfide, a potential reformate impurity, on fuel cell performance.
- Screened potential cathode catalysts with reduced platinum loadings.

- Developed new MEA fabrication protocols leading to enhanced catalyst utilization and overall fuel cell performance.

Future Directions

- Investigate alternative catalyst materials for use in reconfigured anodes.
- Evaluate new potential CO tolerant catalysts.
- Further study hydrogen sulfide fuel stream impurity effects and develop technologies to minimize associated performance reduction.
- Screen new potential cathode catalyst materials.
- Continue to develop modified MEA fabrication protocols.

Introduction

The reforming of hydrocarbon fuels is one of the leading processes under consideration for producing hydrogen to power PEM fuel cells. However, the hydrogen stream generated by the reforming process can contain volatile chemical compounds that significantly diminish the fuel cell performance. Two approaches to solving this problem are to lower the level of impurity resulting from the reformation process, or to modify the fuel cell itself to be more tolerant toward those compounds. This study has taken the latter approach; ways were investigated to improve the anode performance in the presence of anticipated reformate impurities.

Fuel cell operation depends not only on hydrogen oxidation at the anode but also on oxygen reduction at the cathode. The oxygen reduction reaction plays a very significant role in limiting the operating efficiency of the fuel cell, and is very dependent on high precious metal loadings in the catalyst layer. Improving the efficiency of this reaction while lowering the precious metal loadings is critical to commercialization of fuel cell technology to automotive applications.

Approach

The predominant deleterious impurity anticipated in the reformate fuel stream is CO. This gas is more strongly absorbed on the surface of the catalyst than hydrogen, effectively blocking the sites where hydrogen oxidation should occur. One method to prevent this from happening is to remove the CO by oxidizing it to harmless carbon dioxide before it can reach and react with the anode surface. This can be accomplished by using the Los Alamos National Laboratory (LANL) reconfigured anode, shown schematically in Figure 1. The reconfigured anode has an outer, non-precious metal catalyst layer added to the standard MEA. Bleeding a low level of air into the fuel stream results in preferential oxidation of the CO at this outer layer.

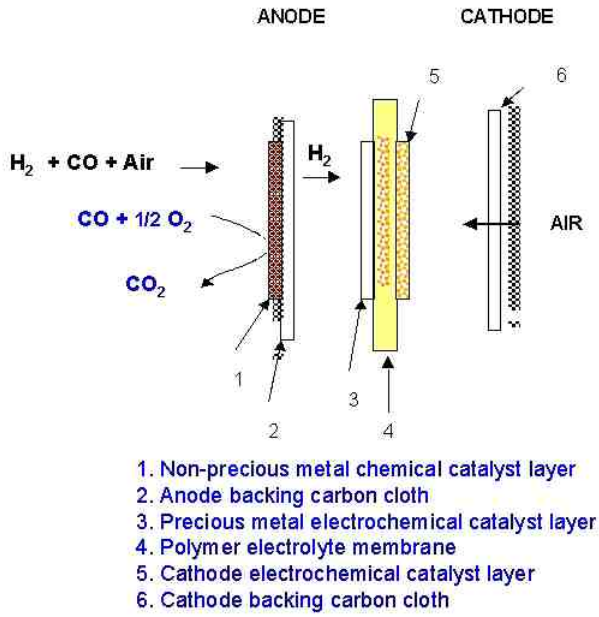

Figure 1. Fuel Cell Schematic with Reconfigured Anode

A second approach to solving the CO problem is to use an anode catalyst that is intrinsically more CO tolerant and that may contain a lower percentage of precious metals. In a given period of time, we receive many new potential catalysts from both commercial and non-commercial sources. These materials are

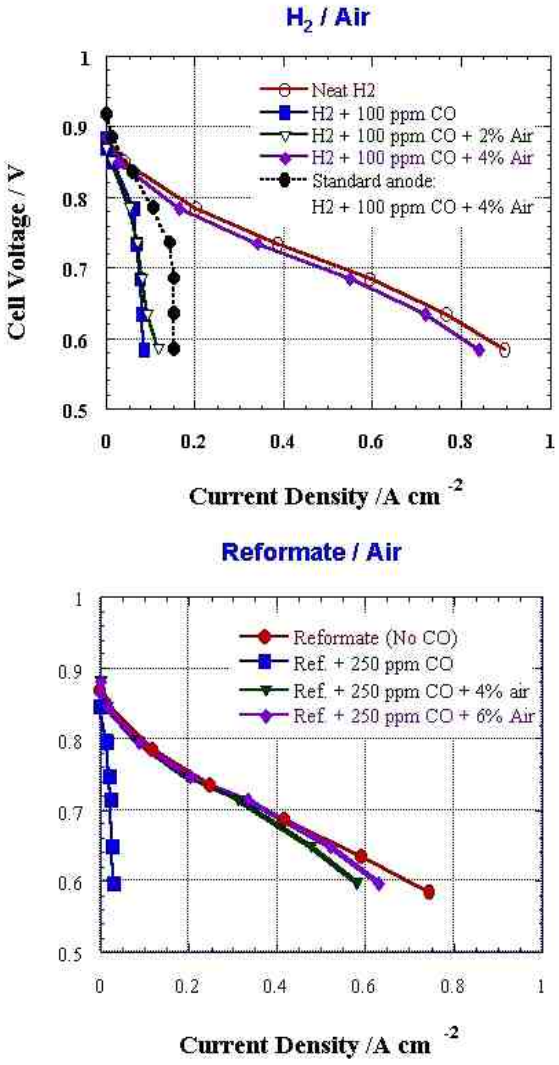

Figure 2. Fuel cell performance at 80°C with reconfigured anode containing a non-precious metal-based chemical catalyst. (0.2 mg Pt/cm^2 at each electrode)

fabricated into MEAs, using a protocol established at LANL, then placed in fuel cells and tested under standard operating conditions.

A third approach to developing better fuel cell anodes is to study the kinetics and mechanisms associated with the reactions of suspected impurities in the reformate stream and various catalysts. The mechanism for CO poisoning of the anode catalyst is fairly well understood, but for other potential poisons that may not necessarily be the case. During this past year such a study has been initiated for hydrogen sulfide, a very likely by-product in reformed fuels initially containing sulfur bearing compounds.

An approach similar to that used to improve anode performance was also applied to the study of the cathode reaction and included the following:

- Develop new MEA fabrication methods to improve catalyst utilization.
- Work with vendors to develop and test new catalyst formulations.
- Study the dependence of performance on catalyst layer structure.
- Study the effects of suspected impurities present in air (sulfur dioxide, nitrogen oxides, particulates) on cathode performance.

Results

Results obtained with the LANL reconfigured anode and platinum anode catalyst are shown in Figure 2. The graph on the top shows the effect of a small amount of CO on the operating characteristics of the fuel cell, with pure hydrogen as a fuel source. There is an almost catastrophic loss of performance when 100 ppm of CO is added to the hydrogen. However, using the reconfigured anode and adding 4% air to the mixture results in essentially complete CO oxidation and restores the performance of the fuel cell. The graph on the bottom shows similar results for a synthetic reformate fuel stream containing 40% hydrogen, 35% nitrogen and 25% carbon dioxide. In this case the effects of adding 250 ppm of CO are fully mitigated with the addition of 6% air.

The second approach of building CO tolerance directly into the anode catalyst has also been confirmed. The most promising results to date were obtained with a catalyst provided by R. Adzic from Brookhaven National Laboratory, composed of 10% ruthenium and 1% platinum on a carbon support. As shown in Figure 3, a significant fraction of the fuel cell performance is restored with the addition of small amounts of air to the fuel stream. Perhaps even more significant is that the total platinum loading of this catalyst is only 18 micrograms per square centimeter, approximately 1/10 that normally used in operating fuel cell anodes.

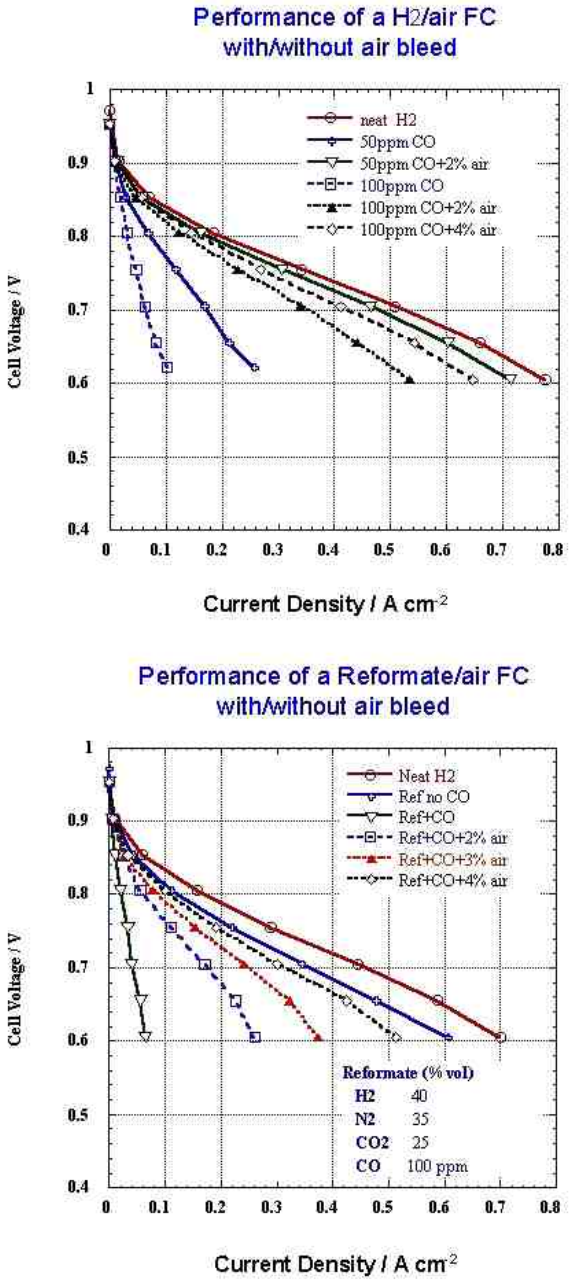

Figure 3. Low Pt Content Anode Catalyst for CO Tolerance (Anode: 0.2 mg Ru-Pt/cm^2; Cathode: 0.2 mg Pt/cm^2)

Preliminary data obtained with hydrogen sulfide, another anticipated reformed fuel impurity, show this compound has an even more serious effect on fuel cell performance than CO. Hydrogen sulfide appears to poison the platinum catalyst irreversibility.

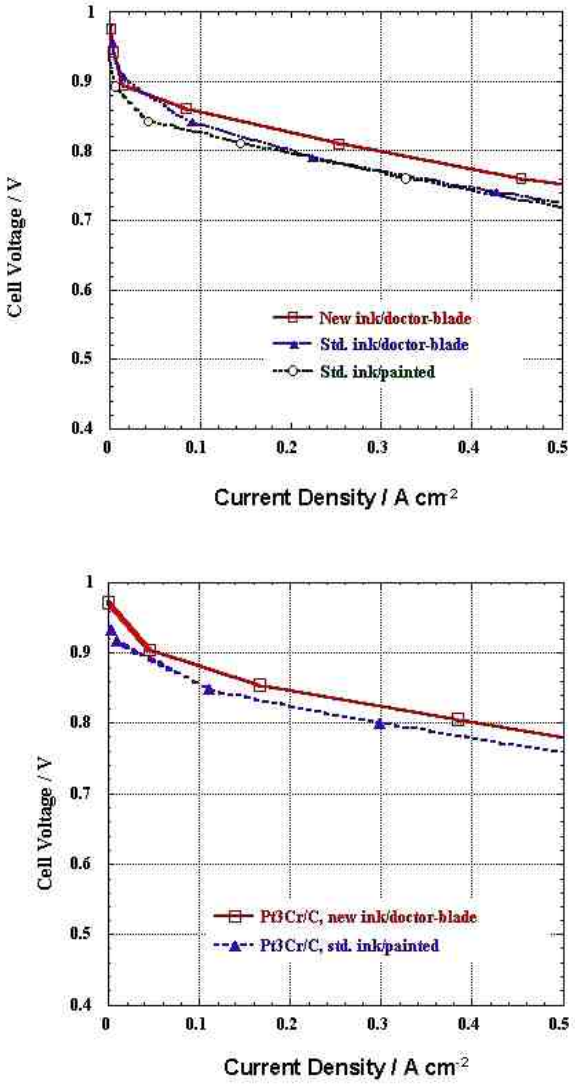

Figure 4. Cathode Optimization: New Catalyst and MEA Preparation (0.2 mg Pt/cm^2 at each electrode)

Results obtained from studies on improving the cathode/oxygen reduction reaction are summarized in Figure 4. This figure shows the effect of changing the catalyst from pure platinum to a platinum-chromium alloy, and of changing the MEA preparation method from the standard painted/decal method to using an automated doctor blade approach. The new catalyst and new preparation method both enhance fuel cell performance.

Conclusions

The performance of fuel cells operating on reformed hydrocarbon fuels is seriously affected by the presence of trace impurities present in the fuel stream. However, a significant fraction of performance losses can be regained by using either a reconfigured anode design or an alternative anode catalyst material. This has been clearly demonstrated for a CO impurity level of up to 250 ppm in the fuel stream. Studies also indicate that using alternative cathode catalyst materials and new MEA preparation methods can still result in further fuel cell performance gains.

FY 2002 Publications\Presentations

1. F. Uribe, S. Gottesfeld and T. Zawodzinski, "The Effect of Ammonia as Potential Fuel Impurity on Proton Exchange Membrane Fuel Cell Performance", J. Electrochem. Soc., 149, A293 (2002).

2. F. Uribe and T. Zawodzinski, "A Study of Polymer Electrolyte Fuel Cell Performance at High Voltages. Dependence on Cathode Catalyst Layer Composition and on Voltage Conditioning". Accepted in Electrochimica Acta. (2002).

3. P. A. Adcock, S. Pacheco, E. Brosha, T. Zawodzinski, and F. Uribe, "Maximization of CO Tolerance of PEMFC Systems Using Reconfigured Anodes". To be presented at the Electrochemical Society Meeting, Salt Lake City, UT (Fall 2002).

4. F. Uribe and T. Zawodzinski, "PEMFC Reconfigured Anodes for Enhancing CO Tolerance with Air Bleed", 201st Electrochemical Society Meeting, Philadelphia (2002). Abstract No. 806.

5. P. Adcock, F. Uribe, J. Valerio and T. Zawodzinski, "New Results for Maximization of CO Tolerance of Hydrogen and Reformate Fuel Cells", 201st Electrochemical Society Meeting, Philadelphia (2002). Abstract No. 814.

6. J. Xie, F. Garzon, T. Zawodzinski, "The Microstructure of the Cathode Catalyst Layer in PEFC's", 201st Electrochemical Society Meeting, Philadelphia (2002). Abstract No. 808.

7. J. Xie, S. Pacheco, K. Wilson, C. Zawodzinski and T. Zawodzinski, "Influence of Ionomer Content in the Cathode Catalyst Layer on the Performance of PEM Fuel Cells", 201st Electrochemical Society Meeting, Philadelphia (2002). Abstract No. 810.

8. E. Brosha, S. Pacheco, P. Zelenay, F. Uribe, F. Garzon and T. Zawodzinski, "Development of Freeze-Dried Catalysts for Hydrogen and Direct Methanol Fuel Cells", Electrochemical Society Meeting, San Francisco, CA (2001). Abstract No. 322.

9. F. Uribe and T. Zawodzinski, "The Effects of Fuel Impurities on PEM Fuel Cell Performance", Electrochemical Society Meeting, San Francisco, CA (2001). Abstract No. 339.

Patent Applications

1. F. Uribe and T. Zawodzinski, "Fuel Cell Anode Configuration for CO Tolerance" (2001).

2. F. Uribe and T. Zawodzinski, "Method for Improving High Cell Voltage Performance for Polymer Electrolyte Membrane Fuel Cell". 2001/0044040 (2001).

IV.D.15 Nondestructive Study of the Water Transport Mechanism Inside Operating PEM Fuel Cells Using Neutron Imaging Techniques

Muhammad Arif (Primary Contact), David Jacobson, Rahul Satija (now at Duke University)
National Institute of Standards and Technology
Gaithersburg, MD 20899
(301) 975-6303, fax: (301) 926-1604, e-mail: arif@nist.gov

DOE Technology Development Manager: Nancy Garland
(202) 586-5673, fax: (202) 586-9811, e-mail: Nancy.Garland@ee.doe.gov

Objectives

Neutron imaging may be the only technique available today that has the realistic possibility of mapping water distribution in flow channels and membranes inside operating PEM fuel cells. This information can be very important to fuel cell developers for designing more robust and efficient fuel cells. Our research objectives are as follows.

- Development of a neutron-imaging facility for studying PEM fuel cell water transport.
- Two-dimensional imaging of time-dependent bulk water distribution in an operating PEM fuel cell and quantification of the results.

Approach

- Phase 1. Define neutron beam characteristics most sensitive to water distribution in fuel cells. Define spatial and temporal resolution parameters for visualization of water/vapor distribution.
- Phase 2. Based on parameters defined in Phase 1, design a new beam line and a charge-coupled device (CCD)-based neutron imaging instrument at the National Institute of Standards and Technology (NIST) nuclear reactor. Make special considerations for easy accessibility and user friendliness of the facility for non-NIST fuel cell researchers.
- Phase 3. Carry out neutron measurements on a working 4-stack PEM fuel cell to define the operating parameters of the new setup and test the limits of achievable spatial and temporal resolution of water distribution and flow dynamics inside a working fuel cell.

Accomplishments

- Designed a state-of-the-art new neutron imaging facility for fuel cell research. This facility will be used for critical water transport studies in the MEA and the flow channels, for the measurement of the hydrogen diffusion co-efficient across the MEA and water/vapor phase, and for evaluation of the integrity of various interfaces. The facility is expected to be operational in October, 2002.
- Using existing facilities, non-destructively imaged and quantified time-dependent water distribution in an operating fuel cell. A near 1 second time resolution was achieved. The total water content inside the fuel cell as a function of time was also quantified.

Future Directions

Three-dimensional imaging of the fuel cell is needed to allow independent measurement of water/vapor distribution parameters within any section or part of the fuel cell.

- Develop neutron-imaging methods to accurately measure water gradients across a fuel cell PEM membrane.
- Determine diffusion coefficient and hydrophobic characteristics of the gas diffusion layer.
- Characterize two-phase flow mechanism in the fuel cell flow field.
- Study the time-dependent membrane-catalyst-gas diffusion layer interface integrity.

Introduction

Compared to most other forms of radiation, neutrons are highly efficient in probing complex structures because of their tremendous penetration capability in almost all known materials and due to their unique ability to distinguish different materials with very similar physical properties. They are particularly effective in detecting hydrogenous materials and other light elements. As a result, neutron imaging is ideally suited for ***non-destructive, in situ visualization and quantification*** of water transport phenomena in operating PEM fuel cells.

Approach and Results

The new setup is being constructed at the BT6 high intensity thermal beam line at the NIST Center for Neutron Research (NCNR) nuclear reactor (Figure 1) to non-destructively characterize water transport mechanism in single or multi-stack PEM fuel cells. The high neutron flux will allow attainment of a time resolution of about 1 sec and a nominal detector spatial resolution of about 30 μm. The imaging process consists of a neutron beam passing through a sample. The beam is attenuated by the presence of hydrogenous material (water vapor/ water) present in the sample (fuel cell as an example). Consequently, an image of the hydrogenous material is formed and recorded by a CCD camera (Figure 2). The digital image is then analyzed to determine the quantity and distribution of water/water vapor inside the fuel cell.

At the imaging station, the largest fuel cell that can be imaged is about 20 cm x 20 cm. A sample of larger length can be imaged section by section through translation of the sample. The fuel cells also can be single- or multi-cell. The facility will operate as a user facility; a proposal will be required and will be reviewed for merit before allocating beam time. A generic fuel cell test station will be available for

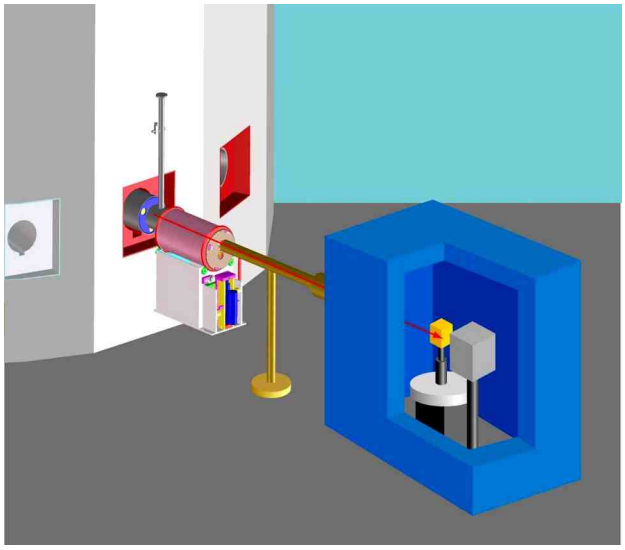

Figure 1. Schematic of New Fuel Cell Imaging Station

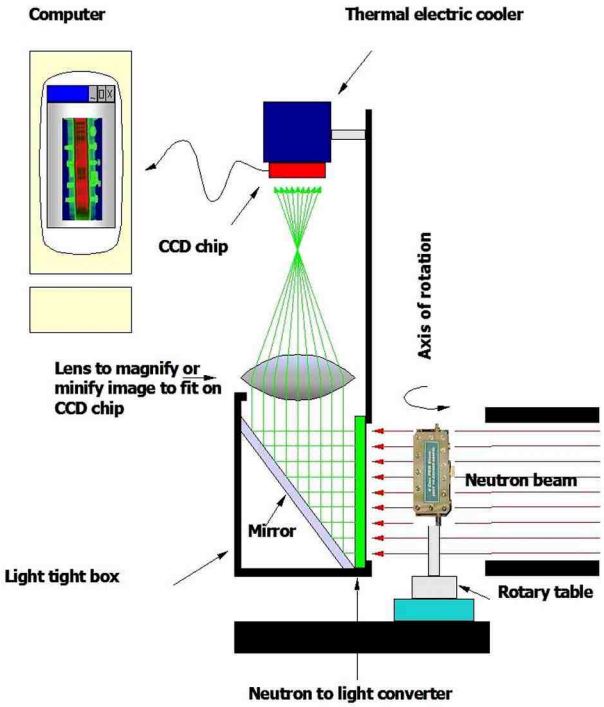

Figure 2. Schematic of Neutron Imaging Setup

general use, but users will be free to bring their own if needed.

To establish operating parameters for the new imaging station, we rotated a 4-cell stack in a high intensity thermal beam at the NCNR reactor and obtained three-dimensional images of the fuel cell as normally done during a medical imaging CAT scan. The cell was imaged while operating with a typical output of about 2.5 A at 3.5 V, and the water (and water vapor) profile in the flow channels was recorded as a function of time (about 1 frame a second). A sample of the water distribution is shown in Figure 3. A graph of the total water content as a function of time is shown in Figure 4. The water content shows periodic behavior with time. From time-lapse images it appears that the water drains only when it reaches a certain volume. The periodic drainage also seems to be un-correlated with the temperature fluctuation and hydrogen flow variations (which were small and random; inconsistent with observed periodicity). The most likely explanation is surface adhesion of water and/or capillary action by the flow channels. We plan to repeat these experiments in a more controlled environment in the near future. The quantification of time-dependent water distribution like this can be very useful in theoretical modeling of fuel cell water transport characteristics.

Conclusions

- A new imaging facility for fuel cell research is expected to be operational in October, 2002. It is a user facility open to researchers from fuel cell manufacturers and automotive companies as well as academic institutions and national laboratories.
- We have been able to observe time dependent water distribution in an operating fuel cell. The result should be useful in modeling water transport mechanism and design of flow channels. We plan to collaborate with University of Miami (among others) in this regard.

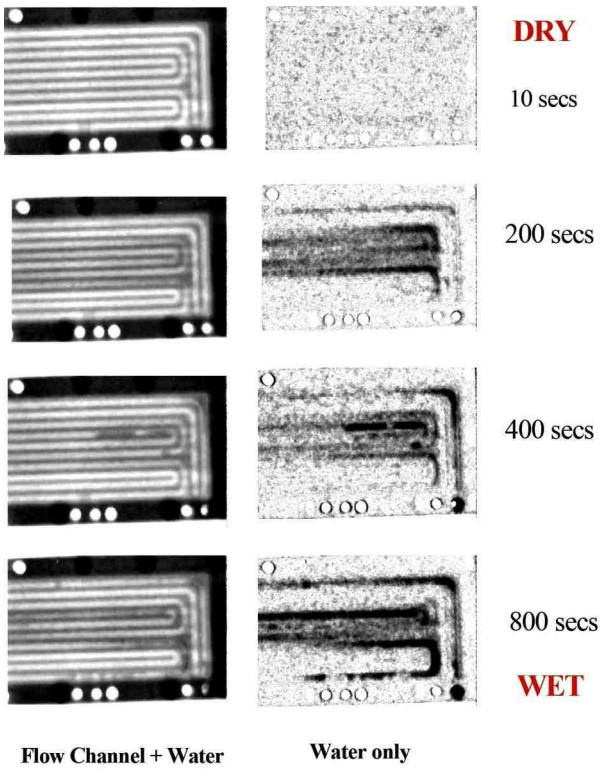

Figure 3. Water Distribution in Flow Channels

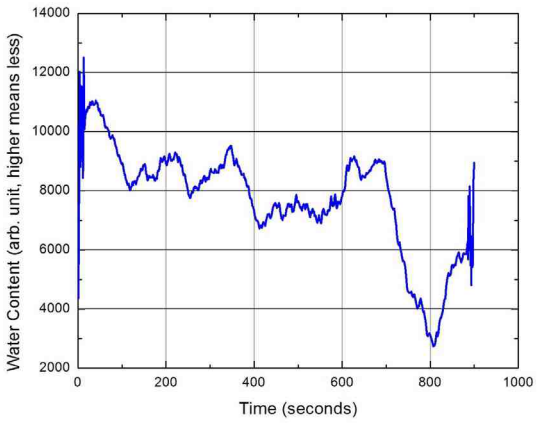

Figure 4. Total Water Content in the Fuel Cell as a Function of Time

IV.D.16 Direct Methanol Fuel Cells

Piotr Zelenay (Primary Contact), Eric Brosha, John Davey, Christian Eickes, Robert Fields, Michael Hickner, Don McMurry, Bryan Pivovar, Geraldine Purdy, John Ramsey, John Rowley, Mahlon Wilson, Christine Zawodzinski, Thomas Zawodzinski, and Yimin Zhu
Materials Science and Technology Division
Los Alamos National Laboratory
Los Alamos, New Mexico 97545
(505) 667-0197, fax : (505) 665-4292, e-mail : zelenay@lanl.gov

DOE Technology Development Managers: Nancy L. Garland and JoAnn Milliken
(202) 586-5673, fax: (202) 586-9811, e-mail: Nancy.Garland@ee.doe.gov
(202) 586-2480, fax: (202) 586-9811, e-mail: JoAnn.Milliken@ee.doe.gov

Objectives

- Develop materials, components and operating conditions of direct methanol fuel cells (DMFCs) for transportation and portable applications optimizing power density, overall fuel conversion efficiency and cost. In particular:
- Design and optimize membrane-electrode assemblies (MEAs) to enhance cell performance.
- Advance electrocatalysis of methanol oxidation and oxygen reduction, thus allowing lower total precious metal loading and/or better cell/stack performance.
- Demonstrate viability of cell components in short- and long-term operation of single cells and stacks.

Approach

- Build and operate single cells and prototype DMFC stacks with different anode and cathode catalysts, membrane materials, flow patterns and optimized MEAs to maximize performance and demonstrate stability.
- Perform complete electrochemical and non-electrochemical testing to gain insight into key factors impacting performance and durability of direct-methanol fuel cells.
- Model, design and fabricate hardware components to optimize performance of single cells and short stacks.

Accomplishments

Catalyst Research

- Identified an alternative binary platinum- patent pending/Carbon (Pt-X/C) cathode catalyst allowing DMFC operation at a voltage 60-80 millivolts (mV) higher than state-of-the-art platinum/carbon (Pt/C) catalysts.
- Established in-house catalyst fabrication capability, by which otherwise unavailable catalysts can be synthesized, e.g., 80 weight percent Pt/C catalyst for the DMFC cathode.
- Optimized composition of cathodes with significantly reduced Pt loading, thus achieving 0.15 watt per centimeter squared (W cm^{-2})with a total precious metal loading of 1.2 milligrams (mgs) cm^{-2} (80°C).
- Completed study of the effect of platinum-to-ruthenium (Pt-to-Ru) ratio on anode performance, demonstrating optimum performance with 55±5 atomic percent of Ru in the anode catalyst layer.

Membrane Research

- Determined sulfonation level and processing method as key to the performance of new sulfonated poly (arylene ether sulfone) membranes (BPSH membranes).
- Developed fabrication techniques and demonstrated BPSH MEAs with relative in-cell selectivity up to 2.5 times that of Nafion®-based MEAs.

Stack Research and Development

- Designed and fabricated components for a new 22 W stack for portable power applications and a new 500 W stack for auxiliary power unit (APU) applications.
- Tested novel hardware designs in single cells and prototype stacks with very good results.

Future Directions

- Continue fundamental research and development of electrocatalysts for methanol oxidation and oxygen reduction.
- Improve performance by optimizing hydrophilic/hydrophobic properties of the cathode.
- Determine the effect of sulfonation on performance of BPSH membranes in DMFCs; narrow the gap between bench-top and fuel cell selectivity of alternative membranes.
- Demonstrate durability of Nafion®-based MEAs in short stacks for 500 hours and alternative MEAs in single cells for 100 hours.
- Investigate composition of the DMFC cathode exhaust at various operating conditions.
- Complete 500 W stack for auxiliary power applications.

Introduction

Direct methanol fuel cell research at Los Alamos National Laboratory (LANL) has focused on developing materials, components and operating conditions relevant to potential applications in portable power (commercial electronics, battery replacement for the military) and transportation (vehicular propulsion, on-board auxiliary power units). The main objective of the LANL research effort in the area of direct methanol fuel cells has been to demonstrate that DMFC-based systems stand a good chance of meeting power-density, overall energy-conversion efficiency and cost targets outlined in the DOE Hydrogen, Fuel Cells and Infrastructure Technologies Program.

Results

In our FY 2002 research, we have focused on the performance of carbon-supported cathode catalysts, especially at low Pt loading. A major achievement has been the introduction of a new binary catalyst, Pt-X (patent application pending). In addition to showing higher activity towards oxygen (concluded from hydrogen/air fuel cell testing), this catalyst appears to be less susceptible to the detrimental action of the crossover methanol than regular Pt/C catalyst. As a consequence of higher activity in the oxygen reduction reaction and improved methanol tolerance, the Pt-X/C catalyst allows DMFC operation at a voltage 60-8-mV high than the voltage achievable with a state-of-the-art commercial PT/C catalyst (De Nora) at the same Pt loading of 0.6 mg cm^{-2} (Figure 1).

We have found that cathodes with significantly reduced Pt loading seem to benefit from the use of carbon-supported catalysts. A comparison of the activity of unsupported Pt cathode catalyst with the activity of carbon-supported Pt catalyst (40% Pt by weight) indicates that carbon-supported catalysts outperform unsupported catalysts as long as Pt loading remains below *ca.* 1 mg cm^{-2}. Also, carbon-supported Pt and Pt-X cathodes both require careful optimization of the ionomer content in the catalyst layer, with the best results obtained at a weight fraction of recast Nafion® between 30 and 40%. Once the anode and cathode catalyst layers are optimized, a very good DMFC performance can be

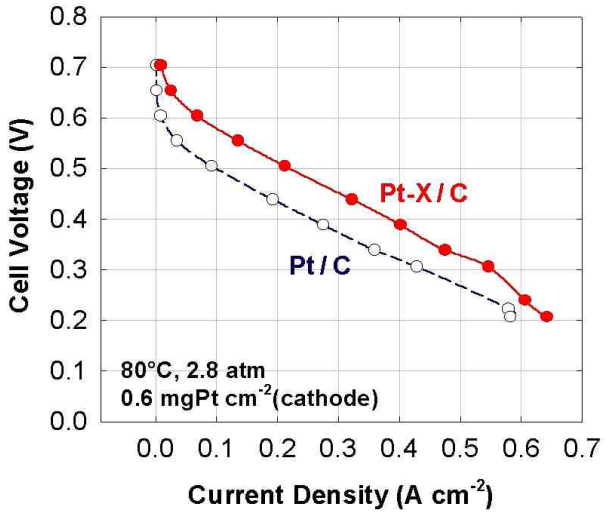

Figure 1. DMFC Performance of Pt-X/C and Pt/C Cathode Catalysts at 80°C - Cathode Pt Loading 0.6 mg cm^{-2}.

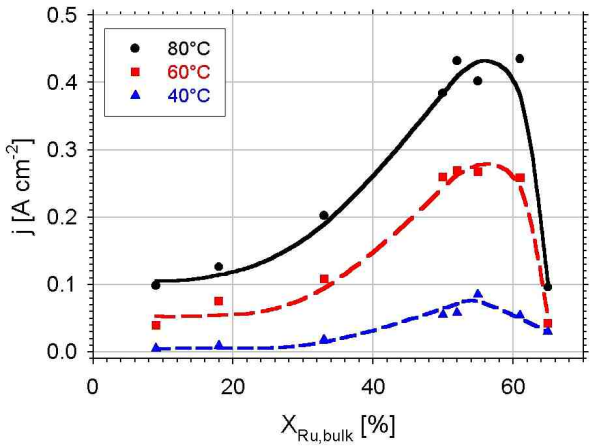

Figure 2. Performance of unsupported Pt-Ru anode catalyst as a function of atomic content of ruthenium in the bulk catalyst phase; current density determined from the anode polarization plots at a potential of 0.35 V *vs.* dynamic hydrogen electrode.

achieved with even moderate Pt loading. One of the highlights of our DMFC research in FY 2002 has been reaching 0.15 W cm^{-2} in aerial power density with a total (anode + cathode) Pt loading of only 1.2 mg cm^{-2} (80°C).

Continuing our anode catalyst effort, we have completed a performance study of unsupported Pt-Ru catalysts, with a Pt-to-Ru atomic ratio ranging from 9:1 to 1:2. This study, conducted in collaboration with Johnson Matthey, has shown that, regardless of the cell operating temperature, the highest activity towards methanol is achieved with catalysts containing 55±5 at% of Ru in the bulk phase (Figure 2). Voltammetric stripping of surface CO has further revealed that the corresponding surface composition of the best-performing catalysts is approximately 30 at% of Ru.

In the past year, we have come considerably closer to the introduction of new ionomeric membranes into direct methanol fuel cells. Most of our membrane/MEA research has focused on the BPSH polymer (collaboration with Virginia Tech). We have found that membrane processing, such as boiling in acidic aqueous solutions, greatly affects the polymer morphology, ability to partially block methanol crossover and, consequently, selectivity in DMFC operation. Once processed, membranes with somewhat lower sulfonation level, BPSH-35 rather than BPSH-40, have been found to perform better in an actual DMFC. A very significant accomplishment of the membrane research in FY 2002 has been successful fabrication and testing of BPSH-based MEAs in direct methanol fuel cells. As shown in Figure 3, these MEAs are capable of performing comparably, if not better, than state-of-the-art MEAs using Nafion®. In addition to offering good cell performance, BPSH MEAs has been found to reduce methanol crossover by as much as 58%, from ~0.12 A cm^{-2} (Nafion® 117) to ~0.05 A cm^{-2} (processed BPSH-35),

Although fundamental research has remained the focal point of the DMFC project at LANL, we have continued prototyping DMFC stacks for the portable power applications and auxiliary power units to prove practical viability of core technology developed at LANL, identify possible scale-up issues, and verify adaptability of the technology to complete systems developed by our partner, Ball Aerospace & Technologies Corporation.

Cell components for a portable power stack have been optimized in single-cell and short-stack testing. The first twenty-two-cell 22 W stack has been built and tested, showing respectable performance at ambient cathode pressure (0.75 atmospheres [atm]),

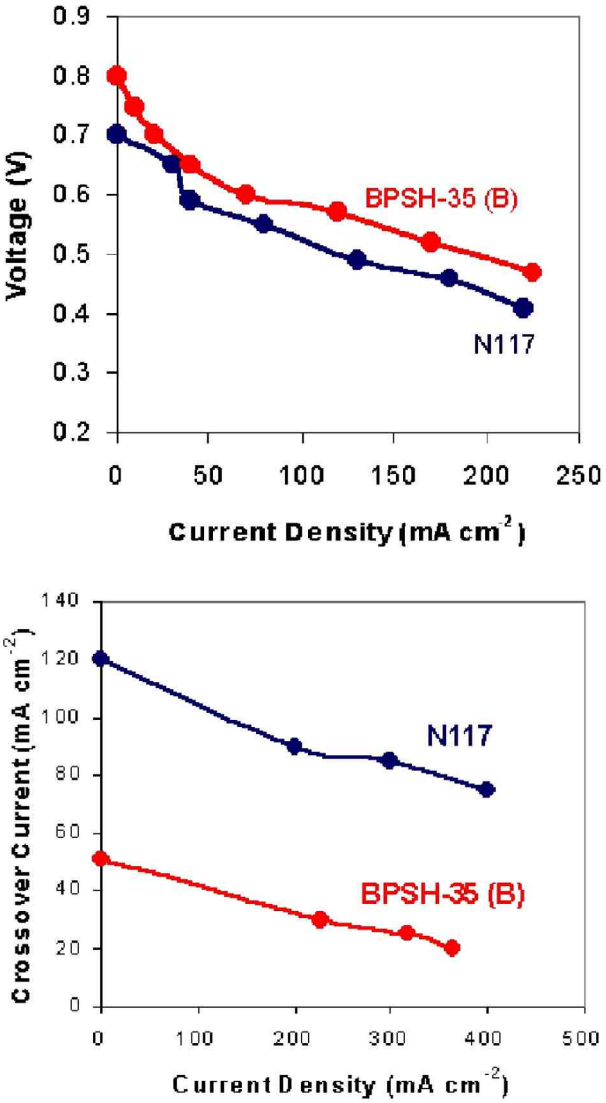

Figure 3. Cell Polarization and Methanol Crossover Plots Obtained with BPSH-35 (pre-processed by boiling) and Nafion® 117 at 80°C - Cell Polarization Data Taken at Ambient Cathode Pressure C_{MeOH}=1.0 mol per liter

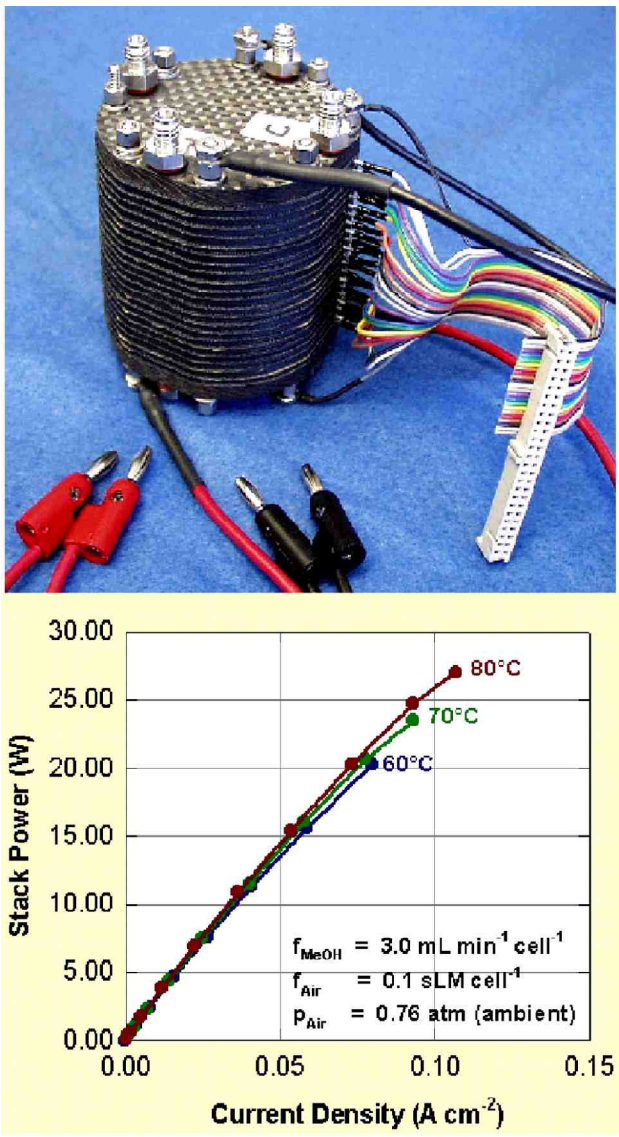

Figure 4. 22 W Portable Power DMFC Stack and selected Performance Data

low air flow (stoichiometry below 3) and relatively high voltage of 0.55 V/cell (Figure 4).

The first-generation APU hardware for MEAs with 100 cm^2 in the active area has been based on high-conductivity graphite plates. The maximum power generated by a single APU cell has been 21 W at a total cathode pressure of 2.8 atm and air stoichiometry of 2.1 (Figure 5). The same cell has delivered *ca.* 11 W at a cathode pressure of 0.76 atm (ambient) and air stoichiometry of only 1.3 (without accounting for the air needed to handle methanol crossover).

Conclusions

DMFC research at LANL in FY 2002 has focused primarily on fundamental issues relevant to potential portable and transportation applications of direct methanol fuel cells, such as cathode and anode electrocatalysis, electrode composition and structure, membrane properties and MEA design. Substantial progress has been achieved in cathode research,

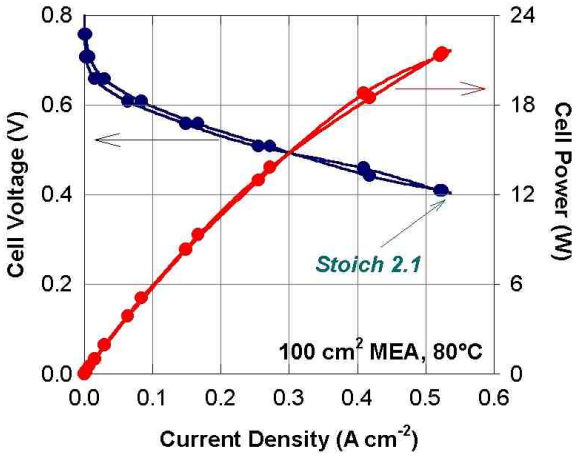

Figure 5. Development of 500 W DMFC stack for auxiliary power system: Single cell polarization and power plots.

which includes the introduction of a highly promising binary catalyst and optimization of catalyst layers at a low Pt loading. The most active composition of the unsupported Pt-Ru anode catalyst has been identified. Major progress has been made in membrane/MEA research, with alternative membrane materials exhibiting greatly reduced crossover rates and in-cell performance at the same, or higher, level as obtained with Nafion® 117. The core MEA technology and fuel cell hardware developed at LANL over the past few years has been incorporated into components for the prototype 22 W and 500 W DMFC stacks for prospective portable and APU use, respectively. The first 22 W stack has been built and tested at ambient cathode pressure and low flow of air, with results clearly demonstrating significant practical potential of DMFCs.

FY 2002 Publications/Presentations

1. Adsorption on Fuel Cell Nanoparticle Electrodes: A Radioactive Labeling Study," P. Waszczuk, A. Wieckowski, P. Zelenay, S. Gottesfeld, C. Coutanceau, J.-M. Léger and C. Lamy, *J. Electroanal Chem.*, 511, 55-64 (2001).

2. Direct Methanol Fuel Cells at Reduced Catalyst Loadings," P. Zelenay, F. Guyon and S. Gottesfeld, in *Direct Methanol Fuel Cells*, S. R. Narayanan, S. Gottesfeld and T. Zawodzinski (Eds.), ECS Proceedings, Electrochemical Society, Pennington, New Jersey, vol. 2001-4, pp. 123-135 (2001).

3. 80 Watt Direct Methanol Fuel Cell Stack for Portable Power Applications", X. Ren, J. Davey, H. Dinh, B. Pivovar, C. Rice, S. Gottesfeld, and P. Zelenay, in *Fuel Cell Technology: Opportunities and Challenges*, Topical Conference Proceedings, 2002 AIChE Spring National Meeting, March 10-14, 2002, New Orleans, Louisiana.

4. Direct Methanol Fuel Cell Performance Using Sulfonated Poly(arylene ether sulfones) Random Copolymers as Electrolytes", B. Pivovar, M. Hickner, J. McGrath, P. Zelenay, and T. Zawodzinski, in *Fuel Cell Technology: Opportunities and Challenges*, Topical Conference Proceedings, 2002 AIChE Spring Meeting, March 10-14, 2002, New Orleans, Louisiana.

5. Influencing the Transport of Water, Methanol and Protons through a Fuel Cell Ion Exchange Membrane", M. Hickner, F. Wang, Y. Kim, B. Pivovar, T. Zawodzinski and J. McGrath, in *Fuel Cell Technology: Opportunities and Challenges*, Topical Conference Proceedings, 2002 AIChE Spring Meeting, March 10-14, 2002, New Orleans, Louisiana.

6. Joint 200th Meeting of the Electrochemical Society and 52nd Meeting of the International Society of Electrochemistry, San Francisco, CA, September 2-7, 2001. Title: "Development of Freeze-Dried Catalysts for Hydrogen and Direct Methanol Fuel Cells"; E. L. Brosha*, S. Pacheco, F. Uribe, H. Garzon, T. A. Zawodzinski.

7. Joint 200th Meeting of the Electrochemical Society and 52nd Meeting of the International Society of Electrochemistry, San Francisco, CA, September 2-7, 2001. Title: "Problems with Membrane Electrode Assemblies for Non-Nafion® Based Membranes"; B. S. Pivovar*, M. Hickner, J. E. McGrath, P. Zelenay and T. A. Zawodzinski.

8. 4th Hawaii Battery Conference 2002, Waikoloa, HI, January 8-11, 2002. Title: "Direct Methanol Fuel Cell Research and Development at Los Alamos National Laboratory" P. Zelenay (*invited lecture*).

9. 2002 Spring National Meeting of American Institute of Chemical Engineers, New Orleans, LA, March 10-14, 2002. Title: "80 W Direct Methanol Fuel Cell Stack for Portable Power Applications"; X. Ren, J. Davey, B. S. Pivovar*, H. N. Dinh, C. Rice, S. Gottesfeld, P. Zelenay.

10. 2002 Spring National Meeting of American Institute of Chemical Engineers, New Orleans, LA, March 10-14, 2002. Title: "Direct Methanol Fuel Cell Performance Using Sulfonated Poly(arylene ether sulfone) Random Copolymers as Electrolytes"; B. S. Pivovar*, M. Hickner, F. Wang, J. McGrath, P. Zelenay, T. A. Zawodzinski.

11. MRS Spring Meeting, San Francisco, CA, April 2, 2002. Title: "System and Material Issues in Direct Methanol Fuel Cells"; B. S. Pivovar (*invited talk*).

12. 223rd Meeting of American Chemical Society, April 7-11, Orlando, FL. Title: "Electrocatalysis in Direct Methanol Fuel Cells"; P. Zelenay (*keynote lecture*).

13. 223rd Meeting of American Chemical Society, April 7-11, Orlando, FL. Title: "DMFC Activity of Pt:Ru Blacks of Different Composition"; C. Eickes*, P. Zelenay, T. Morita and D. Thompsett.

14. 223rd Meeting of American Chemical Society, April 7-11, Orlando, FL. Title: "Novel Pt/Ru Catalyst for the DMFC Anode: Electrochemical Cell and DMFC Testing"; P. Waszczuk, H.-S. Kim, A. Wieckowski, Y. Zhu, P. Zelenay*.

15. 201st Meeting of the of the Electrochemical Society, Philadelphia, Pennsylvania, May 12-17, 2002. Title: "DMFC Cathode Catalyst with Improved Methanol Tolerance"; Y. Zhu*, P. Zelenay.

16. Annex XI Meeting of International Energy Agency Meeting, May 17-18, 2002, Philadelphia, Pennsylvania, Title: "80 W DMFC Stack and Performance Data"; X. Ren, J. Davey, B. S. Pivovar, H. N. Dinh, C. Rice, S. Gottesfeld, P. Zelenay*.

IV.D.17 Development of Advanced Catalysts for Direct Methanol Fuel Cells

S. R. Narayanan
Jet Propulsion Laboratory
California Institute of Technology
Pasadena, California 91109
(818) 354-0013, fax: (818) 393-6951, e-mail: s.r.narayanan@jpl.nasa.gov

DOE Technology Development Managers:
JoAnn Milliken: (202) 586-2480, fax: (202) 586-9811, e-mail: JoAnn.Milliken@ee.doe.gov
Nancy Garland: (202) 586-5673, fax: (202) 586-9811, e-mail: Nancy.Garland@ee.doe.gov

Objectives

- Reduce catalyst cost for direct methanol fuel cells (DMFCs).
- Demonstrate feasibility of reducing Pt-Ru catalyst loading to 0.5 mg/cm^2 using thin film deposition techniques.
- Develop a low-cost manufacturing technique for MEA fabrication.
- Prepare and identify low-cost alternatives to Pt-Ru based on Ni, Zr, and Ti catalysts.

Approach

- Utilize direct current (DC) magnetron sputter-deposited multi-component catalyst layers.
- Employ reactive sputter-deposition of alloys and oxides.
- Characterize half-cells and full cell MEAs electrochemically.
- Characterize structural and electronic properties.

Accomplishments

- Platinum-Ruthenium alloy films of various compositions have been sputter-deposited and characterized in half-cells and full cells.
- Fuel cell performance has been improved from 100 mW/mg to 800 mW/mg at 0.1 mg/cm^2 of catalyst at the anode.
- Effect of reactive co-sputtering of RuO_x has been studied and determined not to have any beneficial effect.
- A unique metal nanostructure has been developed by pretreatment of Nafion films.

Future Directions

- Prepare and characterize ternary Pt M_x M_y films by December 2002.
- Deposit corrosion resistant alloy films of base metals by June 2003.
- Demonstrate 2000 mW/mg by June 2003.
- Characterize metal/metal oxide systems by December 2003.
- Demonstrate 2500 mW/mg by June 2004.

Introduction

Fuel cells offer the possibility of reduced emissions and high efficiency for transportation applications. Of the various fuel cells being considered, the direct methanol fuel cell (DMFC) is very attractive due to the key advantages of reducing system complexity and potentially improving transient response compared to reformate-air fuel cell systems. However, DMFCs currently require unsupported noble metal catalysts at high loadings of 2.5 – 4.0 mg/cm^2, leading to a high catalyst cost of $100-150/kW. Also, to keep the overall fuel cell cost low, the preferred method of catalyst application must be designed for manufacturing. Thus, cost presents a major obstacle to commercialization of DMFCs. Enhancement of the efficiency of this fuel cell is also necessary to achieve the required weight and volume required for transportation applications. This research effort aims at addressing these key issues of cost and efficiency.

The overall objective is to develop new methods of preparing electrocatalysts, novel electrode structures, and new-low cost electrocatalysts that will result in overall cost reduction and improved performance of direct methanol fuel cells.

The specific objectives are:

- Reduce the catalyst loading levels of Pt-alloy in DMFCs to 0.5 mg/cm^2 or less
- Develop new low-cost methods of fabricating membrane-electrode assemblies
- Prepare catalysts with enhanced activity for methanol electro-oxidation
- Develop non-noble metal methanol oxidation catalysts.

Approach

The Jet Propulsion Laboratory (JPL) has researched the stated objectives by investigating sputter-deposition (SD) of designed anode and cathode nanostructures of Pt-alloys, and electronic structures and microstructures of sputter-deposited catalyst layers. JPL has used the information derived from these investigations to develop novel catalysts and membrane electrode assemblies (MEAs) that will meet the DOE objectives of lower fuel cell cost and high performance.

SD is routinely used to deposit thin films and has proven benefits from economies of scale in the metallization of plastics. The technique has already been used to create enhanced and unique MEAs for H_2-air proton exchange membrane fuel cell (PEMFC) systems. In this project, JPL is pursuing the use of SD to create DMFC membrane electrode assembly structures with highly electro-active catalyst layers that will reduce the amount and cost of the Pt-alloy catalyst at the fuel cell anode.

The research involves the development of techniques for deposition of porous catalyst layers by defining the conditions of pressure, sputter rates, and target configurations that will result in appropriate compositions and morphology for the catalyst layer. The effect of catalyst structure and composition on the activity of the catalyst layers will be characterized by x-ray diffraction (XRD), x-ray photoelectron spectroscopy (XPS), scanning electron microscopy (SEM), x-ray absorption spectroscopy (XAS), and electrochemical polarization studies in half cells and full cells. New base metal and noble metal alloys and oxides will also be studied with an aim to identify new compositions that will result in enhanced activity. The catalyst activity target is 2500 mW/mg of anode catalyst.

Results

The main focus of this year's effort has been on the deposition and characterization of platinum-ruthenium films of various compositions produced by co-sputtering of the individual elements. The effect of ruthenium deposited by reactive co-sputtering has also been studied. The sputtering chamber was modified with a linear drive to be able to produce films on graphite foils, porous carbon structures, and on membranes. Thin films were deposited on graphite foil electrodes and characterized by XRD, XPS, SEM and polarization experiments.

XRD results indicate that the alloy phase exhibits continuous change in lattice parameter and a change in structure from a face-centered cubic (fcc) to a hexagonal close pack (hcp) lattice consistent with the

formation of a solid solution. The alloy deposit exhibits fine grain characteristics with crystallite size of about 15-25 nanometers. These grain sizes are about 3 to 4 times smaller than those observed in chemically prepared materials. Electrochemical activity as measured in half-cells and full-cells increases with platinum content, and the lowest Tafel slopes were obtained for a bulk composition of 50/50 atomic weight % of Pt/Ru. XPS analysis indicated small amounts of oxides of platinum and ruthenium on the surface. The oxide content was approximately 30% and did not seem to depend on the metal composition.

Cyclic voltammetric studies indicated that the activity of the Pt-Ru films increased with operating temperature just as in conventional catalyst layers produced from unsupported catalyst inks. Membrane electrode assemblies were fabricated from Pt-Ru films of the most active compositions, and a power density of 800 mW/mg was realized for anodes that were deposited with about 0.1 mg/cm^2 of Pt-Ru (see Figure 1). Applying the catalyst layers by sputter deposition on the electrode was found to yield better performance than applying them on the membrane. This was attributed to the enhanced electrical connectivity achieved when the catalyst layer is applied on the electrode. However, this is only true for very thin films. When thicker composite films are produced, such as those planned later in this project, good electrical connectivity may be achieved even with membrane deposition.

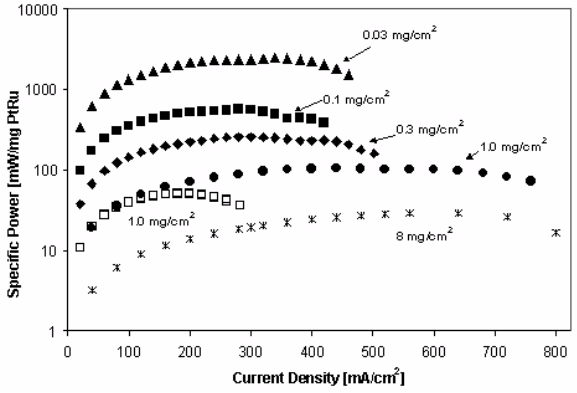

Figure 1. Catalyst Utilization Curves for Sputter-Deposited (filled symbols), Carbon Supported (□, 1.0 mg/cm^2), and Conventional (∗, 8.0 mg/cm^2) Pt-Ru

SEM photographs of sputtered films show that the layers are fairly dense and appear to crack into platelets when subjected to MEA fabrication. The dense films do not lend themselves to high surface areas; therefore, there is substantial scope for enhancement of performance if the surface area can be increased. This may be achieved by producing porous 3-D Pt-Ru layered structures. One such method for creating such 3-D structures, that seem to be extremely promising, involves the pre-treatment of the membrane surface by ion-beam etching, which is then followed by sputter-deposition of the metal. This results in substantially enhanced surface area and very rough nanostructures. Next year's effort will include characterization of such films.

Electrodes were fabricated with catalyst layers containing platinum-ruthenium alloys and platinum-ruthenium oxide. Membrane electrode assemblies were fabricated with such cells, and the performance was evaluated in a full cell configuration. Although ruthenium oxide is a proton conductor and is expected to enhance the rate of proton transport from the interface during methanol oxidation, no noticeable improvement in activity of the catalyst layer was observed by addition of ruthenium oxide. The role of other metal oxides such as tungsten oxide will be investigated next year, along with evaluation of non-noble metal catalysts based on nickel, titanium, and zirconium.

Conclusions

High catalyst activity and utilization of sputtered thin films was demonstrated in operating fuel cells. Optimal sputter-deposition conditions for platinum-ruthenium alloys have been determined. The effect of composition on the performance of Pt-Ru films was studied, and optimal composition has been determined. Novel methods of enhancing surface area and improving porosity have been identified. Co-sputtered ruthenium oxide has been demonstrated not to have any significant beneficial effect on the activity of the catalyst layers. While cost presents a major obstacle to commercialization of DMFCs for mobile applications, this project demonstrates novel means to reduce the catalyst costs in DFMC fuel cells. Efficiency enhancements that are also necessary for DMFCs to be viable will be addressed

in the subsequent phases of the project under the development of new catalysts.

Publications and Presentations

1. C. K. Witham,T.I. Valdez, and S. R. Narayanan, "Nanostructured Catalysts for Direct Methanol Fuel Cells", 200th Electrochemical Society Meeting, Philadelphia, May 2002

2. C. K. Witham, T. I. Valdez, and S. R. Narayanan, "Methanol Oxidation Activity of Co-Sputter Deposited Pt-Ru Catalysts", Proceedings of the Symposium on Direct Methanol Fuel Cells, Electrochemical Society, PV 2001-4, p.123

IV.D.18 Carbon Composite Bipolar Plates

T. M. Besmann (Primary Contact), J.W. Klett, and J. J. Henry, Jr.
Surface Processing and Mechanics Group and Carbon and Insulating Materials Group
Oak Ridge National Laboratory, P.O. Box 2008, MS 6063, Bldg. 4515
Oak Ridge, TN 37831-6063
(865) 574-6852, fax: (865) 574-6198, e-mail: besmanntm@ornl.gov

DOE Technology Development Managers:
JoAnn Milliken: (202) 586-2480, fax: (202) 586-9811, e-mail: JoAnn.Milliken@ee.doe.gov
Nancy Garland: (202) 586-5673, fax: (202) 586-9811, e-mail: Nancy.Garland@ee.doe.gov

ORNL Technical Advisor: David Stinton
(865) 574-4556, fax: (865) 574-6918, e-mail: stintondp@ornl.gov

Objectives

- Develop a slurry molded carbon fiber material with a carbon chemical vapor infiltrated sealed surface as a bipolar plate.
- Collaborate with potential manufacturers with regard to testing and manufacturing of such components.

Approach

- Fabricate fibrous component preforms for the bipolar plate by slurry molding techniques using carbon fibers of appropriate lengths.
- Fabricate hermetic plates using a final seal with chemical vapor infiltrated carbon.
- Develop commercial-scale components for evaluation.

Accomplishments

- Developed carbon composite material with graphite particulate filler to control pore size and speed surface sealing.
- Further characterized and measured mechanical properties of carbon composite plate material.
- Significantly improved wetting of bipolar plate surface.
- Determined surface roughness of finished bipolar plate components.
- Supported scale-up efforts at licensee Porvair Fuel Cell Technology.

Future Direction

- Develop bipolar plate materials/configurations to meet various users' unique requirements.
- Improve wetting properties of carbon surfaces.
- Decrease component thickness.
- Transfer technology and aid in scale-up with Porvair.

Introduction

In FY 2002, the Oak Ridge National Laboratory (ORNL) carbon composite bipolar plate effort has achieved several programmatic goals in measuring plate properties and improving wetting. It is necessary to have accurate mechanical property information for the bipolar plates in order to assure they will survive handling, assembly, and service. These measurements need to go beyond simple tensile or flexure strength, since the relatively thin plates will be subjected to combined tension-torsion loading in assembly and to potentially high rates of stress during handling and service. Thus, torsion behavior and fracture toughness are particularly important to understand. Measurements of these properties, along with methodologies to demonstrate material uniformity through thermal imaging, have been developed.

Approach

Fibrous component preforms for the bipolar plate are prepared by slurry molding techniques using 100-µm carbon fibers (e.g., Fortafil) in water containing phenolic resin followed by curing. Molds are used to impress channels and other features into the preform, and the surface of the preform was sealed using a chemical vapor infiltration (CVI) technique in which carbon is deposited on the near-surface fibers sufficient to make the surface hermetic. In the current work, differing amounts of carbon flake filler were used and the effects on properties determined. Infrared imaging to identify defects and inhomogeneities was performed by heating one side of the samples and imaging the opposite side. Shear stress is a good measure of torsion behavior. Thus, the Iosipescu method was used to measure shear properties, whereby the shear strength of one of the different material shear planes of a composite may be determined by loading a coupon in the form of a rectangular flat strip with symmetric centrally located V-notches using a mechanical testing machine and a four-point asymmetric fixture. Failure of the specimen occurs by shear between the V-notches. The efforts to improve wetting of the carbon surface consisted of briefly heating the components to 1000°C in air.

Results

Slurry-molded preforms 2.5 mm in thickness were produced and cut into 5-cm squares. Illustrative results of the thermal imaging are seen in Figure 1. The relative uniformity indicates little density difference within the plates and between plates. There is some indication of delamination along the edges, although this is likely due to cutting of a larger plate into the 5 cm samples.

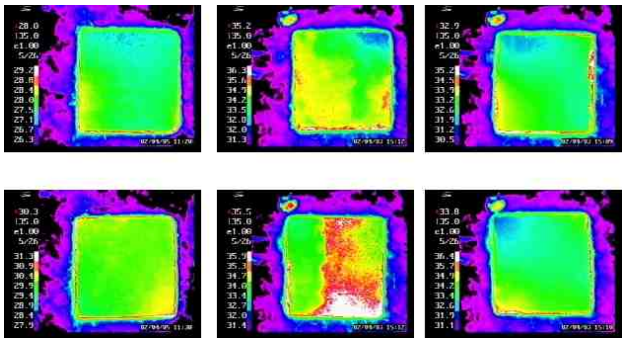

Figure 1. Infrared Images of Carbon Composite Bipolar Plate Material Samples

The Iosipescu torsion measurement results are given in Table 1, with an example stress-displacement curve shown in Figure 2. These values are indicative of a relatively torsion-resistant material, particularly given the low density of the carbon composite. The stress-displacement curves indicate little delamination or other failures until ultimate failure.

Sample (% Filler)	Strength Measurement
PMP10R (0%)	25.9±9.9 MPa
PMP10T (0%)	19.3 MPa (1 test)
PMP09K (15%)	24.4±11.8 MPa
PMP11E (30%)	43.3±2.7 MPa
PMP11G (30%)	17.1±1.1 MPa
PMP11H (30%)	18.7±4.7 MPa

Table 1. Measurements of Shear Stress by the Iosipescu Method for Carbon Composite Samples with Differing Amounts of Carbon Flake Filler

The dramatic improvement in wetting of the carbon composite surface with treatment is seen in Figure 3. Whereas, prior to oxidative treatment, water appeared to have a small wetting angle on the surface of the carbon composite, water readily spread

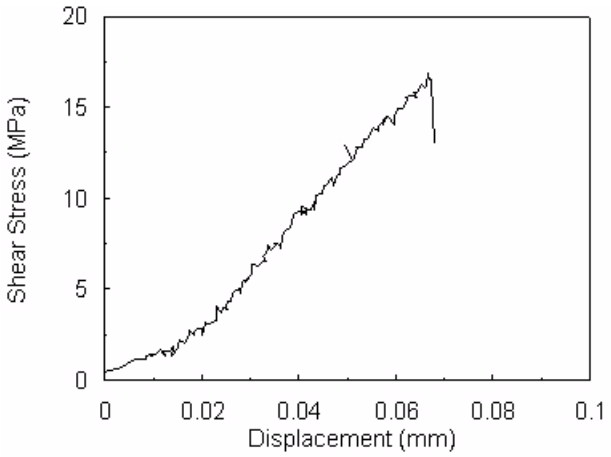

Figure 2. Typical Stress-Displacement Curve for the Iosipescu Torsion Measurement of the Carbon Composite Bipolar Plate Material

on the surface after treatment with an apparent large wetting angle.

Conclusions

During this period, the mechanical properties of the carbon composite bipolar plate material were assessed, including measurements of uniformity and defect distribution by infrared imaging. The results indicate good material uniformity and substantial resistance to torsional stresses. Significant improvement in the wetting of the material was demonstrated after a simple oxidation treatment.

FY 2002 Publications/Presentations

1. T. M. Besmann, J. W. Klett, J. J. Henry, Jr., and T. D. Burchell, "Carbon Composite Bipolar Plates for PEMFC," 26th Annual International Conference on Advanced Ceramics and Composites, January 13-18, Cocoa Beach, FL.

2. T. M. Besmann, J. W. Klett, J. J. Henry, Jr., and E. Lara-Curzio, "Carbon/Carbon Composite Bipolar Plate for PEM Fuel Cells," National Meeting of the American Institute of Chemical Engineers, March 10-14, New Orleans, LA.

3. T. M. Besmann, J. W. Klett, J. J. Henry, Jr., and T. D. Burchell, "Carbon Composite Bipolar Plate for PEMFC," Future Car Congress, June 3-5, Arlington, VA.

Figure 3. Water Illustrates a Much Larger Wetting Angle on the Carbon Composite after Oxidative Treatment

IV.D.19 Cost-Effective Surface Modification for Metallic Bipolar Plates

M.P. Brady
MS 6115, Oak Ridge National Laboratory
P.O. Box 2008, Oak Ridge, TN 37831-6115
(865) 574-5153, fax: (865) 241-0215, e-mail: bradymp@ornl.gov

DOE Technology Development Managers:
JoAnn Milliken: (202) 586-2480, fax: (202) 586-9811, email: JoAnn.Milliken@ee.doe.gov
Nancy Garland: (202) 586-5673, fax: (202) 586-9811, e-mail: Nancy.Garland@ee.doe.gov

ORNL Technical Advisor: David Stinton
(865) 574-4556, fax: (865) 574-6918, e-mail: stintondp@ornl.gov

Objective

- Develop a low-cost metallic bipolar plate alloy that will form an electrically conductive and corrosion resistant nitride surface layer during thermal nitriding to enable use in a PEM fuel cell environment.

Approach

- Conduct a study of the nitridation behavior of a series of model Ni-X and Fe-X base alloys (X = nitride forming elements such as Cr, Nb, Ti, V) that can potentially meet DOE bipolar plate cost goals.
- Identify the most promising combination of X additions, ternary and higher order alloying addition(s), and nitridation reaction conditions that result in the formation of an adherent, dense nitride surface layer.
- Evaluate corrosion behavior in 80°C sulfuric acid solutions to simulate PEM fuel cell environments (in collaboration with K. Weisbrod and C. Zawodzinski of Los Alamos National Laboratory and I. Paulauskas and R.A. Buchanan of the University of Tennessee)
- Characterize nitride layer microstructure and composition by x-ray diffraction, electron probe microanalysis, scanning electron microscopy, and transmission electron microscopy. Use this information in a feedback loop to modify alloy chemistry and nitridation processing conditions to optimize the protectiveness of the nitride surface layer.
- Measure electrical conductivity of select nitrided alloys by D.C. four-point probe.
- Down-select model Ni-Fe-X alloy for in-cell performance evaluation and begin modification and optimization of alloy composition/nitridation conditions for commercial scale up and/or identify nitridation conditions suitable for commercially available alloys (if feasible).

Accomplishments

- A model nitrided Ni-50Cr wt% alloy exhibited no discernible degradation after 1 week immersion in pH 2 sulfuric acid at 80°C and a corrosion current density of less than 1 x 10^{-6} A/cm^2 up to ~ 0.9 V vs. standard hydrogen electrode (SHE) in pH 3 sulfuric acid at 80°C. This level of corrosion resistance is in the range of the goal for metal bipolar plates and warrants scale-up to in-cell testing and evaluation. Further, the Cr-nitride layers formed on the Ni-50Cr alloy grow in a very robust manner such that lack of coverage over features such as stamped flow fields does not appear to be a major issue. Preliminary measurement of electrical properties of a nitrided coupon indicated an electrical conductivity in the $10^4\Omega^{-1}cm^{-1}$ range, which is two orders of magnitude greater than the DOE target.

- Coupons of nitrided Ni-50Cr were delivered to Los Alamos National Laboratory for further corrosion testing and evaluation. Preliminary feedback from ongoing exposure in the Corrosion Test Cell indicate stable electrical resistance (collaboration with K. Weisbrod).
- A United States provisional patent disclosure was submitted in April 2002 for nitrided Ni-Cr and related base alloys.

Future Directions

- Pursue in-cell testing of nitrided Ni-50Cr to determine if the promising corrosion resistance translates to in-cell performance.
- Optimize nitridation conditions and reduce the level of Cr to below 40-42 wt.% in order to improve the cold formability of the alloy and reduce processing and raw material costs (based on input from commercial alloy producers).
- Investigate the nitriding characteristics of existing commercial high-Cr-, Ni- and Fe- base alloys to determine if a similar corrosion resistant Cr-nitride layer can be formed in order to facilitate scale-up and transfer of this technology.
- Establish partnerships with alloy producers and fuel cell manufacturers.

Introduction

The bipolar plate is one of the most expensive components in proton exchange membrane (PEM) fuel cells. Thin metallic bipolar plates offer the potential for significantly lower cost than conventional machined graphite bipolar plates and reduced weight/volume and better performance than developmental carbon fiber and graphite bipolar plates currently under consideration. However, inadequate corrosion resistance can lead to high electrical resistance and/or can contaminate the proton exchange membrane. Metal nitrides (e.g. TiN or Cr_2N) offer electrical conductivities up to an order of magnitude greater than that of graphite and are highly corrosion resistant. Unfortunately, most conventional coating methods for metal nitrides are too expensive for PEM fuel cell stack commercialization or tend to leave pin-hole defects, which result in accelerated local corrosion and unacceptable performance.

Approach

The goal of this effort is to develop a bipolar plate alloy that will form an electrically conductive and corrosion resistant nitride surface layer during thermal (gas) nitriding. There are three advantages to this approach. First, because the nitriding is performed at elevated temperatures, pin-hole defects are not expected because thermodynamic and kinetic factors favor complete conversion of the metal surface to nitride. Rather, the key issues are nitride layer cracking, adherence, and morphology (discrete internal precipitates vs. continuous external scales), which can potentially be controlled through proper selection of alloy composition and nitridation conditions. Second, thermal nitridation is an inexpensive, well-established industrial technique. Third, the alloy can be formed into final shape by inexpensive metal forming techniques such as stamping prior to thermal nitridation.

Results

A series of model Ni-base alloys with additions of (5-15)Ti, (5-10)Nb, (10-15)V, (5-10)Nb + (5-15)V and (35-50)Cr wt%, to form external Ti, Nb, V, Nb+V, or Cr based nitride layers, was studied (Table 1). Ni was selected as the initial alloy base because it is relatively inexpensive ($2-4/lb), has good ductility, doesn't compete with Cr during thermal nitridation, and exhibits a relatively low permeability to nitrogen, which favors external nitride layer formation.

Corrosion behavior was screened by a 1 week immersion in pH 2 sulfuric acid at 80°C in order to optimize alloy composition and nitridation conditions. Anodic polarization testing was then conducted on the most promising nitrided alloys in aerated pH 3 sulfuric acid at 80°C to quantify

Alloy Base (wt.%)	Nitridation Conditions (high-purity nitrogen)		Nitrogen Uptake (mg/cm^2)
	Temperature	Time (h)	
Ni-(5-15)Ti	1000-1100°C	8-48	0.1-1
Ni-(5-10)Nb	900-1100°C	1-48	0.1-2
Ni-(10-15)V	1100°C	24-48	0.5-1
Ni-(5-10)Nb-(5-15)V	1100°C	24-48	0.5-1
Ni-(35-50)Cr	1100°C	1	1.5-2

Table 1. Summary of Nitriding Conditions

corrosion resistance. A corrosion current density of less than 1 x 10^{-6} A/cm^2 up to a range of approximately 0.9 V vs. standard hydrogen electrode (SHE) was considered indicative of sufficiently promising behavior to warrant further development and future in-cell stack testing.

Nitrided Ni-(5-10)Ti base alloys (to form an external TiN base layer) exhibited relatively low corrosion currents (Figure 1). However, regions of through thickness local attack of the TiN surface layer were evident in most of the coupons. Nitrided Ni-(5-10)Nb + (5-15)V wt% base alloys formed external Ni-Nb-V-N and Nb-V-N scales which resulted in good corrosion resistance in the 1 week immersion screening in pH 2 sulfuric acid at 80°C (weight loss <-0.05 mg/cm^2) but exhibited high corrosion currents in the anodic polarization testing (10^{-5}– 10^{-4} A/cm^2 range at 0.9 V vs. SHE). The Ni-(10-15)V wt% alloys formed external V-N layers after the nitridation treatment, but exhibited relatively high weight losses in the sulfuric acid immersion screenings (3-5 mg/cm^2 loss after 1 week). External Nb-N layers could not be formed on Ni-(5-10)Nb wt.% alloys under the nitridation conditions used in the present work (Table 1).

Of the nitrided alloys examined, Ni-50Cr wt.% exhibited the most corrosion resistance and met the target corrosion current of less than 1 x 10^{-6} A/cm^2 up to ~ 0.9V vs SHE in pH 3 sulfuric acid at 80°C (Figure 1 and Table 1). The post-nitridation microstructure of all the Ni-Cr alloys (35Cr, 45Cr, 50Cr wt.%) examined, nitrided for 1-2 h at 1100°C in nitrogen, consisted of external Cr_2N overlying a

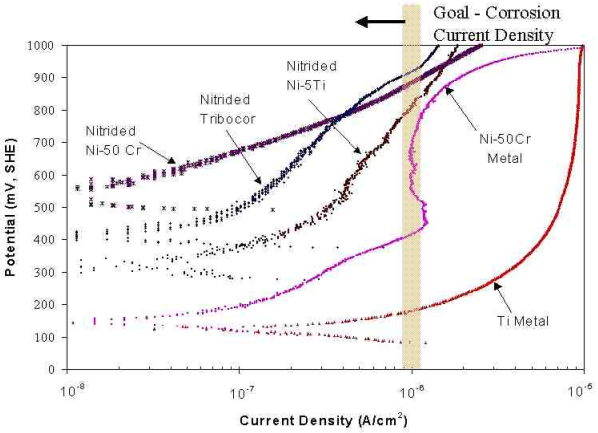

Figure 1. Anodic polarization data in aerated pH 3 sulfuric acid at 80°C (scan rate of 0.1 mV/s)

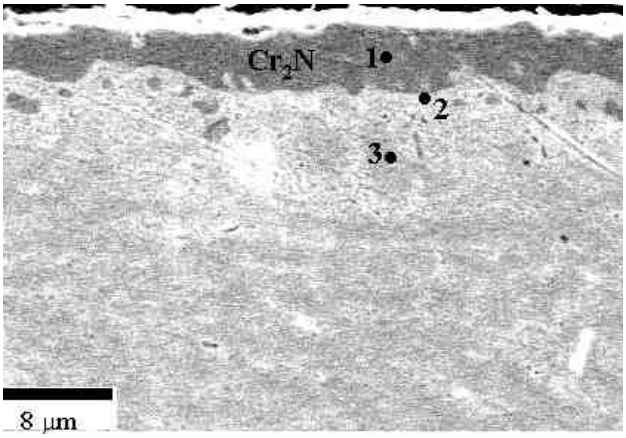

Figure 2. Scanning electron microscopy cross-section of Ni-50Cr wt% nitrided for 2 h at 1100°C in N_2. point 1- external Cr_2N scale: 69Cr-30N-1Ni atomic percent (at.%), point 2- Cr-depleted Ni(Cr) metal (light): 68Ni-32Cr at.% (71Ni-29Cr wt%), point 3- subscale ternary Ni-Cr-N phase (dark): 52Cr-14N-34Ni at.%. Compositions determined by electron probe microanalysis using pure element standards for Ni, Cr and a Cr_2N standard for nitrogen.

mixed zone of Cr-depleted Ni(Cr) and a ternary Ni-Cr-N subscale nitride (Figure 2) (occasional examples of internal Cr_2N were also observed in the lower Cr alloys). The degree of continuity, and hence protectiveness, of the external Cr_2N improved with increasing alloy Cr content, with a dense nearly continuous or continuous layer formed on Ni-50Cr. Optical analysis after testing revealed no evidence of significant corrosion or breaching of the nitride layer

formed on the Ni-50Cr. Uncoated Ni-50Cr metal also exhibited relatively low corrosion currents (Figure 1) but showed evidence of pitting after the test exposure.

The nitridation of the Ni-50Cr alloys was very robust, with no evidence of inadequate coverage at sharp corners or edges. Figure 3 shows a coupon of Ni-50Cr that was hand stamped with the letters "ORNL", nitrided, and then immersed in pH 2 sulfuric acid at 80°C for 1 week; there was no attack evident in the stamped regions. These results suggest that the present approach is amenable to coverage and protection of stamped flow field features in a bipolar plate. Bulk electrical conductivities were in the range of 1-2 x 10^4 $\Omega^{-1}cm^{-1}$ after nitriding, which surpasses the DOE electrical conductivity target by two orders of magnitude.

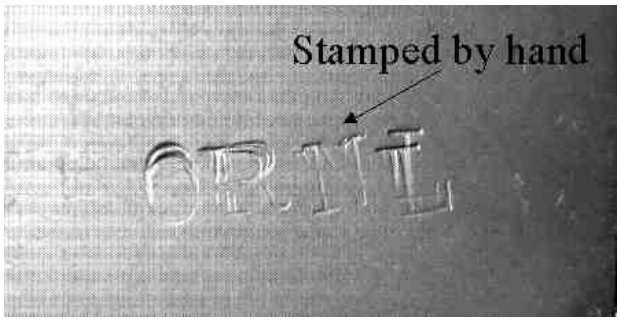

Figure 3. Macrograph of stamped and nitrided Ni-50Cr coupon after 1 week exposure in pH 2 sulfuric acid at 80°C (coupon dimensions 1" X ½").

Conclusions/Future Work

These results indicate that nitrided Ni-Cr base alloys show potential for use as bipolar plates in PEM fuel cells. Future work will focus on in-cell testing of nitrided Ni-50Cr to determine if the promising corrosion resistance demonstrated in the anodic polarization testing translates to good in-cell performance. From a cost and alloy processing perspective, lower levels of Cr are needed, ≤ ~ 40-42 wt% range [1], particularly in terms of the rate of work hardening during cold rolling, to allow the economical production of alloy sheet. The critical level of Cr needed to form an external nitride layer on binary Ni-Cr alloys is in the range of 30-40 wt% Cr [2], so a reduction below 50 wt% Cr appears feasible with proper adjustment of nitridation conditions (e.g. temperature, N_2 vs. NH_3 environments, initial surface condition) to form a sufficiently continuous and dense Cr_2N (or possibly CrN) layer. Reduction in Cr level may also be achievable through ternary alloying additions that form nitrides of intermediate thermodynamic stability between those of Cr and Ni, ie. secondary gettering [e.g. 3]. For example, the level of Al needed to form an external alumina layer on Cu-Al alloys can be significantly reduced by additions of Zn [e.g. 3]. It may also be possible to form similar corrosion resistant nitride layers on Fe-Cr or Ni(Fe)-Cr base alloys, which would also further reduce alloy cost. Investigation of the nitriding characteristics of existing commercial Ni-Fe-Cr alloys will also be performed. Emphasis in the next year will be placed on establishing collaborations with commercial alloy producers and fuel cell manufacturers to facilitate technological assessment (particularly in-cell testing) and scale-up of this approach.

References

1. G. Smith and M. Harper, Special Metals Corp., private communication (2002)

2. R.P. Rubly and D.L Douglass, Oxid. Met., 35, 259 (1991)

3. M.P. Brady, B. Gleeson, I.G. Wright, JOM, 52(1) 16 (2000).

FY 2002 Publications

1. "Assessment of Thermal Nitridation to Protect Metal Bipolar Plates in PEM Fuel Cells", M.P. Brady, K. Weisbrod, C. Zawodzinski, I. Paulauskas, R.A. Buchanan, and L.R. Walker, submitted to *Electrochemical and Solid State Letters*.

Patents

1. "Metallic Bipolar Plate Alloys Amenable to Inexpensive Surface Modification for Corrosion Resistance and Electrical Conductivity", M.P. Brady, J.H. Schneibel, B.A. Pint, and P.J. Maziasz, United States Provisional Patent Disclosure, April 2002.

IV.D.20 Scale-Up of Carbon/Carbon Composite Bipolar Plates

David Haack (Primary Contact), Ken Butcher, Earl Robert Torre
Porvair Fuel Cell Technology, Inc.
700 Shepherd Street
Hendersonville, NC 28792
(800) 843-6105, fax: (828) 697-7960; e-mail: dhaack@pamus.com

DOE Technology Development Manager: Donna Ho
(202) 586-8000, fax: (202) 586-9811, e-mail: Donna.Ho@ee.doe.gov

ANL Technical Advisor: Thomas Benjamin
(630) 252-1632, fax: (630) 252-4176, e-mail: Benjamin@cmt.anl.gov

Main Subcontractor: UTC Fuel Cells, Inc., South Windsor, Connecticut

Objectives

- Develop carbon/carbon composite materials for bipolar plates that meet or exceed target property criteria
- Evaluate the performance of the bipolar plate materials through fuel cell stack testing
- Design and construct a research-scale production line for materials development efforts
- Design and construct a pilot-scale production line to demonstrate high volume, low-cost bipolar plate manufacturing

Approach

Phase I

- Design, construct and install material forming, pressing and thermal treatment equipment
- Systematically investigate material forming techniques and composition ingredients
- Systematically investigate material processing variables and test material properties
- Perform fuel cell testing to evaluate plate performance at UTC Fuel Cells
- Investigate forming techniques aimed at rapid, low-cost production

Phase II

- Design, construct and install a pilot-scale production line for 300 plates per hour capacity
- Design and implement quality assurance system for pilot line
- Evaluate pilot line performance and estimate pilot and mass bipolar plate production costs
- Evaluate pilot line bipolar plates for fuel cell performance and deliver fuel cell stack

Accomplishments

- Developed two-sided embossed bipolar plates with excellent material properties, exhibiting the potential for low-cost production
- Designed, constructed and installed research material forming and processing equipment
- Developed improved bipolar plate materials, exhibiting improved material properties and low-cost ingredients

- Began investigation into rapid-forming techniques
- Began fuel cell testing at UTC Fuel Cells

Future Directions

- Continue material development efforts for improved material properties and reduced raw materials
- Continue rapid-forming investigations
- Continue fuel cell testing

Introduction

In April 2001, Porvair Fuel Cell Technology, Inc. (PFCT) licensed a carbon/carbon composite bipolar plate formation technology from Oak Ridge National Laboratory (ORNL). The goal of PFCT is to transfer this technology from the laboratory to full-scale, low-cost mass production to meet the emerging need of the rapidly developing fuel cell industry. This program is directed at further developing the carbon/carbon bipolar plate material to meet the performance, durability and cost demands of the fuel cell industry, and to demonstrate a pilot-scale manufacturing line to produce this material in reasonable pilot quantities (300 plates per hour).

The process involves formation of a carbon perform by a low-cost slurry molding process. The pre-form is pressed and a flow field pattern is embossed in the surfaces. The porosity of the plate is then filled to the desired density by chemical vapor infiltration.

Approach

The path to final production demonstration is split into two major parts in this program. Phase I focuses upon material and composition refinement to satisfy the fuel cell property and performance requirements. Also in Phase I, investigations and demonstrations of research-scale rapid material formation techniques will be performed.

The approach in material development is to systematically perform statistically designed experiments. Techniques include fractional factorial designs, Grecko-Latin squares, and self-directed optimization. Data collected is statistically evaluated to determine primary and combined effects of the variables of investigation. Properties of importance will be measured using standard techniques; they include material electrical conductivity, strength, flexure, hydrogen permeability, and corrosion rate. Our commercial partner in this endeavor, UTC Fuel Cells, will measure bipolar plate performance in out-of-cell testing and in-cell testing (both single and multiple cell stacks).

Phase II focuses upon process development to result in a pilot production line capable of producing 300 bipolar plates per hour. Our goal is a complete functional pilot line, including all relevant quality assurance, failure mode and effects analysis, and statistical manufacturing characterization processes. This will be completed by transferring the most promising mass-production technique to larger-scale and continuous equipment operation in a dedicated production line.

Results

The project to this point has focused primarily upon process design and equipment installation, although some material and process development has been performed. A laboratory space has been arranged for the bipolar plate development activities. A research vacuum forming system (Figure 1) has been installed for use in manufacturing experimental material. Material pressing equipment, material property testing equipment, and thermal processing equipment has also been installed. Figure 2 shows the laboratory-scale CVI furnace used for preliminary materials development efforts. Because the capacity of this furnace limits productivity, a larger furnace has been designed and installed (Figure 3) to provide capacity suitable to produce an average of 10 plates per hour (a Phase I productivity goal).

Figure 1. Photograph of carbon/carbon composite vacuum forming equipment.

Materials development activities have focused upon improving material properties and reducing the costs of the raw materials composing the bipolar plate. The original work done at ORNL focused primarily upon the use of short graphite fibers as the backbone of the bipolar plate. The fiber material utilized, however, is quite expensive (projected high volume costs of ~$5/lb) and may limit the achievement of desirable material properties. A two-level fractional factorial design investigating fiber type and content was undertaken to reduce the quantity of fiber in the product or to displace the expensive fiber material with lower cost alternatives. Results showed that much of the fiber within the material could be displaced, resulting in a lower-cost product with superior material properties.

The potential of embossing flow field patterns in the preform materials has also been investigated. A two-sided proprietary flow field pattern has been successfully transferred to the carbon/carbon material yielding near-net-shape bipolar plates. Subsequent materials property testing has confirmed adequate material properties.

Table 1 shows preliminary materials properties measured on non-optimized bipolar plate materials produced through initial development work at PFCT. Comparisons with published DOE goals are made in the table. Sealing of the plate through - through plate permeability is accomplished through the application

Figure 2. Photograph of laboratory-scale chemical vapor infiltration (CVI) furnace

of a thin non-permeable layer on the exterior surface of the material. Figure 4 is an SEM micrograph of such a surface. Permeability testing with nitrogen gas at room temperature has been performed (ASTM D1434), showing no detectable permeability. The experimental setup to allow testing with hydrogen is still under development.

Table 1. Carbon/Carbon Material Properties

Property	Value	DOE Target
Electrical Conductivity (S/cm) (ASTM C611)	> 300	> 100
Density (g/cc)	1.00 - 1.30	-
Flexural Strength (psi)	5700	> 600 (crush)
Flexibility (%) (deflection at mid-span)	1.5 - 3.5	3 - 5
Nitrogen Permeability (cc/cm^2/sec) (ASTM D1434)	Not detected	< $2x10^{-6}$ (Hydrogen)

Figure 3. Photograph of Phase I development CVI furnace in assembly.

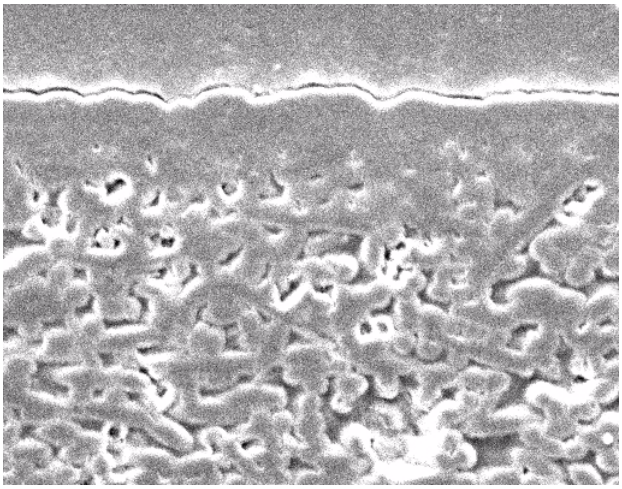

Figure 4. SEM micrograph of a molded carbon/carbon composite material. Figure shows thin skin coating on plate exterior to provide plate sealing.

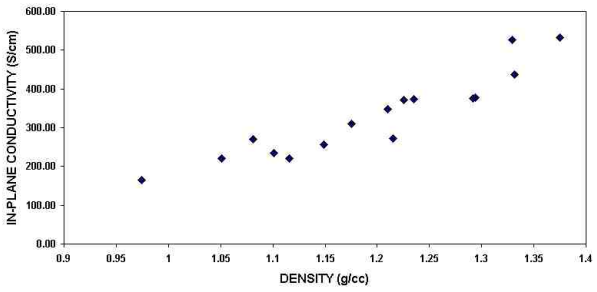

Figure 5. Density influence on through-plane electrical conductivity from an array of experimental compositions.

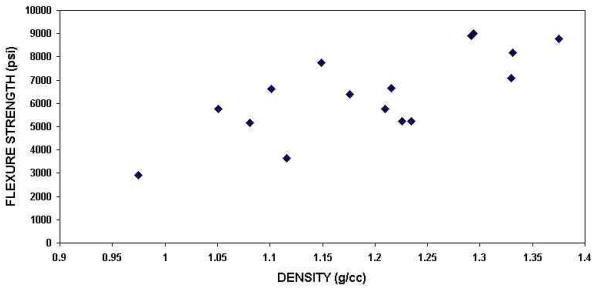

Figure 6. Density influence on flexural strength from an array of experimental compositions.

Some material trends have been established through continued experimental investigation. Figure 5 is a chart of material conductivity as a function of material density. Figure 6 is a similar chart showing material flexure strength. The process and material developed to date shows considerable flexibility to tailor material properties to desired levels. As seen in Figures 5 and 6, a trade-off exists between material density and material properties - a lightweight material will not be as strong or conductive as a heavier material. However, material properties measured appear to be well above the DOE targets, even with low-density materials. Further material optimization is continuing.

UTC Fuel Cells, Inc. is testing both machined and pattern-embossed materials in single fuel cell operation. Initial results, although not ready for publishlication, appear promising.

Conclusions

Preliminary work completed in this project includes laboratory and equipment setup and installation, and preliminary rounds of material optimization and process development. Full size bipolar plate prototypes have been produced with full double-sided flow patterns, demonstrating the potential of the manufacturing process. Process and material development has resulted in the characterization of material properties under a variety of composition levels. Material properties meeting or exceeding DOE targets have been measured, and bipolar plates, both machined and pattern-embossed, have been submitted to UTC Fuel Cells for in and out of cell testing. Phase I work will

continue this year in the optimization of the material composition for cost and performance, in the development of potential mass-production techniques, and in expanded in-cell testing.

IV.D.21 Carbon Foam for Fuel Cell Humidification

J. W. Klett (Primary Contact), Nidia Gallego, April McMillan, Lynn Klett
Carbon Materials Technology Group
Oak Ridge National Laboratory, P.O. Box 2008, MS 6087, Bldg. 4508
Oak Ridge, TN 37831-6087
(865) 574-5220, fax: (865) 576-8424, e-mail: klettjw@ornl.gov

DOE Technology Development Managers:
JoAnn Milliken: (202) 586-2480, fax: (202) 586-9811, e-mail: JoAnn.Milliken@ee.doe.gov
Nancy.Garland: (202) 586-5673, fax: (202) 586-9811, e-mail: Nancy.Garland@ee.doe.gov

ORNL Technical Advisor: David Stinton
(865) 574-4556, fax: (865) 241-0411, e-mail: stintondp@ornl.gov

Objectives

- Determine how graphite foams can be used to enhance the humidification of the fuel cell inlet air.
- Determine what characteristics of the foam require optimization to allow the combination of power electronics cooling with humidification of the inlet air.

Approach

- Design and construct a humidification test cell to utilize different foam structures to aid evaporation of water.
- Perform tests to characterize the humidification potential of the foam and develop optimized designs to minimize pumping power while maximizing humidification with heat generated from power electronics.

Accomplishments

- Foam was demonstrated to successfully humidify dry inlet air to 87% saturation at 60°C using a simulated power electronic device.
- Optimization of foam density uniformity, batch consistency, and thermal properties was performed and showed that a foaming rate of 3.5°C/min and a graphitization rate of 1°C/min produced the best foam structures.
- A mathematical model for heat transfer in foams was developed, which can simulate power electronics cooling by fluid flow through the foam.

Future Directions

- Apply optimized foam structures to humidification systems to show improvement in humidification potential.
- Apply mathematical model to design optimized humidification systems (i.e., lowest pressure drop, highest humidity, and lowest heater temperature).
- In collaboration with a fuel cell manufacturer, develop a full-scale prototype humidifier for fuel cell applications.

Introduction

The efficiency of the automotive proton exchange membrane (PEM) fuel cell is dependent on many factors, one of which is the humidification of the inlet air. If the inlet air is not sufficiently humid (saturated), then the stack can develop dry spots in the membrane and efficiency and voltage will drop. Therefore, it is necessary to ensure that humid inlet air at the proper elevated temperature is supplied to the stack. Current methods involve utilizing a spray nozzle to atomize water droplets onto a cloth or wire mesh substrate. As the ambient inlet air passes over the cloth it picks up moisture; however, the relative humidity drops as the air is heated in the fuel cell. If heat could be supplied to the water efficiently, the system would become independent of the ambient conditions, the inlet air could become more humid at the proper temperatures, and the overall stack could maintain a high level of efficiency. Previous work with power electronic heat sinks and automotive radiators has demonstrated the high efficiency of carbon foam for heat transfer. Utilizing the carbon foam in the PEM fuel cell may reduce the inlet air humidification problems.

The unique graphite foam, shown in Figure 1, has a ligament conductivity greater than 1500 W/m·K, equivalent to artificial diamond. The high thermal conductivity of the foam combined with the very high surface area (>4 m^2/g) result in heat transfer coefficients that are two orders of magnitude greater than those of conventional heat exchangers. Therefore, we believe that graphite foam can be effectively utilized to capture waste heat from power electronics to heat and humidify ambient air entering the fuel cell. To characterize the behavior of the foam in a humidification system, a test chamber normally used for evaluating heat sinks is utilized (see Figure 2). A block of carbon foam is brazed onto an aluminum plate and placed in a cavity through which cooling air flows. A simulated power inverter capable of generating up to 800 W, or 30 W/cm^2, is mounted to the back of the aluminum plate. As cooling air passes through the system, the temperature of the heater and the inlet and outlet air can be measured.

Several tests were run to determine the efficacy of using waste heat from power electronics to heat and humidify ambient inlet air. Testing was initiated by flowing 5 SCFM of ambient (~20°C) air through the heat sink (test system) that was dissipating 10 W/cm^2 of heat. The temperature of the outlet air increased to about 104°C. The test was repeated with the addition of 10 cm^3/min of water to not only heat but also humidify the air. The temperature of the outlet air increased to 73°C at a relative humidity of 24%. The test was repeated a second time with the addition of 20 cc/min of water for humidification. The temperature of the outlet air increased to ~59°C at a relative humidity of 87%.

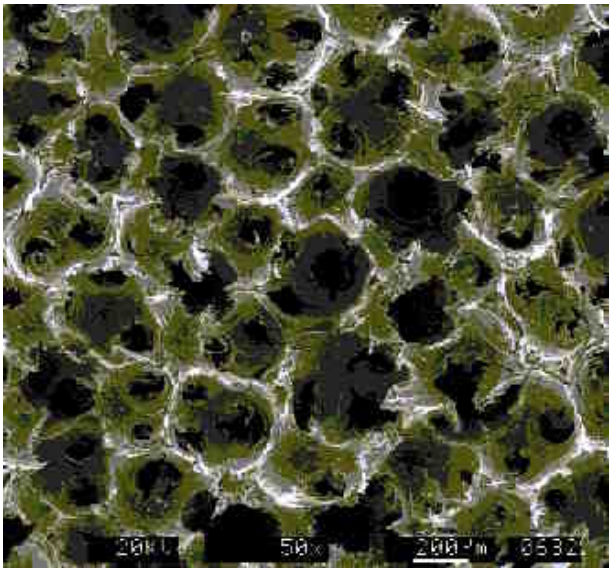

Figure 1. ORNL Graphite Foam

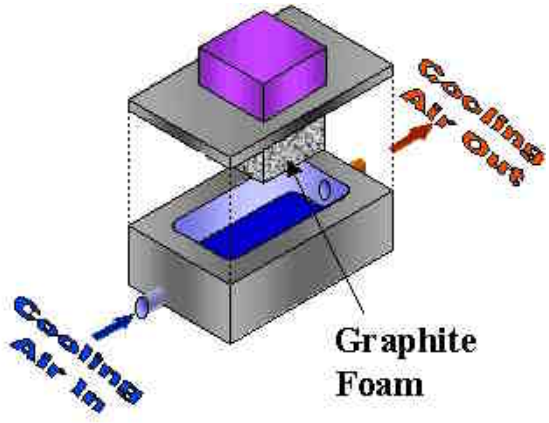

Figure 2. Schematic of Test Rig to Evaluate Heat Sink Geometries

The successful operation of a fuel cell vehicle will likely require about 4.5 m^3/min or 160 SCFM of inlet air at a temperature of about 80°C. Our calculations show that there should be sufficient heat generated by the power electronics to adequately heat and humidify this volume of air. Unfortunately, very large quantities of water would be required to humidify this large volume of air. In fact, a hybrid electric vehicle would consume more water per mile or per hour than gasoline. In order to make humidification systems practical, very efficient systems that recycle moisture from the exhaust stream will be required. Hence, understanding the structure-processing relationship of the foam as a means of tailoring the foam properties will be required to optimize the humidification system. In addition, developing a model that can predict heat transfer and developing better joining methods to reduce thermal resistance will be critical to the success of this project. Therefore, efforts were initiated in several of these areas.

Approach and Results

Foam Optimization

For many carbon materials the heat treatment rate during graphitization is critical to optimizing the material properties. Commercial heating rates of approximately 0.1°C/minute to 2800°C are typically used for graphitization. Because graphitization takes so long, it is expensive and energy intensive; thus, finding the maximum heating rate which yields the desired properties is critical to minimizing costs. Therefore, the influence of heating rate during graphitization on key properties of the foam such as density, thermal diffusivity and crystalline parameters was examined in this research.

Density Uniformity: The first characterization of the foams was the measurement of the density uniformity after carbonization. Several billets of foams were made with two different foaming rates: 3.5°C/min and 10°C/min. Test billets were heat treated in the top and bottom positions in the furnace, as illustrated in Figure 3. This provides an understanding of the temperature uniformity within the furnace and its effects on the resulting foam. Table 1 reports the density uniformity for the billets processed at different foaming rates and positions in the furnace. The density of samples heat treated at the top of the furnace is much more uniform than samples heat treated at the bottom of the furnace. While there appears to be a slight effect on density uniformity due to the foaming rate, this effect is small comared to the effect of the position of the pan in the furnace. This implies that the temperature at the bottom of the furnace (most likely a lower temperature) during the foaming is not sufficient to produce uniform temperature profiles in the foam, thereby leading to non-uniform foam density plots.

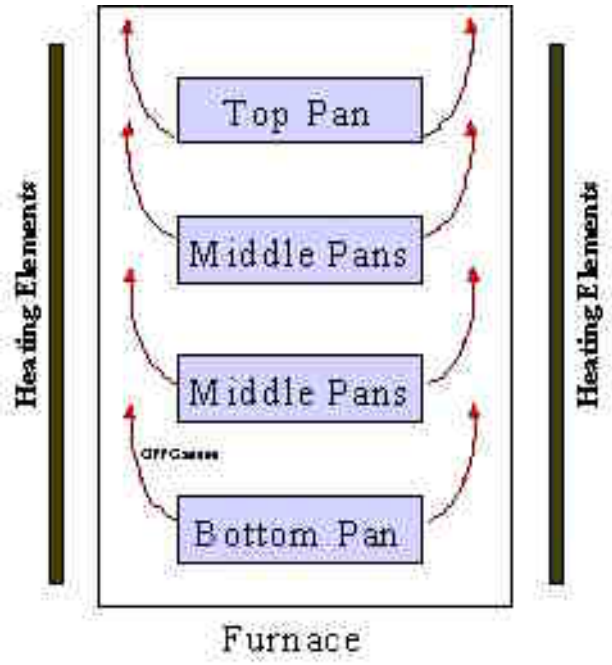

Figure 3. Furnace Diagram with Locations of Billets of Foam

	Bottom Pan		Top Pan	
Foaming Rate [°C/min]	Avg. Density	Max Deviation	Avg. Density	Max Deviation
3.5	0.474	10.6%	**0.448**	**3.7%**
10	0.434	13.1%	**0.430**	**3.8%**

Table 1. Density (in g/cc) Uniformity of Billets

Thermal Properties: Cubes cut from each billet were separated into groups of four and fired to

2800°C at five different heating rates (0.5, 1, 5, 10, and 15°C/min). The thermal properties of the samples were then measured in x, y, and z directions with a Xenon flash diffusivity apparatus. The thermal conductivity of the samples was calculated from their thermal diffusivity. Table 2 lists the Z-direction thermal conductivity values for each graphitization heating rate and position within the furnace. From these data, it is clear that the thermal conductivity is directly related to the graphitization heating rate. A similar trend was observed in the crystal properties of the foams determined from X-ray diffraction (not shown here for brevity). However, it is not understood why there is a maximum at 1°C/min.

Graphitization Heating Rate	Bottom Pan		Top Pan	
	Foaming Rate		Foaming Rate	
	3.5°C/ min	10°C/ min	3.5°C/ min	10°C/ min
0.5	118.6	85.8	132.9	109.4
1.0	134.7	111.9	148.9	115.5
5	130.7	104.3	133.9	114.1
10	123.7	96.6	126.4	112.7
15	98.7	88.4	125.1	115.3

Table 2. Z-direction Thermal Conductivity (in W/m·K) after Graphitization

The effect of the location of the samples in the foaming furnace on the final thermal properties is also noteworthy. It is clear that in the Z-direction (the direction with the highest conductivity), both billets that were located in the top of the furnace exhibited the highest overall thermal conductivity, irrespective of foaming rate. However, it is also evident that the foaming rate does affect the final thermal properties, with the lower foaming rate yielding graphitized foam with the higher thermal conductivity. While these trends are also true for the x and y directions, the effects are less pronounced due to the lower thermal conductivities in these directions.

Modeling of Heat Transfer

A mathematical model was developed to predict the thermal transfer in the foams. This is critical to developing engineered structures which provide both humidification and electronic cooling. This model uses the equations of energy, motion, and continuity to develop a finite element solution with a commercial package, FLEXPDE. For the hypothetical model, heat is assumed to be added to the top of the foam (simulating a heater), and the fluid flows perpendicular to the heat flow (see Figure 4). The following equations were input to the model:

Darcy-Forcheimer Equation for flow through porous media

$$0 = -\nabla p - \frac{\mu}{\kappa}\mathrm{v} + \frac{\mu\rho}{\sqrt{\kappa}}|\mathrm{v}|\mathrm{v}$$

Equation of Continuity

$$0 = -\nabla^2 P - \left(\frac{\mu}{\kappa} - \frac{\mu\rho}{\sqrt{\kappa}}|\mathrm{v}|\mathrm{v}\right)(\nabla\cdot\mathrm{v})$$

Heat Equation in Fluid

$$0 = \nabla\cdot\left(-k_w\nabla T_w\right) - \rho C_p DT + \dot{q}_{gained}$$

Heat Equation in Foam

$$0 = \nabla\cdot\left(-k_f\nabla T_f\right) - \dot{q}_{loss}$$

Model heat transfer from foam to fluid as a source/ loss term - q

$$\dot{q}_{loss} = \dot{q}_{gained} = -h_{loc}\cdot A_{spec}\cdot(T_f - T_w)$$

The results were exceptional, as shown in Table 3. The model adequately predicts the output fluid temperature and heater temperatures for various conditions in power input and flow rates. Now that the model is validated, it can be applied to engineering concepts to easily predict and design the optimum configurations to produce humid inlet air while cooling devices such as power electronics.

Figure 4 illustrates the results of the simulations. First, the model can predict the flow field of the fluid, in this case a plug flow, which is optimum for heat transfer. Next, the model predicts the isotherms of the foam and water, giving the designer important visualization of the system, thereby allowing easier engineering of optimum designs.

Power Input (W)	**300**	**300**	**600**	**600**
Water Flow Rate [gph]	**25**	**45**	**25**	**45**
Pressure Drop [psi]	**3.5**	**7.0**	**3.5**	**7.0**
Measured Base Plate Temperature [C]	**300.3**	**296.8**	**308.7**	**303.4**
Predicted Base Plate Temperature [C]	**299.6**	**297.2**	**308.4**	**303.6**
Measured Outlet Water Temperature [C]	**293.8**	**292.6**	**296.3**	**293.9**
Predicted Outlet Water Temperature [C]	**293.7**	**292.4**	**295.8**	**293.9**

Table 3. Heat Transfer Model Results

Conclusions

It was shown that carbon foam is beneficial to humidification systems for fuel cells. The foam has demonstrated the ability to utilize waste heat from power electronics to both heat and humidify ambient inlet air to ~80°C and 80% relative humidity.

The foaming process was characterized to optimize both the foaming rate and the graphitization rate of the foams. It was found that the temperature uniformity of the foaming furnace is critical to the density uniformity and batch consistency of the foam billets. It was found that a foaming rate of 3.5°C/min produced foams with more uniform densities and higher thermal conductivities than a higher foaming rate. It was also found that a graphitization rate of less than 1°C/min produces foams with the highest thermal conductivities.

Last, a mathematical model was developed which accurately predicts heat transfer from the foam to a fluid flowing through the pores of the foam. This is critical to developing optimized designs for humidification devices that both humidify and provide cooling potential.

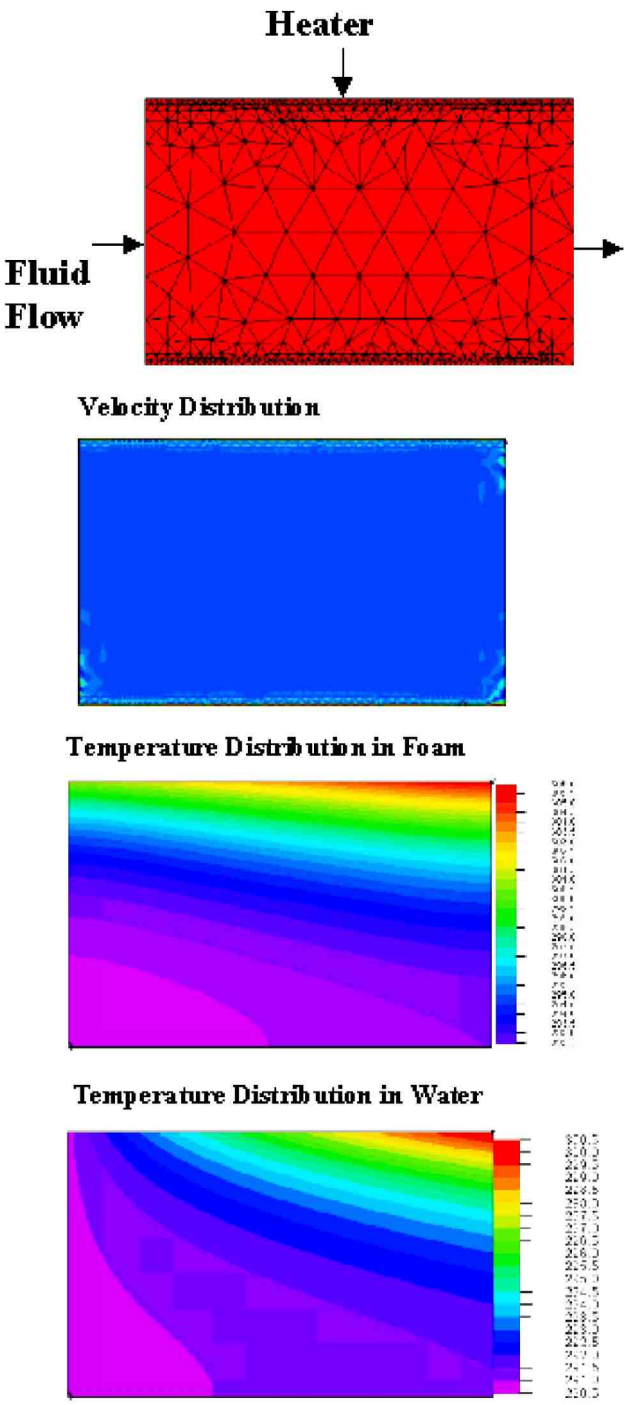

Figure 4. Model and Results of Simulated Heat Transfer from Foam to Fluid Flowing through Foam

IV.D.22 Carbon Monoxide Sensors For Reformate Powered Fuel Cells

Fernando Garzon (Primary Contact), Eric Brosha and Rangachary Mukundan
MS D429, MST-11 Group
Los Alamos National Laboratory
Los Alamos, New Mexico, 87545
(505) 667-6643, fax: (505) 665-4292, e-mail: garzon@lanl.gov

DOE Technology Development Managers:
Nancy Garland: (202) 586-5673, fax: (202) 586-9811, e-mail: Nancy.Garland@ee.doe.gov
JoAnn Milliken: (202) 586-2480, fax: (202) 586-9811, e-mail: JoAnn.Milliken@ee.doe.gov

Objectives

- Hydrogen reformate gas powered fuel cell systems require sensors for carbon monoxide level monitoring and feedback control.
  - Develop a high temperature sensor for measurement of 0.1 to 2% carbon monoxide in reformate gas for fuel processor control.
  - Develop a low temperature sensor for measuring 10-100 ppm range concentrations for stack poisoning control.

Approach

- Two electrochemical sensor types are being investigated for high and low temperature carbon monoxide sensing:
  - An oxide solid electrolyte device based on the kinetics of the electrode reactions is being developed for the high temperature application.
    - Yttria-doped zirconia and gadolinia-doped ceria oxygen ion conductors and strontium yttrium zirconium oxide proton conductors are being investigated as the solid electrolyte.
    - Several metals including Pt, Pd, Au, Ru and Ni are being evaluated as the sensing and reference electrodes.
  - A amperometric device based on carbon monoxide inhibition of hydrogen oxidation kinetics using either a perfluorosulfonic acid polymer electrolyte or an inorganic acid electrolyte is being evaluated for the low temperature application.

Accomplishments

- A cerium oxide based high temperature sensor has been developed. The sensor responds well to 10-500 parts per million of carbon monoxide in air.
- Strontium zirconate proton conducting thin film electrolytes have been successfully synthesized and characterized.
- Amperometric low temperature carbon monoxide sensors have been developed and tested under a variety of conditions. These devices respond well at ambient temperature to carbon monoxide in hydrogen streams.

Future directions

- Modify the electrodes in the cerium (or zirconium) oxide devices to detect CO in the presence of hydrogen.

- Increase the operating temperature of the low temperature devices from room temperature to approximately 80^{o}C.
- Optimize low temperature amperometric devices for fast response time.
- Evaluate catalyst composition, loading and particle size effects on sensor performance.
- Investigate alternative electrolytes.
- Test the sensor prototypes in actual reformate gas streams.

Introduction

The detection and measurement of carbon monoxide in high temperature reformate streams is of vital importance to the successful implementation of fuel cells for transportation. Much research is being performed to optimize low-cost fuel reformer systems that convert liquid hydrocarbon fuels to hydrogen gas containing fuel streams. This hydrogen gas typically feeds a polymer electrolyte membrane (PEM) fuel cell utilizing a platinum based anode. It is well known that low concentrations of carbon monoxide (~10-100) ppm impurities in hydrogen can severely degrade the performance of PEM fuel cell anodes. This performance degradation is due to strong adsorption of carbon monoxide on the electro-active platinum surface sites where hydrogen is normally oxidized to protons.

The proper design of fuel reformer systems must pay careful attention to the minimization of carbon monoxide before the processed fuel stream enters the fuel cell stack. Many reformer systems use a secondary preferential oxidation reactor that selectively oxidizes the carbon monoxide present in reformate streams. In most transportation applications the steam reformer and the selective oxidation reactors do not operate under steady state conditions; large transients may occur which produce relatively large amounts of carbon monoxide. It is highly desirable to have a low-cost real-time carbon monoxide measurement system that provides feedback control to the fuel processing system in order to protect the PEM fuel cells from performance degrading concentrations of carbon monoxide.

Current fuel cell systems use air-bleeding methods to reduce the carbon monoxide poisoning of the Pt anode. Since this method involves the mixing of 2-6% air with the fuel stream, it results in a decrease in the energy efficiency of the fuel cell system and thus should only be used for carbon monoxide transients. Hence, a CO sensor that measures the CO content of the anode stream can be used for feedback control of the air-bleeding system thus allowing these systems to operate at maximum energy efficiency. We are designing and developing solid-state electrochemical sensors meeting these criteria, including the demonstration of prototype sensors.

Approach

High temperature carbon monoxide sensors

Los Alamos is developing high temperature zirconia- and ceria-based electrochemical sensors to measure 0.1-2% CO in hydrogen streams. These sensors would operate at 400-600^{o}C and can be used for feedback control of the reformer system. We have successfully developed novel mixed-potential sensors that are capable of measuring ppm levels of CO in air[1]. We are currently working on modifying the electrodes of these devices to enable them to work in a hydrogen atmosphere. We are also exploring the possibility of using proton-conducting electrolytes and using these sensors in an amperometric mode.

Low temperature carbon monoxide sensors

Low temperature carbon monoxide sensors based on the reversible carbon monoxide adsorptive poisoning of precious metal electrodes are also being developed by Los Alamos National Laboratory. The addition of metals such as ruthenium to the platinum electrode material greatly improves the hydrogen oxidation kinetics in the presence of CO. An amperometric sensor that senses the CO inhibition of the hydrogen oxidation can be fabricated from a platinum electrode, a proton conductor and a platinum ruthenium alloy electrode. While the

current density of the platinum electrode will be influenced by the surface coverage of carbon monoxide, the current density at the Pt/Ru alloy electrode should be relatively unaffected. This difference in the electrode current density in the presence of CO can be used to fabricate a low temperature CO sensor.

Results

During FY 2002 we prepared several low temperature sensors based on a Nafion® electrolyte and various metal electrodes. We evaluated the CO response of Pt, Pt/Ru and Ru metal electrodes at various loadings. Figures 1 and 2 illustrate the current vs. voltage curves from two sensors using precious metal loadings of approximately 0.2 mg/cm^2. These electrodes were carbon supported electrodes and were prepared using a decal technique similar to typical fuel cell electrodes. Figure 1 illustrates that the Pt and Pt/Ru electrodes are poisoned by CO at room temperature, and the hydrogen-oxidation current is greatly decreased. However, this process was found to be difficult to reverse and the original current vs. voltage curves could not be obtained even after the CO was removed from the gas stream. It is seen from Figure 2 (inset) that the CO poisoning of the Ru electrode is

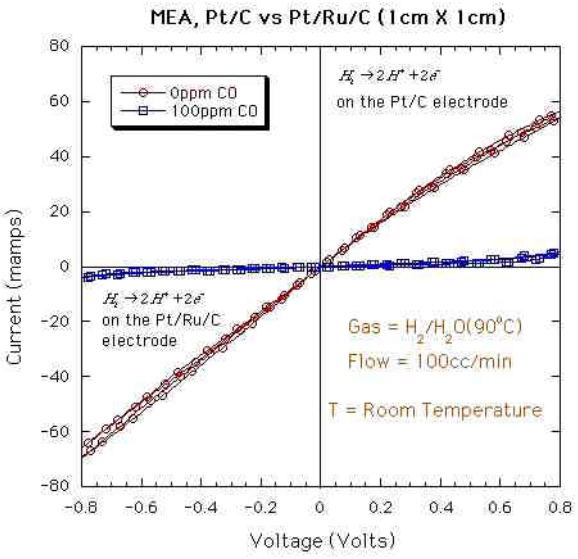

Figure 1. Current-Voltage Characteristics of a "0.22 mg/cm^2 Pt/C // Nafion® // 0.25 mg/cm^2 Pt/Ru/C" sensor at room temperature.

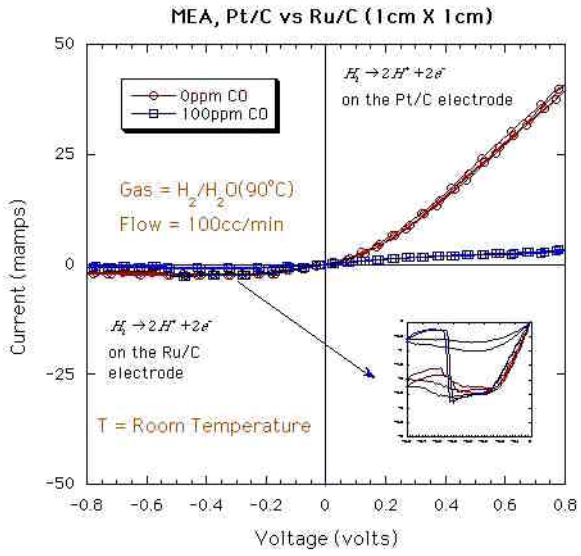

Figure 2. Current-Voltage Characteristics of a "0.22 mg/cm^2 Pt/C // Nafion® // 0.12 mg/cm^2 Ru/C" sensor at room temperature.

reversible, and the CO can be cleaned by the application of a voltage <-0.5 V. However, due to the low hydrogen-oxidation kinetics of this electrode, a sensor based on this electrode would have very little sensitivity to CO.

In order to improve the reversibility of the CO adsorption, several electrodes with higher catalyst loadings were evaluated. Pt, Ru and Pt/Ru black catalysts mixed with Nafion® and without carbon support were painted onto Nafion® membranes at approximately 10 mg/cm^2 loadings. The current vs. voltage curves of a "Pt/ Nafion®/ Pt-Ru " device are shown in Figure 3, where the Pt/Ru alloy electrode is relatively unaffected by the presence of 100 ppm of CO while the Pt electrode is poisoned. Moreover the CO from the Pt electrode can be easily cleaned by the application of a voltage >0.4 V. Therefore, this device, when biased at a voltage <0.4 V can be used as a CO sensor. The CO response obtained from this device at a bias of 0.3 V is illustrated in Figure 4.

Figure 5 illustrates the current vs. voltage curve of a "Pt/ Nafion® /Ru" device and indicates that the CO poisons both the Pt and the Ru electrodes in a reversible manner. The poisoning of the Ru electrode can also be used to yield a sensor response when the bias is >-0.6 V. Figure 6 illustrates the

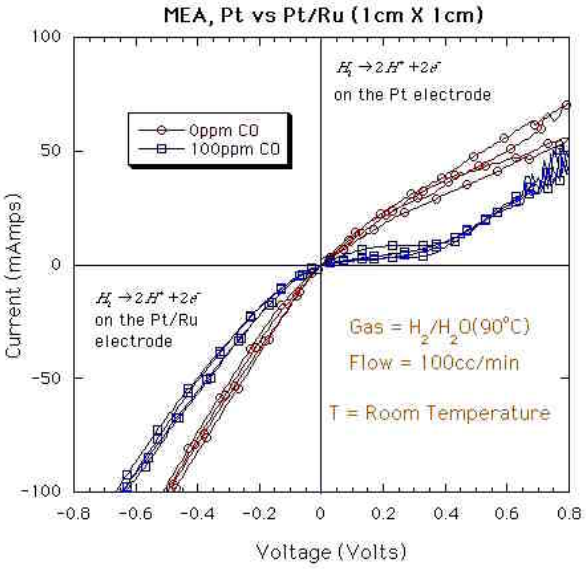

Figure 3. Current-Voltage Characteristics of a "10 mg/cm^2 Pt // Nafion® // 10 mg/cm^2 Pt/Ru" sensor at room temperature.

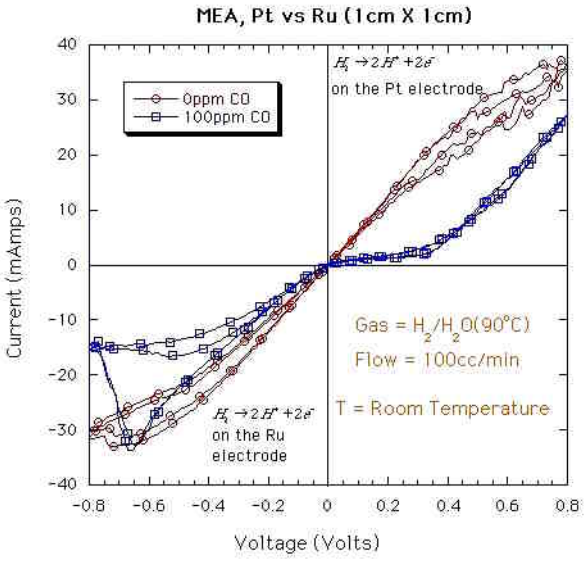

Figure 5. Current-Voltage Characteristics of a "10 mg/cm^2 Pt // Nafion® // 10 mg/cm^2 Ru" sensor at room temperature.

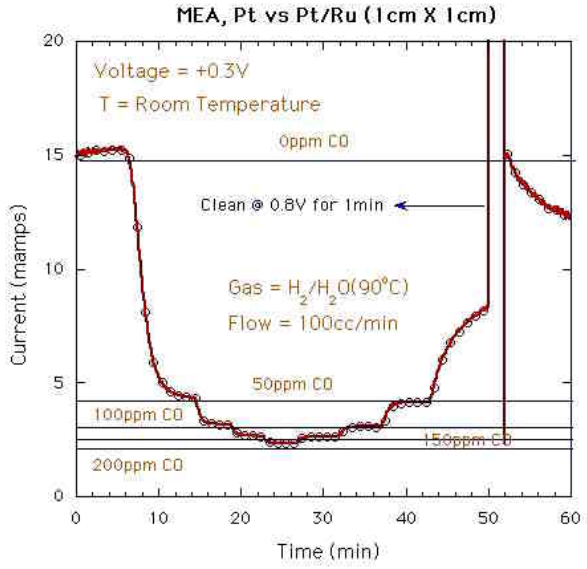

Figure 4. Response of the "10 mg/cm^2 Pt // Nafion® // 10 mg/cm^2 Pt/Ru" sensor to 0, 50, 100, 150, 200 ppm of CO in H_2.

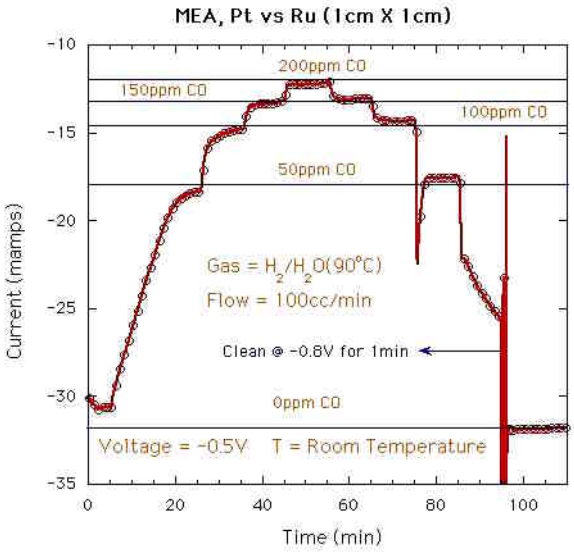

Figure 6. Response of the "10 mg/cm^2 Pt // Nafion® // 10 mg/cm^2 Ru" sensor to 0, 50, 100, 150, 200 ppm of CO in H_2.

response of this device to CO when the bias is set at –0.5 V. This sensor shows excellent sensitivity to CO and can be used to measure CO concentration in the 10-100 ppm range in a hydrogen stream. Although the CO desorption is fast at most CO levels, a bias of –0.8 V was found to restore the baseline of the sensor upon removal of the CO.

Conclusions

We have successfully developed low temperature sensors for the monitoring of carbon monoxide gas in a hydrogen stream. The sensors can detect parts per million concentrations of carbon monoxide in either a pure hydrogen or a hydrogen/carbon-dioxide

stream. Future work includes the raising of the operating temperature of the sensor to approximately 80^{o}C (fuel-cell operating temperature) and the optimization of the sensor response time and sensitivity.

References

1. R. Mukundan, E. L. Brosha, D. R. Brown, and F. H. Garzon. A mixed potential sensor based on a $Ce_{0.8}Gd_{0.2}O_{1.9}$ electrolyte and platinum and gold electrodes. *Journal of the Electrochemical Society,* **V 147(4)**, 1583-1588 (2000)

IV.D.23 Electrochemical Sensors for PEMFC Vehicles

Ai-Quoc Pham (Primary Contact)
Lawrence Livermore National Laboratory
P.O. Box 808, L-350
Livermore, CA 94550
(925) 423-3394, fax: (925) 422-6892, e-mail: pham2@llnl.gov

DOE Technology Development Managers: JoAnn Milliken and Nancy Garland
(202) 586-2480, fax: (202) 586-9811, e-mail: JoAnn.Milliken@ee.doe.gov
(202) 586-5673, fax: (202) 586-9811, e-mail: Nancy.Garland@ee.doe.gov

Objectives

- Develop a hydrogen safety sensor operating at 500°C or below, having 1s response time and being insensitive to humidity and hydrocarbons.
- Develop a hydrogen sensor for reformate fuel monitoring for hydrogen concentrations ranging between 10 to 100%.
- Develop a carbon monoxide (CO) sensor for reformate fuel monitoring.

Approach

- Use proven technology, i.e., solid state electrochemical sensors similar to the well-know oxygen sensor used in automobile exhaust gas
- Use mixed potential signal to eliminate the need for a reference gas compartment
- Use nanocrystalline electrode material for faster response time
- Develop micro-sensors for minimum power consumption

Accomplishments

- Data were obtained on temperature effect on sensor response
- Sensors with nanocrystalline electrodes were fabricated and tested
- Sensors with response time of a few seconds at 500°C were demonstrated
- Preliminary testing indicated no baseline drifting over several hundred hours

Future directions

- Complete characterization of hydrogen safety sensor
- Investigate limiting current type hydrogen fuel sensors
- Develop mixed potential CO sensors
- Develop micro-sensors with incorporated self heating device
- Transfer to industrial partners

Introduction

Proton exchange membrane fuel cells (PEMFCs) are among the most promising clean power system technologies being developed for transportation applications. The introduction of this new transportation technology implies important changes in vehicle design as well as incorporation of new features that do not currently exist in internal combustion engine automobiles. For example, the use of hydrogen, in particular, and combustible gases in general, requires additional safety devices to

prevent fire and explosion hazards. In addition, if hydrogen fuel is supplied by an on-board fuel reformer that delivers a hydrogen stream containing several other gases, additional control and monitoring devices are needed in order to protect and to efficiently operate the PEMFCs.

The purpose of this project is to design, develop, and demonstrate solid state electrochemical sensors for the various controls and monitoring on PEMFC vehicles. During this first phase of the project, we focus on the development of a hydrogen safety sensor.

Approach

A number of hydrogen and combustible gas sensors are commercially available. However, none of them appears to straightforwardly satisfy all the stringent requirements for automobile applications. In particular, the commercial hydrogen safety sensors suffer from significant long-term drifting as well as cross-sensitivity. Our approach is to use solid-state electrochemical sensor technology which has proven to be robust and reliable in automobile applications. Our sensor consists of an oxygen-conducting electrolyte membrane sandwiched between two electrodes, one serving as reference and one as working electrode. The working electrode has mixed potential response when exposed to an atmosphere containing hydrogen, i.e., due to the competing oxidation-reduction reactions of hydrogen and oxygen on the electrode surface, the potential of the mixed potential electrode departs from the actual thermodynamic value. The reference electrode, which is designed to reach thermodynamic equilibrium, will thus have a different potential. The potential difference between the two electrodes is thus the sensor voltage. This sensor voltage is dependent on the hydrogen concentration. This type of sensor does not require a separate reference gas compartment.

Accomplishments

This project started in January 2001. During FY01, we successfully developed a mixed potential type sensor with response time as fast as 1 second. However, a fairly high operating temperature (600°C or higher) was needed in order to have fast reaction kinetics. While this high operating temperature is not a major issue if a micro-sensor with enough insulation is used, the power consumption to maintain that temperature could still be fairly high. Therefore, our goal was to lower the operating temperature to 500°C or below.

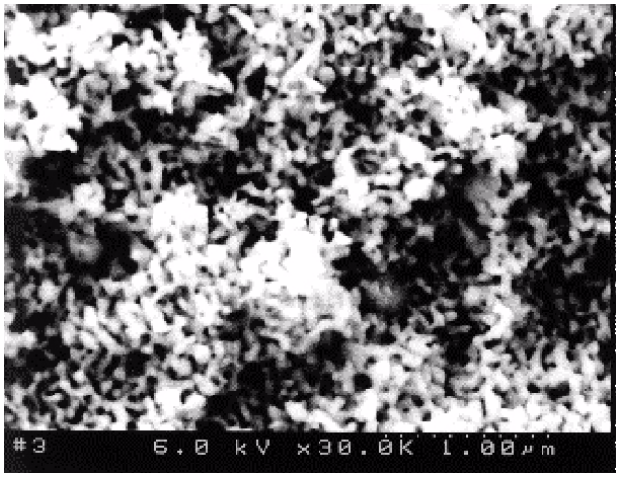

Figure 1. Micrograph of the Porous Nanocrystalline Electrode

We studied the effect of temperature on the sensor response. It was found that the lower the temperature, the higher was the signal amplitude while the response time became longer. We also found that the smaller the particle size of the electrode material, the faster was the sensor response. It was then concluded that using nanocrystalline material would be beneficial to accelerate sensor response, especially at low temperatures. Figure 1 shows the scanning electron microscopy picture of such a porous nanocrystalline electrode. The electrode was deposited using the colloidal spray deposition technique. The average particle size is less than 100 nm. At 500°C, the sensor response to hydrogen in air was 2 seconds for a flow rate of 2 liters per minute. A fast response to hydrogen was also observed at 400°C, however, the signal tended to overshoot before stabilizing at steady state.

Some of the characteristics of the new sensor are: no humidity effect on sensor response, high selectivity versus methane (see Figure 2) and virtually no baseline drifting over several hundred hours of operation. However, some issues still need to be improved, including the over-shooting that was

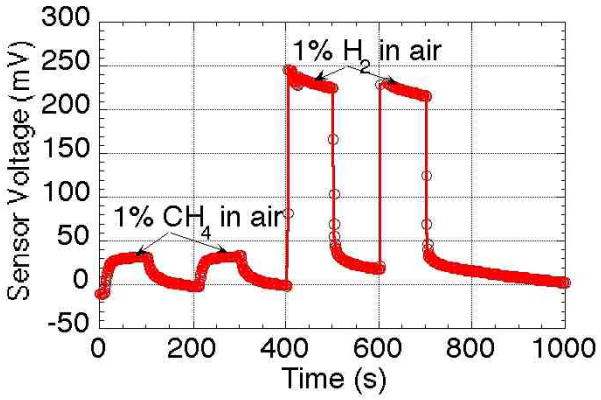

Figure 2. Sensor Response to Methane and Hydrogen

observed at time and the slow recovery upon removal of hydrogen from ambient air.

Conclusion and Future Work

We have demonstrated the possibility to reduce the sensor operating temperature from 600°C to 500°C. The sensor has some highly viable characteristics such as stability and selectivity.

Further work is needed in order to demonstrate a commercially viable device. For practical use, we will develop a self-heated micro-sensor for reduced power consumption as well as for minimum heat generation.

IV.D.24 Development of Sensors for Automotive Fuel Cell Systems

Brian A. Knight (Primary Contact)
United Technologies Research Center
411 Silver Lane Mail Stop 129-30
East Hartford, CT 06108
(860) 610-7293, fax: (860) 610-7669, e-mail: knightba@utrc.utc.com

DOE Technology Development Manager: Nancy Garland
(202) 586-5673, fax: (202) 586-9811, e-mail: Nancy.Garland@ee.doe.gov

Main Subcontractors: ATMI, Inc., Danbury, Connecticut; Illinois Institute of Technology, Chicago, Illinois; NexTech Materials, LTD, Worthington, Ohio

Objectives

- Develop technology and a commercial supplier base capable of supplying physical and chemical sensors required to optimize the operation of proton exchange membrane (PEM) fuel cell power plants in automotive applications.

Approach

- Obtain representative samples of physical parameter sensors currently available.
- Determine the suitability of state of the art physical parameter sensors for the extreme environment of a PEM fuel cell power plant by testing them in a combination of laboratory and simulated fuel cell flow stream environments.
- Assist the sensor manufacturers, where necessary, to modify the sensors to achieve the requisite performance, cost, and durability goals.
- Modify baseline chemical sensing technology to create sensors capable of making the measuring the parameters of Table 3.2 in a PEM fuel cell operating environment.
- Validate and document the performance and durability of the developed sensors by exposing them to a combination of laboratory and simulated fuel cell flow stream environments.
- Install the developed sensors on a breadboard PEM fuel cell at United Technologies Company fuel cell (UTCFC) for final testing.

Accomplishments

- This contract is still under negotiation; there has been no technical progress to date.

Introduction

The present state of the art in fuel cell powerplant sensor technology is embodied in the UTCFC PAFC PC 25 and PEM S200 powerplants. However, none of the chemical sensors, and only a very few of the physical sensors are "on-board" the powerplant. Furthermore, only temperature and stack differential pressure, in the S200, are measured continuously for control purposes. Production automotive fuel cell powerplants require all of these sensors to be on-board the powerplant, and to provide data signals on a continuous basis to optimize fuel cell operation and protect the cell stack from damage.

The measurement technology used by the PC 25 and S200 "off-line" chemical analyzers cannot be adapted to provide the basis for on-board, continuously measuring chemical sensors. IFC and

its team members have identified three candidate technologies that have the potential to achieve these goals.

Approach

Table 1 identifies the two technologies and the specific parameters the technologies will be targeting during the development effort. The sections below discuss each technology that we plan to use to develop the required capability.

Table 1.

Technologies	CO	H_2	SO_2	H_2S	NH_3	O_2
Electrochemical	X		X	X	X	X
MEMS		X	X	X	X	

CO = carbon monoxide, H_2 = hydrogen, SO_2 = sulfur dioxide, H_2S = hydrogen sulfide, NH_3 = Ammonia, O_2 = diatomic oxygen

Electrochemical

Electrochemical sensing is based on the interaction of an electrically conductive film with a molecular species in its environment. Typically an inorganic film is deposited on a semiconducting film, which, in turn is deposited over a series of interdigitated electrodes. The temperature of the device is maintained at a predetermined temperature to facilitate the desired interaction. As the target compound adsorbs to the sensing film, a change in the conductance of the semiconducting film between the interdigitated electrodes is produced, sensed and a signal is generated for external use.

NexTech Materials is pursuing the development of low-cost electrochemical carbon monoxide (CO) sensors that will meet the requirements of the fuel cell application. NexTech has recently demonstrated detection of parts per million (ppm) CO in a 50% hydrogen stream using copper/chlorine (CuCl) thick films. Figure 1 shows the response of NexTech's sensor when cycling between 50:50 vol% nitrogen/ hydrogen (N_2/H_2) and 1000 ppm CO in N_2/H_2. The hydrogen content was varied between 25 and 75 vol% (balanced with nitrogen) with no change in the baseline resistance noted. The sensing approach is based on the change in electrical resistance that occurs when carbon monoxide is selectively adsorbed by an inorganic film of a semiconducting

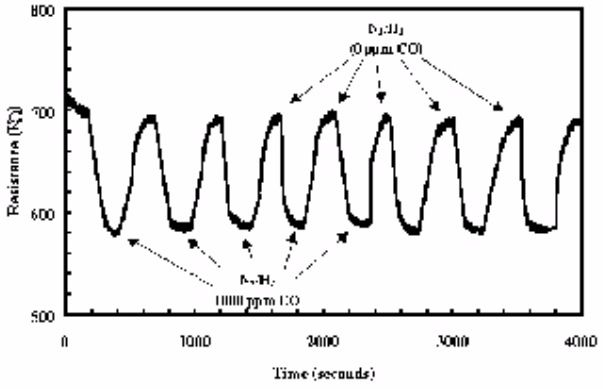

Figure 1. Effect of carbon monoxide (1000 ppm) on resistance of NexTech sensor in a baseline gas composition of 50% hydrogen and 50% nitrogen.

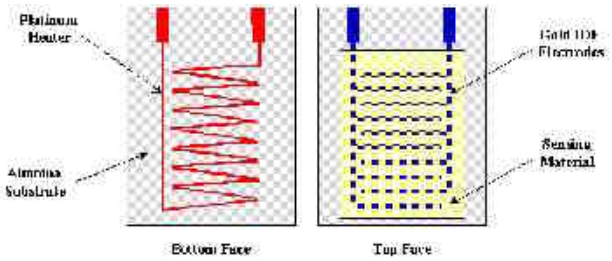

Figure 2. Sensor Construction Detail

material. The sensing material is deposited onto a substrate with interdigitated electrodes, with temperature being controlled by a thick-film heater deposited on the underside of the substrate, as shown in Figure 2. NexTech's results have demonstrated that this resistance change occurs rapidly (with either increasing or decreasing CO content), varies with the amount of CO from the gas stream, is insensitive to the presence of hydrogen, and can be used to detect low carbon monoxide levels. This type of sensor has the potential to be manufactured at a cost of $5 to $10 in volume. However, these sensors were used at a single temperature and CO concentration in the range of 100 -1500 ppm. More work is needed to determine the capability of this material for sensing CO at higher temperatures and/or higher CO concentration. Effort to explore the range of operation of the sensors will accelerate under this project.

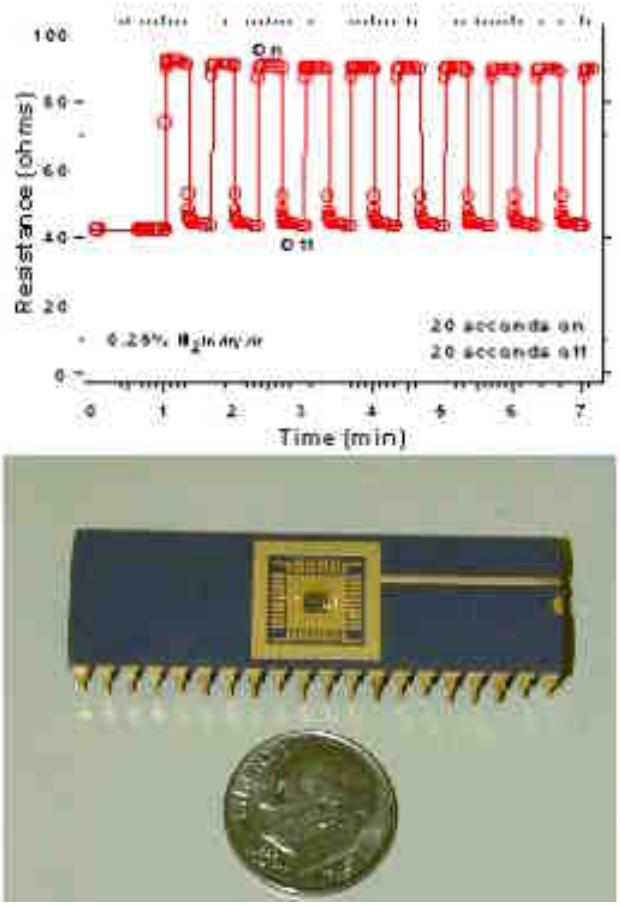

Figure 3. MEMS Hydrogen Sensor

Micro Electro Mechanical Systems (MEMS)

MEMS is a method to produce microscopic three-dimensional sensor arrays from a solid substrate. Sensing mechanisms such as the hydrogen-induced transition from a metallic di-hydride to a semiconducting tri-hydride can be deposited on a MEMS substrate. The reduced size, mass, subsequent thermal rise and fall times of the tiny devices, often called microhotplates, makes it possible to pulse the sensor to a desired operating temperature in milliseconds, make a measurement, and step to another measurement condition. Power consumption of such devices can be brought to very low values, response times can be in the sub second range, and sensitivity can be controlled by the actual reaction taking place in the uppermost sensing film.

The micro-hotplate gas sensor is a conductometric MEMS-based sensor that uses the change in conductance of the sensing layer as a function of temperature and time to measure the gases present. A critical step in developing these gas sensors is the selection of a specific chemi-resistive reactive layer for each target gas. ATMI has demonstrated the development of a high performance-low cost MEMS based H_2 gas sensor, (U.S. Patent, 09/231277, Allowed 2000) using palladium (Pd) alloy coated metal hydrides as the gas sensitive layer.

Figure 3 shows a typical unit of this design and the response to 0.25% hydrogen in dry air. These sensors have shown over a 100% change in resistivity to 0.25% H_2 in air, at speeds of response of less than 0.5 second.

UTCFC and its team members will investigate each of these platforms as a technology for part of the chemical-sensing requirement. No single platform is believed capable of addressing the entire chemical sensing requirement; therefore, each of the team members will develop its platform toward the requirement indicated in Table 3 1. The goal is to develop at least one applicable technology for each species and demonstrate them on an on-line S300 system

Current Technology for Physical Sensing

The state of development of physical sensor technology is dramatically different from that of the chemical sensors. Demand for high performance temperature, humidity and pressure sensors by the automotive and heating, ventilating, air conditioning and refrigeration (HVAC) industries have resulted in a large variety of different sensors. Consequently, the primary goal of this section of the effort will be to evaluate and modify, as necessary, commercial off-the-shelf sensors to fill the need. The physical sensors used by the PC 25 and S200 physical powerplants can be used as the basis of on-board continuously measuring sensors. Additionally, it is possible that more recently developed sensors for measuring the same parameters may be a better starting platform than the PC25/S200 sensors. The team will continually monitor the evolution of new physical sensors during the performance of this project.

The UTCFC team will select a baseline device for each sensor and to confirm its ability to fully meet the DOE specification. If there are deficiencies, we will work with the manufacturer to modify the sensor to conform. Table 2 identifies current sensors and the properties expected to limit their application. The potential limitations will be carefully evaluated in lab testing and subsequent on-line testing if they successfully complete the lab-testing phase.

Table 2.

Physical Sensor	Current Manufacturer	Operating Range	Items to be Confirmed in Testing
Temperature	Gulf Sensors Inc.	0 - 1900^{o}F	Corrosion resistance; repeatability
P Cell Stack	Atmos Engineering	1-3 atm; -50^{o}C to +100^{o}C	Survivability in gas stream; linearity; drift; accuracy, cost
Relative Humidity	General Eastern	0 to 100% RH; -10^{o}C to 100^{o}C gas stream	Corrosion resistance; sensor drift; repeatability, cost
Mass Flowmeter	Sierra Instruments	30 - 300 SLPM @ 80^{o}C	Accuracy, corrosion resistance; repeatability, cost

UTCFC will evaluate these sensors in the appropriate test facilities, supplying a synthesized gas stream of known inlet gas composition, and determine the response accuracy of each sensor at the required operating temperature. By controlling the inlet gas composition and mass flow, a fixed reference will be established to which the sensor response will be compared as a function of time. This effort will be conducted in United Technologies Research Center (UTRC), IIT and UTCFC facilities. Baseline sensor technology taken from a combination of production PC25, S200 and fuel cell development laboratory applications will be subjected to a series of performance, durability and cost reduction studies. Concurrent with this portion of the task, a detailed review of alternate sensors will be conducted. Appropriate sensors will be ranked according to probability of successful test outcome. This ranking will be used to identify replacement candidates should any baseline sensor fail the full suite of evaluations. Initial qualification tests will be conducted by IIT in the PEM Fuel Cell Benchmark Facility. These tests will consist of installation and exposure of baseline sensor technology to precisely controlled temperature, humidity, pressure, and gas mixture conditions. Sensor response versus these parameters will be logged.

Second level testing will be conducted at UTRC. During these tests, the sensors will be installed in a chamber through which gases simulating an ATR exhaust stream (created by mixing gases, heating, and humidifying as necessary to obtain the desired composition) will flow. The sensors will be evaluated for accuracy, speed of response, cross sensitivity to non-target parameters and test gas parameters. The tests will operate continuously for 40 hours, during which time a PC utilizing National Instruments LabView software will control and log all test parameters, including gas composition, sensor output, and control safety systems.

It is assumed that repetition of the above testing cycle will be required due to non-performance of some sensors. If baseline sensors cannot demonstrate superior performance, alternates will be selected.

References

1. J.N. Huiberts, et al, Nature 380 231(1996).

IV.D.25 Design and Development of New Glass-Ceramic Proton Conducting Membranes

Steve W. Martin (Primary Contact), Steven A. Poling, Jacob T. Sutherland
Iowa State University, Materials Science and Engineering Department
3053 Gilman Hall
Ames, Iowa, 50011
(515) 294-0745, fax: (515) 294-5444, e-mail: swmartin@iastate.edu

DOE Technology Development Manager: Roxanne Danz
(202) 586-7260, fax: (202) 586-9811, e-mail: Roxanne.Danz@ee.doe.gov

Objectives

- Investigate a new class of proton conducting membranes using thio-acids for hydrogen fuel cell applications.
- Produce anhydrous solid membranes having minimal fuel crossover capability and address many of the problems associated with current hydrogen fuel cell technologies.
- Optimize thio-acid membranes to yield high proton conductivities (10^{-6} to 10^{-3} Siemens per centimeter [S/cm]).
- Demonstrate performance, thermal stablility, and chemical stability with exposusre to water (H_2O) and diatomic oxygen (O_2) in a typical fuel cell setup.

Approach

- Synthesize new thio-acids.
- Synthesize membrane materials from thio-acids; final product may be a glass, glass/ceramic, or ceramic structure with stable sulfur-hydrogen groups.
- Measure the proton conductivity between -70^{o}C and 500^{o}C.
- Determine thermal stability.
- Determine chemical stability with respect to H_2O and O_2.
- Determine electrochemical properties, including reduction and oxidation potentials, and cyclic voltammetry.
- Cooperatively fabricate and test membrane electrode assembly (MEAs) using the most promising membranes. This is to be done in partnership with an external company specializing in fuel cells.

Accomplishments

- Two new thio-acids have been synthesized, a thiogermanic acid and a thiomolybdic acid. Additionally, the synthesis route is able to produce hydrosulfides and sulfides from many different hydroxide and oxide precursors.
- Thiogermanic acid, dihydrogen tetragermanium sulfide ($H_2Ge_4S_9$), is the thermally stable form of nanostructured tetrahydrogen tetragermanium sulfide ($H_4Ge_4S_{10}$). Tetrahydrogen tetragermanium sulfide with n molecules of H_2S ($H_4Ge_4S_{10} \bullet nH_2S$) has a measurable conductivity of 10^{-5}S/cm at room temperature; at higher termperatures it decomposes to $H_2Ge_4S_9$ with a reduced conductivity and greater thermal stability.
- Thiomolybdic acid H_2MoS_4 appears to conduct both protons and electrons. Possible catalytic behavior, electrode application, and storage capability of this acid are undetermined at this time.

- Thermally and chemically stable membranes have been synthesized from thio-acids. Conductivities of 10^{-7} S/cm at ~ 352°C were achieved with materials thermally stable to at least 500°C and chemically stable with H_2O for prolonged exposures.

Future Directions

- Reaction kinetics involving liquid hydrogen sulfide (H_2S) solution are being studied for the germanium oxide (GeO_2) and germanium sulfide (GeS_2) systems. This study is exploring the effects of water, temperature, time, and pressure on the kinetics of these types of reactions. At this point, it is clear that hydration by water speeds the reaction. A high pressure phase, which is more thermally stable, is also realized from long reaction times.
- Investigation into new thio-acid compounds from oxide, hydroxide, and sulfide precursors is being excuted. One new compound has recently demonstated 10^{-3}S/cm at 100°C.
- Efforts to thermally stabilize these thio-acids with large alkali metal cations are underway. This may also produce primitive rotating phases with higher proton conduction values.
- Work is now underway to produce thermally and chemically stable membranes from these thio-acids. This involves bonding thio-acid units to known chemically and thermally durable compounds.

Introduction

Hydrogen-based fuel cells are becoming increasingly popular as an alternative to petroleum-fueled internal combustion engines. Specifically, hydrogen can be converted to electricity through the use of a (H_2-O_2) fuel cell. The by-product of this type of a fuel cell is water, making this a "green" or environmentally friendly technology. At the heart of the fuel cell is the proton exchange membrane (PEM), which transports the proton from the anode to the cathode while providing electronic insulation between them. There are many types of PEMs, each with specific limitations [1].

With current PEMs, there remains a temperature region between ~200°C and ~700°C that currently no one membrane can provide for optimum performance. We propose the use of chalcogenide glass-ceramic proton conducting membranes to help fill this temperature performance regime. These membranes are being developed to be highly conducting to protons, anhydrous in nature, thermally stable up to ~500°C, and chemically stable with respect to H_2O and O_2. Being solid in nature, these membranes are not expected to exhibit fuel cross-over problems. Proton conductivities of these membranes are expected to be orders of magnitude higher than their oxide counterparts, assuming they follow the trend exhibited by alkali cations such as lithium (Li) and silver (Ag) in chalcogenide verses oxide host materials [2].

Approach

Oxide, hydroxide, and sulfide compounds capable of forming thio-acids in liquid H_2S solution are being identified. As an example, the reaction of GeO_2 with liquid H_2S at room temperature produces the thio-acid ($H_4Ge_4S_{10} \bullet xH_2S$). Membranes may be produced by bonding thio-acid units with known thermally and chemically stable sulfide or oxide compounds. Taking a glass or ceramic material that has one or more thio-acid analogs and reacting it in a liquid H_2S solution is one way to accomplish this.

Proton conductivity in the glasses and glass-ceramics is being determined through impedance measurements as a function of temperature and frequency. Direct current polarization experiments have been used to determine the electronic verses ionic conductivity of the samples. Physical properties of the glass-ceramic proton conducting materials have been determined, including decomposition, sublimation, crystallization, and glass transition temperatures. Structural comparisons have been used to examine stability with exposure to H_2O and O_2.

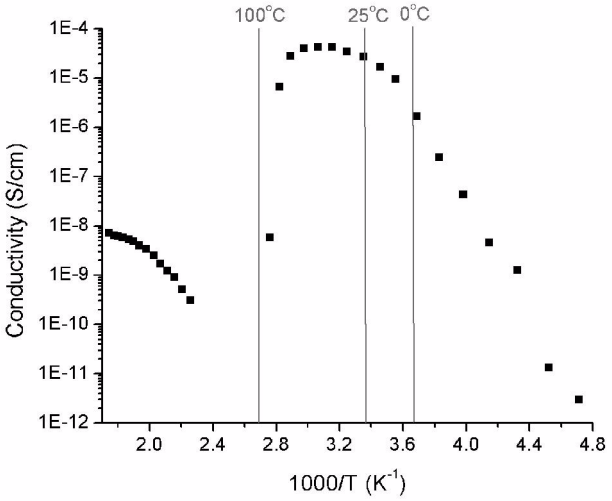

Figure 1. Proton Conductivity Values for the Thiogermanic Acid between -61°C and 300°C

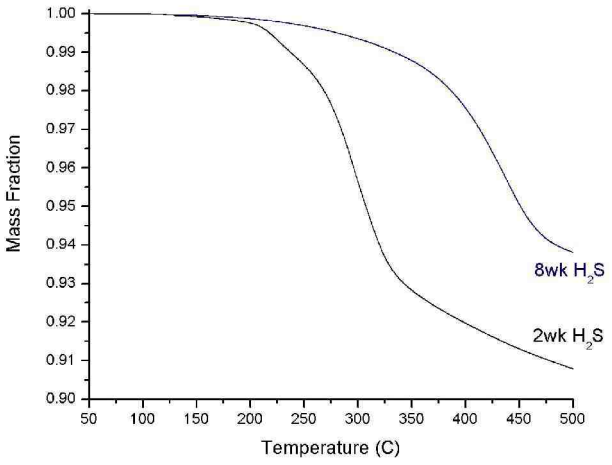

Figure 2. TGA Scan at 10°C/min of the Thiogermanic Acid

A cooperative effort to fabricate and test MEAs using our most promising membranes is being carried out in partnership with an external company specializing in fuel cells.

Results

Proton conduction has been demonstrated for our anhydrous thio-acid materials. Figure 1 shows the resulting proton conductivity values for

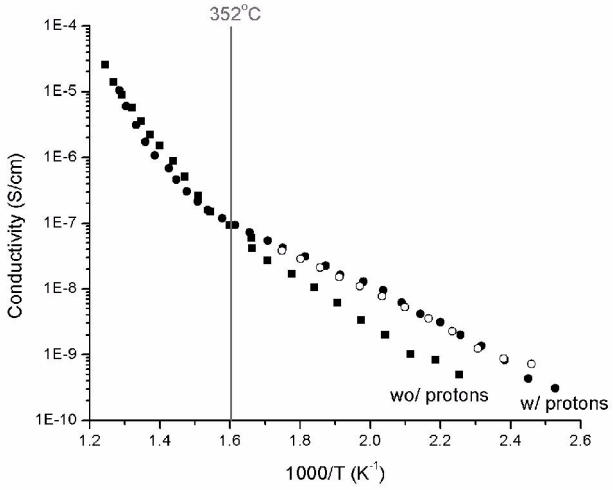

Figure 3. Proton Conductivity Values of the 0.14 Ga_2S_3 + 0.86 GeS_2 + H_2S System between 110°C and 500°C

nanostructured $H_4Ge_4S_{10} \bullet nH_2S$ produced by reacting GeO_2 with liquid H_2S for four weeks. The data is presented in the temperature range of 61°C to 300°C; a conductivity of 10^{-5}S/cm is realized at room temperature before the nanostructured $H_4Ge_4S_{10}$ material decomposes to the thiogermanic acid $H_2Ge_4S_9$. Effort is currently underway to stabilize the nanostructured $H_4Ge_4S_{10}$ material, thereby increasing the conductivity and useable temperature range.

Figure 2 illustrates thermogravimetric analyzer (TGA) spectra of the thiogermanic acid $H_2Ge_4S_9$. Longer reaction times, i.e. eight weeks versus two weeks, with liquid H_2S appears to produce a more thermally stable crystal phase.

Figure 3 demonstrates proton conduction for one of our thermally and chemically stable thio-acid membranes. A conductivity of 10^{-7}S/cm at ~ 352°C as achieved in the 0.14 gallium sulfide (Ga_2S_3) + 0.86 GeS_2 + H_2S system. This material is thermally stable to at least 500°C and chemically stable with prolonged H_2O exposures.

Figure 4 presents preliminary proton conduction for one of our new thio-acid compounds. Conductivity of 10^{-3}S/cm at ~100°C was achieved (this is close to the commercial PEM Nafion® ~

10^{-2} S/cm). Beyond 100°C this compound decomposes. Effort is currently underway to

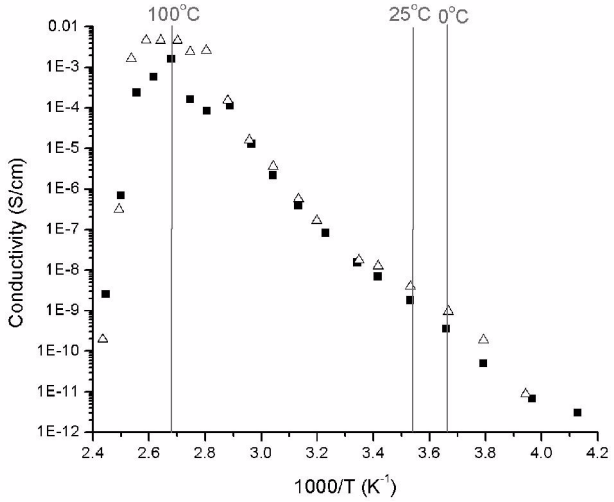

Figure 4. Preliminary Conductivity Values for a Newly Synthesized Compound between -31°C and 136°C

thermally stabilize this new thio-acid compound, and to increase its proton conductivity and useable temperature range.

Conclusions

- A synthesis route for producing thio-acids, hydrosulfides, and sulfides has been identified; effort to decrease production time is underway.The structure, conductivity, thermal and chemical stability of many potential thio-acids have been investigated; many more are being pursued.
- Two new thio-acids have been identified and synthesised for the first time, namely thiogermanic acid and thiomolybdic acid.
- Preliminary ionic conductivity as high as 10^{-3}S/cm at ~100°C has been realized from one new compound; this is close to the commercial membrane material Nafion®.
- Structural modifications to thio-acid compounds and thio-acid membranes are underway to increase thermal stability and conductivity.

References

1. Martin, S.W., Poling, S.A., Sutherland, J.T., "Design and Development of New Glass-Ceramic Proton Conducting Membranes." DOE Hydrogen Program Annual Review, Proceedings (2002): NREL/CP-610-32405.

2. Angell, C.A. 1992. "Mobile Ions in Amorphous Solids." Annual Review of Physical Chemistry, 43:693-717.

FY 2002 Publications/Presentations

1. "Design and Development of New Glass-Ceramic Proton Conducting Membranes," Steve W. Martin, Steven A. Poling, and Jacob T. Sutherland, DOE Hydrogen Program Annual Review, Proceedings (2002): NREL/CP-610-32405.

2. "Synthesis and Structure of Thiogermanic Acid $H_2Ge_4S_9$," Steven A. Poling, Steve W. Martin, and Jacob T. Sutherland, to be submitted.

3. "Design and Development of New Glass-Ceramic Proton Conducting Membranes," Steve W. Martin, Steven A. Poling, and Jacob T. Sutherland, DOE Hydrogen Program Annual Review, Golden, CO, May 6-10, 2002.

4. "Synthesis and Characterization of a New Class of Ceramic Proton Conducting Solid Electrolytes," Steve W. Martin, Steven A. Poling, and Jacob T. Sutherland, 201st Meeting of The Electrochemical Society, Philadelphia, PA, May 12-17, 2002.

5. Invited Talk, "Preparation and Characterization of New Proton Conducting Chalcogenide Glasses and Glass-Ceramics," University of Muenster, Muenster, Germany, July, 2002.

6. Invited Talk, "Preparation and Characterization of New Proton Conducting Chalcogenide Glasses and Glass-Ceramics," University of Dortmund, Dortmund, Germany, July, 2002.

7. "Invited Talk, "Preparation and Characterization of New Proton Conducting Chalcogenide Glasses and Glass-Ceramics," University of Montepellier II, Montepellier, France, July, 2002.

8. "Protonated Chalcogenide Materials for Fuel Cell Electrolyte Membranes," poster at the104th Annual Meeting and Exposition of the American Ceramic Society, Steve W. Martin, Steven A. Poling, and Jacob T. Sutherland, St. Louis, MO, April 29-May 1, 2002.

Special Recognitions & Awards/Patents

1. Provisional Patent: "Synthesis and Uses of Thio Acids" Steve W. Martin, Steven A. Poling, Jacob T. Sutherland, Iowa State University, ROI ISURF 2894, February 8, 2002. Provisional filing date of July 26, 2002.

IV.D.26 Fuel Cell System Durability

Rod Borup (Primary Contact), Michael Inbody, Troy A. Semelsberger, Francisco Uribe, and José Tafoya
P.O. Box 1663
Los Alamos National Laboratory
Los Alamos, NM 87545
(505) 667-2823, fax: (505) 665-9507, e-mail: Borup@lanl.gov

DOE Technology Development Managers:
JoAnn Milliken: (202) 586-2480, fax: (202) 586-9811, e-mail: JoAnn.Milliken@ee.doe.gov
Nancy Garland: (202) 586-5673, fax: (202) 586-9811, e-mail: Nancy.Garland@ee.doe.gov

Objectives

- Achieve DOE system durability target of 5,000 hours on reformate.
- Quantify fuel cell component durability
  - Fuel processor durability reforming liquid hydrocarbons (gasoline)
  - Fuel cell durability on reformed gasoline
  - Fuel cell durability on hydrogen
- Quantify fuel reformate effects on fuel cell system (fuel processor and fuel cell stack) durability
  - Determine stack durability limits of operation with reformed fuel
    - Determine reformate effect on electrocatalyst durability
    - Determine reformate effect on proton exchange membrane durability
  - Determine fuel and fuel impurity effects on fuel processor catalyst durability
  - Identify reformate species which limit fuel cell anode durability

Approach

- Measure single cell fuel cell performance with hydrogen and gasoline reformate
  - Measure stack component durability with hydrogen
  - Measure stack component durability with gasoline reformate from fuel processor
- Operate modular fuel processor system with liquid hydrocarbons to generate real reformate
  - Measure fuel processor operation and reformate composition over long operational period (1000 hrs)
    - Analyze fuel processor catalysts to determine structural and elemental changes
    - Analyze reformate to determine low level of impurities
  - Characterize membrane electrode assemblies (MEAs) during operation
    - Electrochemical polarization curves, high frequency measurements
    - Hydrogen adsorption/desorption

Accomplishments

- Operated fuel processor system with liquid hydrocarbon fuels for over 1000 hrs
  - Measured fuel reformate impurities
    - Near-zero NH_3 formation (<0.5 ppm) with normal operating conditions

  - Measured catalyst surface area after extended operation (~1,200 hours)
    - Decrease of 20% to 90% observed in autothermal reforming (ATR) and preferential oxidation (PrOx) catalysts, including loss in activity and CO conversion in PrOx
- Improved fuel processor subsystem (carbon formation and fuel processor hydrocarbon breakthrough)
  - Carbon formation limited by precious metal steam reforming catalysts, high steam-to-carbon (S/C) ratio (1.3), and high reforming temperature (>725^{o}C)
  - Hydrocarbon breakthrough limited by additional S/C and reforming catalysts (<20 ppm C_2 compounds)
- Measured hydrogen proton exchange membrane (PEM) performance
  - Operated single cells with reformate and hydrogen – low performance observed with reformate

Future Directions

- Improve fuel processor conversion to eliminate high molecular weight hydrocarbon formation
- Study stack operation on reformed petroleum-based fuels to evaluate reformate effects:
  - Pure fuel components and components blends
  - Real fuels such as reformulated gasoline
- Measure fuel cell stack durability with hydrogen and reformate for direct comparison of reformate effects

---

Introduction

This report describes our FY02 technical progress in examining the durability of fuel cell systems to support the DOE target for 5,000 hour durability of these systems. The goal of this research is to identify the factors limiting the durability of fuel cells and fuel processors. This includes PEM fuel cell durability issues for operating on pure hydrogen, as well as those that arise from the fuel processing of liquid hydrocarbons (e.g., gasoline) as a function of fuel composition and impurity content. Benchmark comparisons with the durability of fuel cells operating on pure hydrogen are used to identify limiting factors unique to fuel processing.

We describe the design, operation and operational results of the durability system, including the operating conditions for the system, fuel processor subsystem operation over 1000 hours, post-mortem characterization of the catalysts in the fuel processor, and single cell operation.

Approach: Durability Gasoline Reformate Production and Single Cell Fuel Cells

Our approach to identify the limiting factors on fuel cell system durability is, first, to develop and operate a modular fuel processor system to examine the fuel composition and impurity effects on fuel processor durability and to generate reformate for testing the durability of fuel cell components. Second, we examine the effects of the reformate on the fuel cell components, primarily the membrane electrode assembly (MEA), by testing MEAs in single-cell fuel cells operating on both reformate and pure hydrogen. Third, we use a combination of fuel processor gas analysis, fuel processor catalyst characterization, and MEA characterization during and after operation to quantify performance losses and to identify limiting factors on durability such as poisons. The modular fuel processor subsystem, shown in Figure 1, was designed and constructed to simulate conventional methods of hydrogen generation for PEM fuel cell stacks. The fuel processor consists of a sequence of reactors: a partial oxidation/steam reformer (POx/SR) or autothermal reformer (ATR), sulfur removal, high-temperature shift (HTS), low-temperature shift (LTS), and preferential oxidation reactor (PrOx). Typical commercial and semi-commercial noble metal oxidation catalysts and noble metal or non-noble metal steam reforming catalysts are used in the ATR. Conventional commercial catalysts also are used in the HTS, LTS, and PrOx to allow full

Figure 1. Fuel Processor System Showing the Stages for POx/SR, HTS, LTS and PrOx

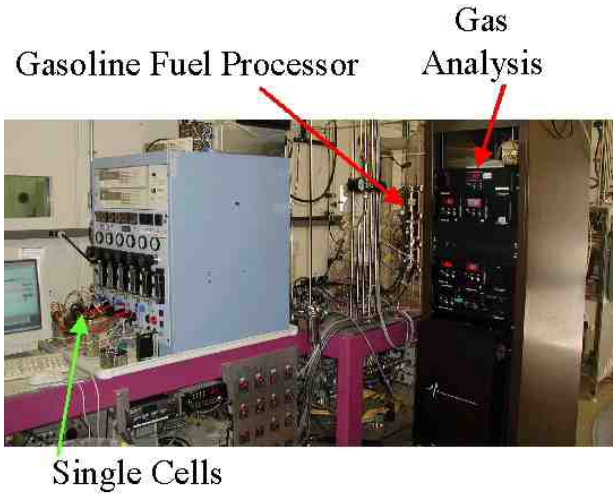

Figure 2. Fuel Processor Coupled with Fuel Cell Test Station and Two PEM Fuel Cell Single Cells

characterization of the catalysts without violating proprietary concerns. The ATR atomic O/C (oxygen/carbon - O from air only) is 0.8 to 0.85, while typical S/C (steam/carbon) is from 1.0 to 1.25. Additional downstream liquid water injection increases the overall S/C ratio to a typical S/C of 2.5 to 3.0. A slipstream of the reformate flow from the fuel processor is routed to the fuel cell test station.

Figure 2 shows the fuel cell test station and single cells coupled with the fuel processor. The fuel

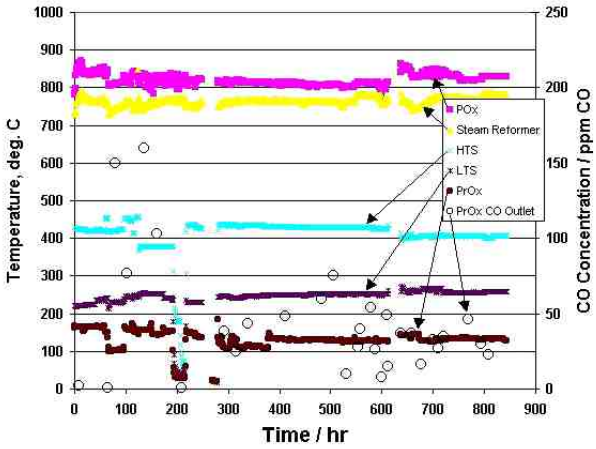

Figure 3. Temperature and PrOx Outlet CO Concentration of Fuel Processor System during ~ 800 hrs Operation with Isooctane

cell test station can operate 3 single-cell fuel cells with either pure hydrogen or with the gasoline reformate. The direct comparison of pure hydrogen and reformate feeds to the single cells is used to identify the effects that fuel processing reformate has on the fuel cell durability. Currently, 50 cm^2 single cell components are being tested. Performance during the durability test is measured with continual monitoring of the voltage/current performance along with periodic polarization curve, AC Impedance, and hydrogen adsorption/desorption (HAD) measurements to monitor the anode catalyst surface area. Following the durability testing, MEAs will be characterized to evaluate degradation mechanisms.

Results: Fuel Processor Operation

The fuel processor subsystem was operated with pure iso-octane to verify its performance. Figure 3 shows 800 hours of the fuel processor operation on iso-octane, showing the temperatures in the different stages, and the CO outlet concentration. The temperature in the partial oxidation stage is about 800 – 825°C, and the outlet temperature of the steam reforming section is 775°C. The average residence time for the ATR section is about 0.5 sec (GHSV ~ 10,000), which should be sufficient for complete hydrocarbon conversion.

The HTS is operated at 400°C, the LTS is operated at 250°C, and the PrOx is controlled to a temperature of 125°C. The outlet CO concentration

from the ATR was typically about 10%; the outlet CO concentration from the LTS was <1%; and the outlet CO concentration from the PrOx varied initially from 0 to 150 ppm, with improved controls keeping the CO concentration below 100 ppm and typically below 40 ppm.

Figure 4 shows operation of the fuel processor subsystem on iso-octane for 11 days, after which the fuel was switched to a simulated gasoline of 74% iso-octane, 20% xylene, 5% methylcyclohexane and 1% 1-pentene. After only two days of operation on this simulated gasoline, the pressure drop between the ATR and HTS increased due to carbon formation. Post characterization of the carbon formed showed that a high concentration of solidified hydrocarbons were present in the carbon (30% by weight). To prevent carbon formation between these reactor sections, the HTS water injection was moved from the inlet to the HTS to the outlet of the steam reformer section.

After extended operation, the catalysts present in the fuel processor were characterized to observe any potential degradation of the catalysts. The relative catalyst surface areas of the ATR, HTS, LTS and PrOx catalysts all decreased after extended operation. The initial portion of the ATR catalyst, where the fuel oxidation occurs, showed a large decrease in surface area, over an order of magnitude decrease from about 3 m^2/g to <0.2 m^2/g (note that the surface area is low because the support material is included in the measurement). Other portions of the ATR catalyst did not show as big a decrease in surface area. The LTS catalyst surface area decreased about 50%, which appears to be independent of the catalyst location in the LTS section. The measured PrOx catalyst surface area, shown in Figure 5, decreased as a function of the axial location in the reactor catalyst volume. The measured PrOx catalyst surface area shows a high decrease in the upstream section, while in downstream sections of the PrOx, approximately 75% of the original surface area is maintained.

Current results indicate operational issues for the fuel processor subsystem to meet the DOE durability target of 5000 hours due to carbon formation and catalyst surface area. Upon post-analysis of the fuel processor, carbon formation was observed regardless

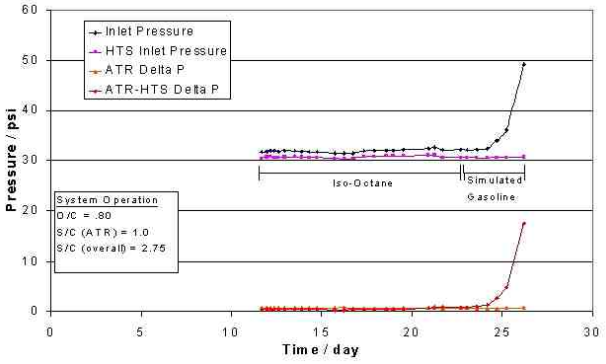

Figure 4. Operation of fuel processor with isooctane and simulated fuel. Inlet pressures and pressure drops are shown, demonstrating the build-up of carbon in between the ATR and HTS.

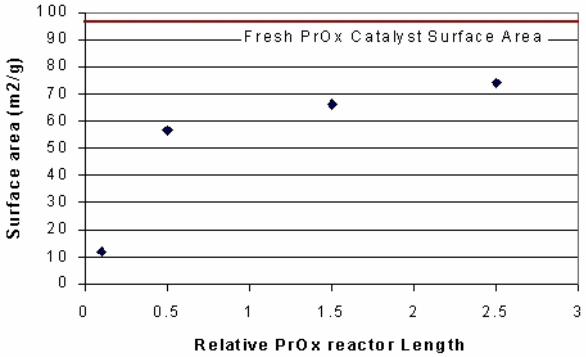

Figure 5. PrOx Catalyst Surface Area after Total On-Stream Time of ~1200 hrs of Operation

of fuel composition and operating condition. When aromatics were present in the fuel, carbon formation was a much a larger issue, such that the amount of carbon formed caused increases in the system pressure drop. Various improvements in the ATR design, including the water injection for the HTS, decreased the amount of carbon formation. In addition, elimination of any nickel steam reforming catalysts has helped decrease carbon formation.

Results: Single Cell Operation

Figure 6 shows a single cell operation for Nafion 112 MEAs on pure hydrogen, and with reformate produced from the fuel processor. The steady state performance of the MEA on pure hydrogen was about 0.9 A/cm^2 at 0.62 V. At hour 48, the pure hydrogen feed was switched to the gasoline

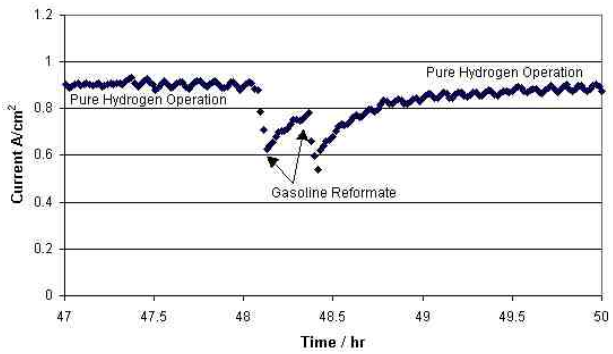

Figure 6. Single Cell Operation on H_2, Followed by Operation on Gasoline Reformate

reformate. Even though the CO content of the fuel processor was below 50 ppm, and air injection was used for the anode of the fuel cell, the performance of the fuel cell was poor, as shown by the rapidly dropping current density of the MEA. As the reformate was switched back to pure hydrogen, the performance recovered quickly, within a few minutes.

Analysis of the fuel processor condensate showed that hydrocarbons were present. The hydrocarbons found in the condensate include hydrocarbons with molecular weights higher than those present in the original fuel, over 150. This could mean that some polyaromatic hydrocarbons are formed. Changes to the catalyst used in the fuel processor ATR section have been made to reduce the hydrocarbon output of the fuel processor section to improve performance of the fuel cells.

Hydrocarbon breakthrough from the fuel processor appears to have limited the durability of the PEM fuel cell anode. The loss of MEA humidification has also been observed to limit MEA durability. Hydrocarbon breakthrough has been eliminated by using small amounts of nickel catalyst in the ATR portion of the fuel processor; however, this resulted in carbon formation, which limited the fuel processor operational durability. Increasing the ATR S/C ration, adding precious metal steam reforming catalyst, and increasing the steam reforming temperature has also eliminated the hydrocarbon breakthrough. Modification of the MEA humidification should eliminate loss of gas feed humidification. These improvements should greatly improve the PEM MEA durability.

Conclusions

Fuel processor operation producing hydrogen with low carbon monoxide content has been demonstrated for over 1000 operational hours. Current results indicate difficulties in operating the fuel processor subsystem continuously for the DOE target of 5000 hours due to carbon formation and reduced catalyst surface area. The catalyst surface decreased in all the stages of the fuel processor, with the amount of decrease depending on the catalyst and its axial location in the catalyst volume. Although the carbon monoxide concentration in the outlet of the fuel processor is low, the performance of the single cells is poor, apparently due to small amounts of hydrocarbons present in the reformate stream. Carbon formation over relatively long periods of time was also an issue between the ATR and HTS stages when fuels containing aromatics were used.

Future work is being conducted to examine fuel processor durability, PEM cell durability on reformate, and operation of PEM fuel cells on hydrogen. The durability of fuel processor catalysts and reactor materials will be examined with 'real' fuel blends with operation and design modified to help prevent carbon formation. This work will evaluate the fuel processor catalyst durability, carbon formation, and changes to the mechanical properties of ATR materials. PEM cell durability studies will concentrate on the operation and causes of degradation of the MEA portion of the fuel cell.

Presentations/Publications

1. Fuels for Fuel Cells for Transportation Applications, Rod Borup, Lee Perry, Mike Inbody, Byron Morton, Troy Semelsberger and Jose Tafoya, AIChE Meeting, Spring 2002, New Orleans, LA, Los Alamos National Laboratory publication, LAUR-02-1207, March 2002.